SATELLITE-BASED SOLAR RADIATION, NET RADIATION, AND POTENTIAL AND REFERENCE EVAPOTRANSPIRATION ESTIMATES OVER FLORIDA

Technical Report
Prepared by

Jennifer Jacobs[1]
John Mecikalski[2]
Simon Paech[3]

July 2008

[1]University of New Hampshire, Department of Civil Engineering, Durham, NH
jennifer.jacobs@unh.edu
[2]University of Alabama in Huntsville, Department of Atmospheric Sciences, Huntsville, AL, johnm@nsstc.uah.edu
[3]University of Alabama in Huntsville, Department of Atmospheric Sciences, Huntsville, AL, simon_paech@hotmail.com

Table of Contents

Executive Summary

In Florida, potential evapotranspiration (PET) and reference evapotranspiration (RET) estimates are used in a number of water resource planning and management activities including estimating water use for permitting and planning, modeling surface water, groundwater, and wetlands dynamics, and characterizing the transport of pollutants through watersheds and aquifers. Both PET and RET estimates require direct measurements of incoming solar radiation. Because the Florida ground-based solar radiation network is extremely sparse from 1991 to present, this project makes PET and RET estimates using solar radiation obtained from Geostationary Operational Environmental Satellites (GOES). The proposed effort provides solar radiation, potential evapotranspiration, and reference evapotranspiration estimates at a 2 km spatial scale and a daily time scale from 1995 to 2004 for the entire state of Florida. The methods used to create these datasets are described in this document. All supporting datasets were transferred to the U.S. Geological Survey, Orlando, Florida and are publicly available via the USGS web portal.

In the process of developing these datasets, several interim conclusions were reached.

The comparison of several methods to estimate PET determined that a tradeoff exists between the Priestley-Taylor (PT) and Penman-Monteith (PM) models. PM is more accurate for small scale studies when at-site parameter values are available, but has extensive data needs, including net radiation, air temperature, relative humidity, and wind speed. Additionally, the PM model has several parameters that cannot be easily measured or estimated over large areas. The PT method, on the other hand, requires only net radiation and air temperature data, has no tuning parameters, does not have a seasonal bias, and is slightly (but not statistically) more accurate over large regions. Based on our analysis, we recommend the use of the PT model. While the Simple method, requiring only incoming solar data, accurately estimates PET for marshlands, it is not found to be broadly applicable for the variable Florida land uses.

The satellite-derived solar insolation dataset required calibration to correct for temporal-, seasonal- and cloudiness-related model biases. This was achieved via comparison with available ground-based pyranometer measurements. Upon calibration, the quality of the solar insolation product was improved.

Net radiation is the most important input for the PT model. The analysis of net radiation approaches suggest that individually estimating the four components of net radiation yields decidedly better results than simple regressions of incoming solar to net radiation. The recommended approach is to use Seller's equation to estimate the clear sky downwelling radiation and the Crawford and Duchon method to correct for cloudy conditions. The surface albedo is best estimated using separate values for the land albedo (0.149) and the water albedo (0.062).

1. Introduction

In Florida, estimates of potential evapotranspiration (PET) and reference evapotranspiration (RET) are needed for a number of water resource planning and managements activities including estimating water use for permitting and planning, modeling surface water, groundwater, and wetlands dynamics, and characterizing the transport of pollutants through watersheds and aquifers. PET estimates typically require direct measurements of net radiation or net radiation derived from measured incoming solar radiation. RET estimates often require direct measurements of incoming solar radiation. However, as the ground-based network of radiation instrumentation is extremely sparse or non-existent from 1991 to present, alternate methods to determine spatially distributed estimates of solar radiation must be used. This project leverages the measurements available from the GOES satellites. Instruments on the satellites are able to provide the hourly estimates of solar radiation that are critical to evapotranspiration calculations. Additionally, their spatial resolution (2 km) is significantly better than that available from the ground-based pyranometer networks.

The overall goal of this project is to provide gridded estimates of solar radiation, net radiation, potential evapotranspiration, reference evapotranspiration, and actual evapotranspiration at a 2 km grid scale and a daily time scale from 1995 to 2004 for the entire state of Florida. This report documents the methods used to achieve these goals in four sections and supporting appendices. Section 2 compares PET estimation methods and makes a final recommendation for the most appropriate model for Florida based on these comparisons. Section 3 presents the approach used to estimate solar insolation from GOES measurements and documents the calibration procedure. Section 4 compares methods to calculate net radiation and provides final recommendations for the most appropriate model for Florida based on these comparisons.

2. Comparison of Potential Evapotranspiration Methods

2.1. Validation sites

Groundwater and surface water models require precipitation and evapotranspiration surface forcings to determine the upper boundary condition. During the past few decades, many models have been developed to simulate water flow in the unsaturated zone, utilizing different techniques to couple the evapotranspiration process with water flow in unsaturated zone. Two approaches are typically used to determine the water lost to the atmosphere from the surface soil layers. One approach is to directly provide daily actual evapotranspiration (DAET). Another approach is to force the model using potential evapotranspiration (PET) and use soil moisture and canopy characteristics to determine the actual evapotranspiration.

Numerous methods exist to estimate PET using atmospheric parameters including wind speed, net radiation, temperature, and relative humidity. While some methods require only temperature data, these methods are not suitable for the humid and cloudy conditions typically found in the southeastern United States. In Florida, the determination of PET requires direct measurements of net radiation or net radiation derived from measured incoming solar radiation. However, as the ground-based network of radiation instrumentation is extremely sparse or non-existent from 1991 to present, alternate methods to determine spatially distributed estimates of solar radiation must be used. The GOES satellites are able to provide hourly estimates of solar radiation that are critical to evapotranspiration calculations with a spatial resolution that is significantly better than that available from the ground-based pyranometer networks.

This report documents the comparison of PET estimation methods and provides a recommendation for the most appropriate model for Florida based on these comparisons. PET results from three models are compared to observed DAET at 18 validation sites across Florida.

2.2. Methodology

2.2.1 Validation sites

18 validations sites having measured evapotranspiration and ancillary climate data were used for the PET intercomparison. The sites were distributed throughout the state and represent a variety of land cover types: open water (3 sites), marshland (4 sites), grassland/pasture (4 sites), citrus (2 sites) and forest (5 sites). Figure 2.1 shows the locations of these sites and Table 2.1 categorizes the sites by water management district (WMD) and general land cover class. Only one site was available in the Suwannee River WMD and no sites were available in Northwest Florida WMD. The remaining WMDs have three or more sites. Table 2.2 lists each site, the land cover, measurement period, climate data measured and average measured ET. Other site information (i.e., latitude/longitude, instrument heights) is included in Appendix 2.2.

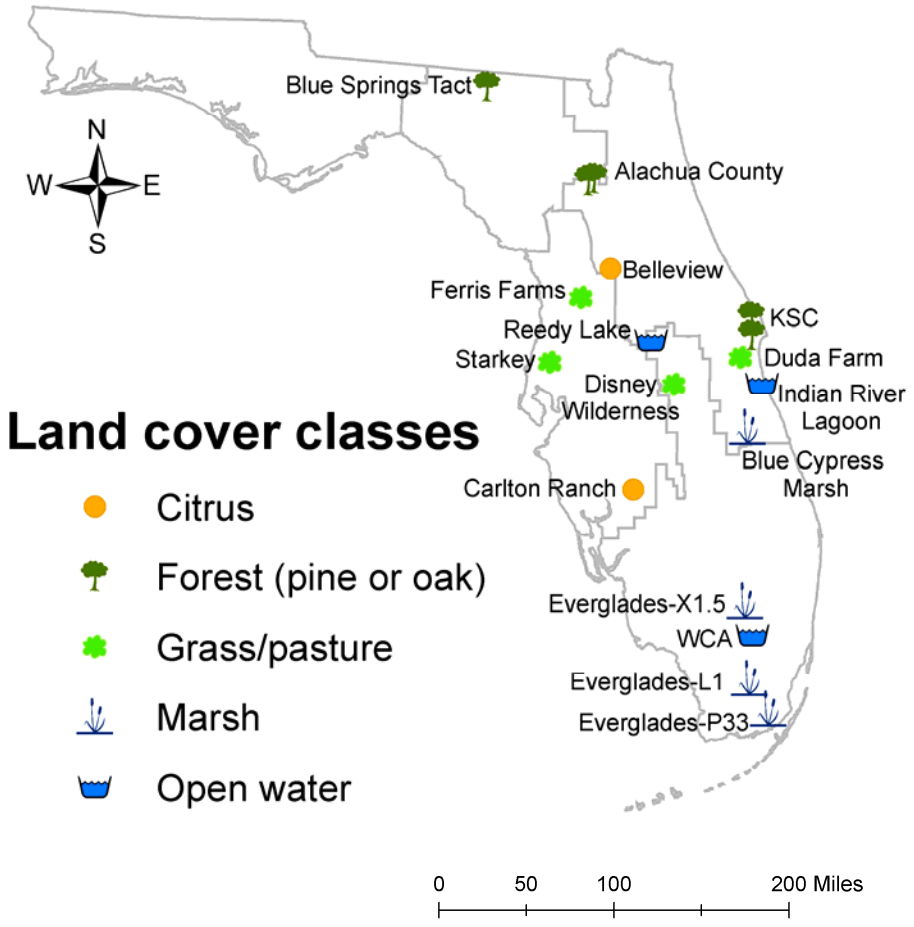

Figure 2.1. Location and generalized land cover type for the 18 validation sites used in this study.

Table 2.1. Validation sites by general land cover type and water management district.

District	Marsh	Grass/ Pasture	Citrus	Forest	Open Water
SRWMD	--	--	--	Blue Springs	--
SJRWMD	Blue Cypress	Duda Farm	Belleview	KSC (2) Alachua (2)	Indian River
SFWMD	Everglades (3)	Disney	--	--	WCA Reedy Lake
SWFWMD	--	Starkey Ferris Farms	Carlton ranch	--	--

Notes: -- denotes no sites available
SRWMD = Suwanee River Water Management District
SJRWMD = St. Johns River Water Management District
SFWMD = South Florida Water Management District
SWFWMD = Southwest Florida Water Management District

Table 2.2. Land cover, experimental period, and meteorological variables collected for each site used in this study.

Site	Land cover	Time Period	Wind speed	Solar radiation	Net radiation	Soil moisture	Air temp	Relative humidity	Latent Heat	Sensible heat
Alachua Cty (Donaldson)	slash pine (immature)	Jan 1999 - Jun 2003	average	average	average	--	min, max, average	min, max	measured	measured
Alachua Cty (Austin Cary)	slash pine (mature)	Jul 2000 - Jun 2002	average[1]	average	average	--	min, max, average	min, max	measured	measured
Belleview	citrus	Jul 2004 - Jul 2005	at 7.28m	average	average	0-6cm	min, max, average	min, max	measured	measured
Blue Cypress	marsh	Jan 2001 - Apr 2005	at 4m	average	average	avg	min, max, average	min, max	measured, gap-filled	measured
Blue Springs Tract	forest (pine)	Jan 2003 - Dec 2004	at 8.5m	average	average	avg	min, max, average	min, max	--	--
Carlton Ranch	citrus	May 2004 - May 2005	avg	average	average	4 cm	min, max, average	min, max	measured, gap-filled	measured
Disney Wilderness	grass	Jul 2000 - Jan 2006	at 3.6m	average	average	0-8 cm and 0-30 cm	min, max, average	min, max	measured, gap-filled	measured
Duda Farm	pasture	Jun 2000 - May 2005	at 2.7 m	average	average	0-30 cm	min, max, average	min, max	measured, gap-filled	measured
Everglades L1	marsh (25% cover)	Nov 2000 - Oct 2003	at 7m	average	average	--	min, max, average	min, max	measured, gap-filled	measured

Table 2.2 (cont'd) Land cover, experimental period, and meteorological variables collected for each site used in this study

Site	Land cover	Time Period	Wind speed	Solar radiation	Net radiation	Soil moisture	Air temp	Relative humidity	Latent Heat	Sensible heat
Everglades P33	marsh (95% cover)	Jan 1996 - Oct 2003	at 7.7m	average	average	--	min, max, average	min, max	measured, gap-filled	measured
Everglades X1.5	marsh (85% cover)	Jan 2002 - Oct 2003	at 9m	average	average	--	min, max, average	min, max	measured, gap-filled	measured
Ferris Farms	grass	Jan 2003 - Feb 2005	at 3m	average	average	0-30 cm	min, max, average	min, max	measured, gap-filled	measured
Indian River Lagoon	open water	Jan 2002 - Jan 2004	average	average	average	--	min, max, average	min, max	measured	measured
Kennedy Space Center	scrub oak	Mar 2000 - Mar 2003	average	average	average	average	min, max, average	min, max	measured	measured
Kennedy Space Center	slash pine	Mar 2002 - Feb 2003	average	average	average	average	min, max, average	min, max	measured	measured
Reedy Lake	open water	Dec 2001 - Oct 2005	average	average	average	--	min, max, average	min, max	measured	measured
Starkey	pasture	Apr 2003 - Dec 2004	average	average	average	20 cm	min, max, average	min, max	measured	measured
WCA	open water	Aug 2002 - Jul 2005	average	average	average	--	min, max, average	min, max	measured, gap-filled	measured

[1] No wind speed data available at Austin Cary site. Used wind speed data from Donaldson site (immature pine), approximately 3 miles away

2.2.2 Potential Evapotranspiration Models

Three PET models are compared in this study: the SFWMD Simple method (Abtew, 1996), the Priestley-Taylor (PT) method (Priestly and Taylor, 1972) and the Penman-Monteith (PM) method (Penman, 1948; Monteith, 1965). The Simple method is a proportional relationship between PET and incoming solar radiation and was developed to estimate PET from marshlands in Florida. The PT method relies on the air temperature and net radiation. The PM method requires measurements of air temperature, net radiation, wind speed, and relative humidity. Additionally, it requires two additional parameters, roughness height and canopy resistance, that are not readily quantified or generalized. A description of these models follows. Equations referenced below (in blue font) are from Shuttleworth (1993).

Model 1. SFWMD Simple Method

The SFWMD Simple Method provides estimates of PET with only measured solar radiation using the following equation

$$\lambda \rho_w ET_o = K_l * R_s \qquad (2.1)$$

where ET_o is the wet marsh potential evapotranspiration (mm d^{-1}), λ the latent heat of vaporization (MJ kg^{-1}), ρ_w the density of water (kg m^{-3}), K_l the coefficient (0.53 for mixed marsh, open water and shallow lakes), and R_s solar radiation received at the land surface (MJ m^{-2} d^{-1}). The method has been validated for cattails and wet marsh vegetation (Abtew, 1996). Using ρ_w = 1000 kg m^{-3} results in the cancellation of the conversion factor from m to mm in the final calculation (Shuttleworth, 1993). We computed a daily value of λ based on the daily average temperature (T_s is in ºC) using eqn 4.2.1.

$$\lambda = 2.501 - 0.002361 T_s \qquad (2.2)$$

Model 2. Priestley-Taylor Method

The Priestley-Taylor method uses the concept of the theoretical lower limit of evaporation from a wet surface as the "equilibrium" evaporation to estimate PET where

$$\lambda \rho_w ET_o = \alpha \frac{\Delta}{\Delta + \gamma}\left(R_n - G\right) \qquad (2.3)$$

where ET_o is the potential evapotranspiration (mm day^{-1}), λ the latent heat of vaporization (MJ kg^{-1}), ρ_w the density of water (kg m^{-3}), Δ the slope of the saturation vapor pressure temperature curve, γ the psychrometric constant, R_n the net radiation (W m^{-2}), and G the soil heat flux (W m^{-2}). Equilibrium conditions reflect evaporation from a wet surface under conditions of minimum advection that result in the actual vapor pressure of the air approaching the saturation vapor pressure. Priestly and Taylor (1972) showed that for conditions of minimum advection with no edge effects, α = 1.26. In this case, the aerodynamic term of the combination equation is effectively assigned a constant percent of the radiation term. In this project, the Priestley-Taylor form with α = 1.26 form was used. Here G is assumed to equal zero over the course of a day.

Again, using ρ_w = 1000 kg m^{-3} results in the cancellation of the conversion factor from m to mm in the final calculation.

The parameters Δ (in kPa ºC), λ (MJ kg^{-1}) and γ (in kPa ºC) were computed using eqns 4.2.3, 4.2.1 (see eqn 2 above) and 4.2.28. respectively:

$$\Delta = \frac{4098 e_s}{(237.3 + T)^2} \tag{2.4}$$

$$\gamma = \frac{c_p P}{\varepsilon \lambda} \times 10^{-3} = 0.0016286 \frac{P}{\lambda} \tag{2.5}$$

where e_s is the saturated vapor pressure (in kPa), c_p is the specific heat of moist air (=1.013 kJ kg^{-1} ºC^{-1}), P is atmospheric pressure (set equal to 101.3 kPa) and T is the minimum daily temperature (in ºC). Saturated vapor pressure was computed from eqn 4.2.2 as

$$e_s = 0.6108 \exp\left(\frac{17.27T}{237.3 + T} \right). \tag{2.6}$$

Model 3. Penman-Monteith

The Penman-Monteith model (Penman, 1948; Monteith, 1965) is an extension of the Penman equations that allows the equation to be applied to a range of surface vegetation through the introduction of plant specific resistance factors and is given as

$$\lambda \rho_w ET_o = \frac{\Delta (R_n - G) + \rho_a c_p D / r_a}{\Delta + \gamma (1 + r_s / r_a)} \tag{2.7}$$

where ET_o is the potential evapotranspiration (mm day^{-1}), λ the latent heat of vaporization (MJ kg^{-1}), ρ_w the density of water (kg m^{-3}), Δ the slope of the saturation vapor pressure temperature curve, γ the psychrometric constant, R_n the net radiation (W m^{-2}) and G the soil heat flux (W m^{-2}). D is the vapor pressure deficit of the air (in kPa). ρ_a is the mean air density at constant pressure, c_p the specific heat of air (1.013 kJ kg^{-1} ºC^{-1}), r_s the bulk surface resistance (s m^{-1}), and r_a the aerodynamic resistance (s m^{-1}).

The mean air density, ρ_a, was computed using 4.2.4

$$\rho_a = 3.486 \frac{P}{275 + T_s} \tag{2.8}$$

where P was set equal to constant 101.3 kPa and T_s was the average daily temperature (in ºC). The vapor pressure deficit, D, was computed as $e_s - e$, where e is the observed daily vapor pressure, which was estimated using measured daily average relative humidity ($e = RH/100 * e_s$ with RH in percent). Daily average RH was computed using an arithmetic average of the

maximum and minimum daily relative humidity measurements. The aerodynamic resistance was computed using Monin-Obukhov similarity and assuming neutral conditions (eqn 4.2.25)

$$r_a = \frac{\ln[(z_u - d)/z_{om}]\ln[(z_e - d)/z_{ov}]}{k^2 u} \quad (2.8)$$

where u is the wind speed (in m s^{-1}) and z_u is the height at which the wind speed was measured, z_e is the height of the vapor pressure/relative humidity instrument, d the displacement height (approximated as $0.67h_c$, where h_c is the average vegetation height), z_{om} the roughness height for momentum, z_{ov} is the roughness height for water vapor (approximated as $0.1z_{om}$) and k is the Von Karmen's constant (0.41). We used literature values for z_{om}, because using a relationship between z_{om} and canopy height is not appropriate for all land cover types. Height of wind measurement (z_u), height of vapor pressure/relative humidity measurement (z_e) and average canopy height (h_c) were obtained from the metadata for each site or from the personnel responsible for collecting the data. z_u and z_e were assumed to be equal unless otherwise noted.

A range of bulk canopy resistance (r_s) estimates for wetlands and for pine forest sites were available from published studies in Florida (Abtew, 1996; Abtew et al., 1995; Jacobs et al., 2002; Powell et al., 2005). We also relied on the ranges of canopy resistance in Breuer et al. (2003), who compiled an extensive list of vegetation parameters such as canopy resistance, canopy height, albedo, etc. from numerous published studies. For grass/pasture sites, we computed r_s using the relationships developed by Sumner and Jacobs (2004):

$$g_s = f(D)g_{\max}(R_n) \quad (2.9)$$

$$f(D) = -0.166\ln(D) + 0.235 \quad (2.10)$$

$$g_{\max} = 5.39\times10^{-5}R_n + 0.0033 \quad (2.11)$$

where g_s is bulk surface conductance (in m s^{-1}), D is vapor pressure deficit (in kPa) and g_{max} is the maximum bulk surface conductance. Bulk surface resistance for grass (r_s, in s m^{-1}) is the reciprocal of g_s. Average bulk surface resistance for the grass/pasture validation sites, calculated for each site, ranged from 284 to 319 s m^{-1} (see Table 2.3) which is consistent with published values. The published value of r_s for marsh/wetland vegetation is 55 s m^{-1} and r_s for open water is zero. For marsh/wetland sites (ie., Blue Cypress, Everglades) r_s was computed as a weighted average based on the proportion of vegetated area and open water area. The parameters used in this analysis are presented in Table 2.3. Also included in Table 2.3, for comparison purposes, are "at-site" r_s values made available for the Alachua County and Kennedy Space Center forested sites.

The Penman-Monteith method (eqn 2.7) is made up of two terms: a radiation term which is determined by the available energy and an advection term which is determined by the vapor pressure deficit and atmospheric resistance. For open water, the surface roughness and wind profiles are different than for a vegetated surface. Shuttleworth (1993) presents an alternative formulation for estimating the advection term for open water (4.2.30):

$$\text{Open water advection term} = \frac{\gamma}{\Delta+\gamma}\frac{6.43(1+0.536u)D}{\lambda} \quad (2.12)$$

which incorporates the r_a formulation for open water (4.2.29)

$$r_a^p = \frac{4.72\left[\ln\left(z_m / z_o\right)\right]^2}{1 + 0.536u} \tag{2.13}$$

where z_m is a standardized measurement height of 2 m and z_o = 0.00137 m.

The Penman-Monteith equation with units as presented in eqn 4.2.27 is not dimensionally homogeneous (see Appendix 2.1 for units analysis). A conversion coefficient of 86.4 was applied to the advection term to make the equation dimensionally consistent.

Table 2.3. Penman-Monteith parameters used for each site.

Site	Land cover		Bulk canopy resistance (s m^{-1})	Humidity height (m)	Wind height (m)	Canopy height (m)
Alachua (Donaldson)[1]	forest (immature pine)[2]		500	15	15	10
		at-site	274	--	--	--
Alachua (Austin Cary)[1]	forest (mature pine)		500	32	32	22
		at-site	245	--	--	--
Belleview	citrus		500	6.65	7.28	5.5
Blue Cypress	marsh		55	2	3	2.1
Blue Springs Tract[3]	forest (pine)		500	8.5	8.5	6
Carlton Ranch[1]	citrus		500	6.4	6.4	5
Disney Wilderness	grass		288	1.2	3.6	0.4
Duda Farm	grass		284	1.1	2.7	0.1
Everglades L1[4]	marsh (25% cover)		14	2.13	2.13	0.8
Everglades P33[4]	marsh (95% cover)		52	2.35	2.35	1.7
Everglades X1.5[4]	marsh (85% cover)		47	2.74	2.74	1.5
Ferris Farm[5]	grass		319	1.9	3.3	0.1
Indian River[6]	open water		0	4.6	4.6	--
Kennedy Space Center[7]	forest (oak)		322	3.5	3.5	1.5
		at-site	157	--	--	--
Kennedy Space Center[7]	forest (pine)		500	18	18	13
		at-site	105	--	--	
Reedy Lake[1]	open water		0	1.9	1.9	--
Starkey[8]	pasture		299	1.4	2.2	0.35
WCA	open water		0	3.2	3.7	0

Notes:

[1]Used wind speed measurement height for Zu and Ze.

[2]Canopy height varied from 9.1 to 11 m due to growth of immature pine stand.

[3]Parameters based on communication from Trey Grubbs.

[4]Parameters based on communication from Ed German.

[5]Average height of grass 8-12 cm, per Sumner & Jacobs, 2005.

[6]Anemometer height above water varied. Used average height for Zu and Ze.

[7]Parameters based on communication from Tom Powell.

[8]Max height is 0.5 m, mowed to 0.2 m twice a year. Used average height.

2.3. Results

2.3.1 Observed Evapotranspiration

Observations were made at 30-minute increments. Daily values were calculated by averaging the 30-minute data over a 24-hour period. When eddy flux measurements were not available for a particular 30-minute increment, ET was estimated using the USGS approach of gap filling using Priestley-Taylor method (see eqn. 2.3). Only those days having measurements for 80% or more of the half-hour increments were used for this study. Most missing values occurred during nighttime or rainfall when ET values would be low (David Sumner, personal communication). These were considered "good" observations. Table 2.4 summarizes the number of days for which ET was measured and those considered to be good. It was necessary to relax this criterion for some of the sites (i.e., the Everglades and Disney Wilderness sites) where ideal measuring conditions were difficult to maintain. For instance, at the Disney Wilderness site, more than 30% of the half-hour measurements were gap-filled due to wind direction with inadequate fetch, excessive misalignment of sonic anemometer, or obscured hygrometer windows. The remote location of the Everglades sites made instrument maintenance difficult (Ed German, personal communication). PET model comparisons were performed using the "good" observations for each site.

Table 2.4. Number of days of daily actual ET observations, the number "good" observations and the number of days in which the Bowen ratio (β) was less than or equal to 1.

		Number of Observations		
Site	Land Cover	Daily	Good	$\beta \leq 1$
Alachua (Austin Cary)	forest (mature pine)	723	606	320
Alachua (Donaldson)	forest (immature pine)	2373	1110	931
Belleview	citrus	365	365	294
Blue Cypress	marsh	2071	1001	982
Blue Springs Tract[1]	forest (pine)	731	676	0
Carlton Ranch	citrus	380	211	171
Disney Wilderness	grass	2004	559	371
Duda Farm	grass	1684	967	826
Everglades L1	marsh (25% cover)	1058	621	613
Everglades P33	marsh (95% cover)	2800	1007	996
Everglades X1.5	marsh (85% cover)	555	167	157
Ferris Farm	grass	790	202	81
Indian River	open water	746	680	674
Kennedy Space Center	forest (oak)	1474	1189	765
Kennedy Space Center	forest (pine)	358	302	272
Reedy Lake	open water	1416	1264	1264
Starkey	pasture	630	310	188
WCA	open water	1089	341	341

[1]None of the data at this site had $\beta \leq 1$. All "good" data were analyzed.

Table 2.5 summarizes the observed DAET statistics by general land cover type and for all 18 sites together. Open water sites had the highest observed DAET (4.35 mm day^{-1}), while grass sites had the lowest DAET (2.43 mm day^{-1}). The coefficient of variability (CV = standard deviation divided by mean) was lowest for the marsh and open water sites. This result indicates that consistent values can be expected for these well watered sites. The CV values were considerably higher for the other land covers with the highest relative variation found for the grass and forested sites. This may be due to variations in vegetation type (scrub oak versus slash pine, open grassland versus mowed pasture), maturity level (immature versus mature stand) and environmental conditions among the sites.

Table 2.5. Median, mean, standard deviation and coefficient of variability (CV) of observed annual average DAET (in mm d^{-1}) by general land cover type.

Land cover	Station count	Mean	Median	Standard deviation	Coefficient of variability (CV)
Citrus	2	3.25	3.25	0.32	0.10
Forest	5	2.59	2.36	0.52	0.20
Grass/pasture	4	2.43	2.55	0.62	0.26
Marsh	4	3.91	3.89	0.06	0.01
Open water	3	4.35	4.42	0.15	0.03
All sites	18	3.21	3.14	0.86	0.27

2.3.2 Characterization of Stress Conditions

Ideally the comparison of results should only use potential evapotranspiration measured values (Stage 1 ET) and eliminate water stressed conditions (Stage 2). The soil moisture content required to transition to water limited conditions is not clearly defined. Previous research shows that potential conditions exist at soil moisture values as dry as 9% (Jacobs et al., 2002) and 3% (MacQuarrie and Nkemdirim, 1991). However, the transition will depend on soils, vegetation, and depth of soil moisture measurement. Under increasingly stressed conditions, the partitioning of available energy between sensible heat (H) and latent heat (LE) will increasingly favor H. The Bowen ratio (β = H/LE) is a measure of this partitioning that is independent of the magnitude of the available energy. Jacobs et al. (2002) reported that the average value of β for a marsh was 0.4. This value is expected to vary among sites.

The Bowen ratio was reviewed as a possible means to discriminate between potential and stressed conditions. Figure 2.2 shows the relationship between β and the time of year (as represented by Julian day) for different land cover types. Here, threshold values for β of 1 and 0.4 (from Jacobs et al., 2002) are drawn to facilitate interpretation. β was found to be consistently less than 1 for the growing season from day 160 to 290 (mid-June to mid-October)

for the sites shown. However, during the remainder of the year, β was highly variable and frequently greater than 1 and infrequently less than 0.4. Additionally, differences among sites are apparent. To test the performance of the PET models under conditions which were as close to PET (Stage 1) as possible, PET model comparisons were repeated on data from day in which β was less than or equal to 1. The number of data points that met these conditions for each site is presented in the last column of Table 2.4.

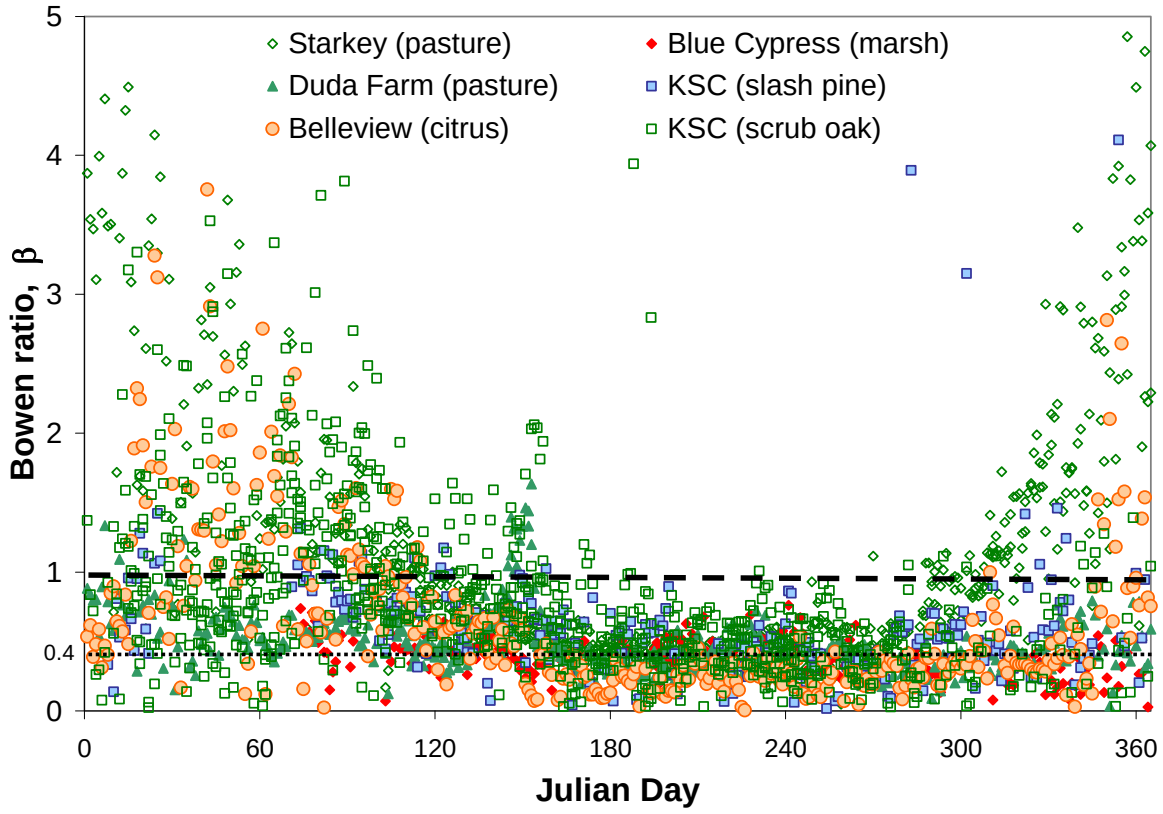

Figure 2.2. Bowen ratio (H/LE) versus julian day for varying land cover types.

2.3.3 PET Methods Comparison Results

2.3.3.1 Mean Annual Results

PET values were calculated for each "good" day and for each day in which β was less than or equal to 1. Calculated values were compared to the observed values using standard statistics methods and regression analysis. Tables 2.6 lists the observed daily average evapotranspiration (DAET) estimates as well as DAET computed by the three models for all "good" days and for days when $\beta \leq 1$. In general, both modeled and observed ET values were lowest for the "dry" sites (grass, pasture, forest, citrus) and highest for the "wet" sites (marsh and open water sites). A noteworthy anomaly is that the literature values for the Penman-Monteith method underestimates the observed ET at treed sites. For these sites, the use of at-site values of canopy resistance greatly improved the Penman-Monteith (PM) mean modeled ET values. This suggests

that existing canopy resistance parameters for trees are not reliable for all forest communities in Florida. Additionally, the PM model shows much better agreement for "wet" sites as compared to "dry" sites.

Figures 2.3, 2.4 and 2.5 graphically illustrate the annual average performance of the Simple, PT and PM models, respectively, for all "good" days (a) and for days when $\beta \leq 1$ (b). Colors were used to categorize by general land cover type. A comparison of Figures 3a and b shows an improvement in the performance of the Simple model when applied only to days when ET is close to PET. Figures 4a and b and 5a and b indicate little improvement in the PT and PM methods when applied to the same conditions. Purple circles represent open water sites, which showed the best match between P-M and observed ET. For the forested sites, at-site canopy resistances were also applied. In Figure 5a and b, blue filled diamonds represent P-M estimates using regional canopy resistance values for forest sites and blue open diamonds represent P-M estimates using at-site canopy resistance values. These figures show that the at-site canopy resistance clearly improves PM model performance. The at-site canopy resistances are considerably lower than the literature values. A sensitivity analysis performed on surface resistance parameter for the forest sites showed that the predicted values change significantly with the change in surface resistance parameter, r_s (see Appendix 2.5). It also suggests that the PM model is highly sensitive to the selection of canopy resistance parameter.

Table 2.7a lists the summary statistics, mean absolute error (MAE) and root mean square error (RMSE) and linear regression coefficients (slope, intercept and correlation coefficient) for each model and site for all "good" days. Table 2.7b lists the same except for days when $\beta \leq 1$. MAE and RMSE were computed as

$$MAE = \frac{1}{n}\sum_{i=1}^{n}\left|ET_{\mathrm{mod},i} - ET_{obs,i}\right| \tag{2.14}$$

$$RMSE = \sqrt{\frac{1}{n}\sum_{i=1}^{n}\left(ET_{\mathrm{mod},i} - ET_{obs,i}\right)^2} \tag{2.15}$$

where $ET_{mod,i}$ and $ET_{obs,i}$ are the modeled and observed ET values, respectively, for each day *i*. MAE and RMSE are aggregate indicators of model performance while the regression statistics are indicators of how well the models predict ET on a daily basis. The overall (all sites) MAE and RMSE statistics presented in Table 2.7b show that for conditions near PET, the Simple method has the smallest error. For the other two models, the difference between the two datasets was not as pronounced. Figure 2.6 compares the RMSE values by site and model, grouped by land cover type. Overall, the highest RMSE values are for the forested sites, followed closely by the citrus sites. The RMSE values are comparable for the grass/pasture, marsh and open water sites. The Priestley-Taylor method has fairly consistently low RMSE values. The Simple method performs best for the wet conditions.

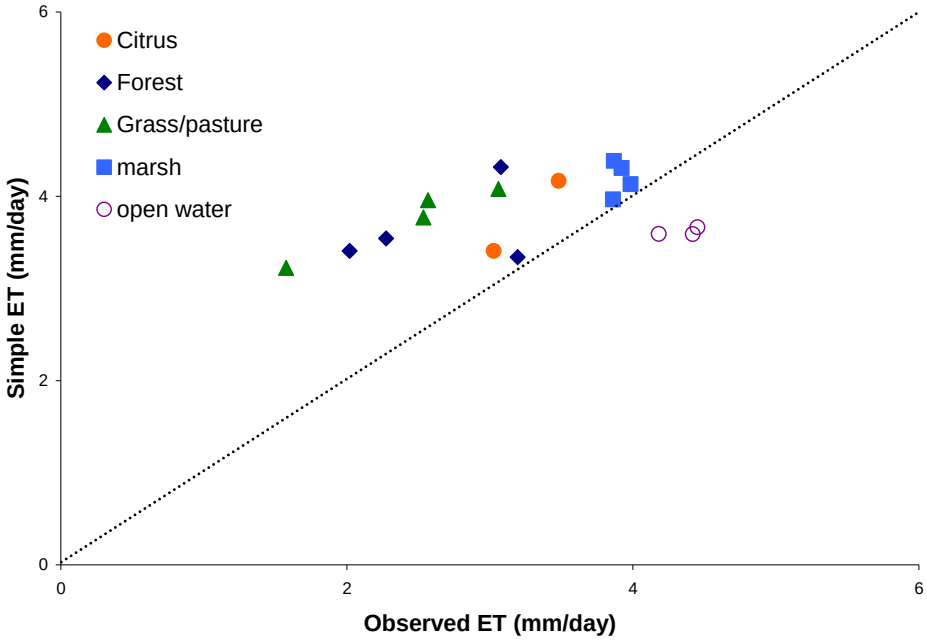

Figure 2.3a: Comparison of annual average daily Simple ET estimates with observations for all "good" days. Different land cover classes are distinguished by color.

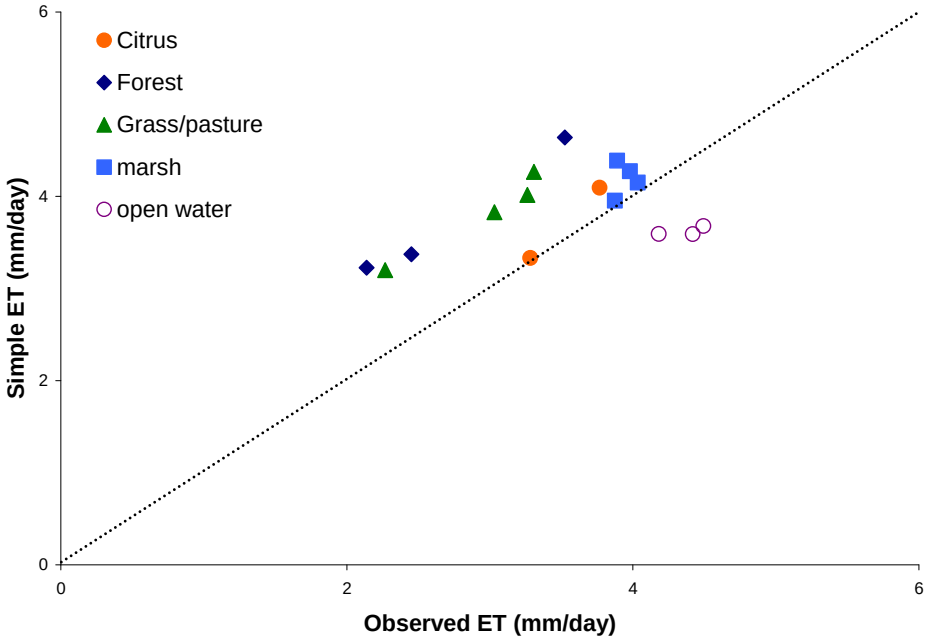

Figure 2.3b: Comparison of annual average daily Simple ET estimates with observations for days when $\beta \leq 1$. Different land cover classes are distinguished by color.

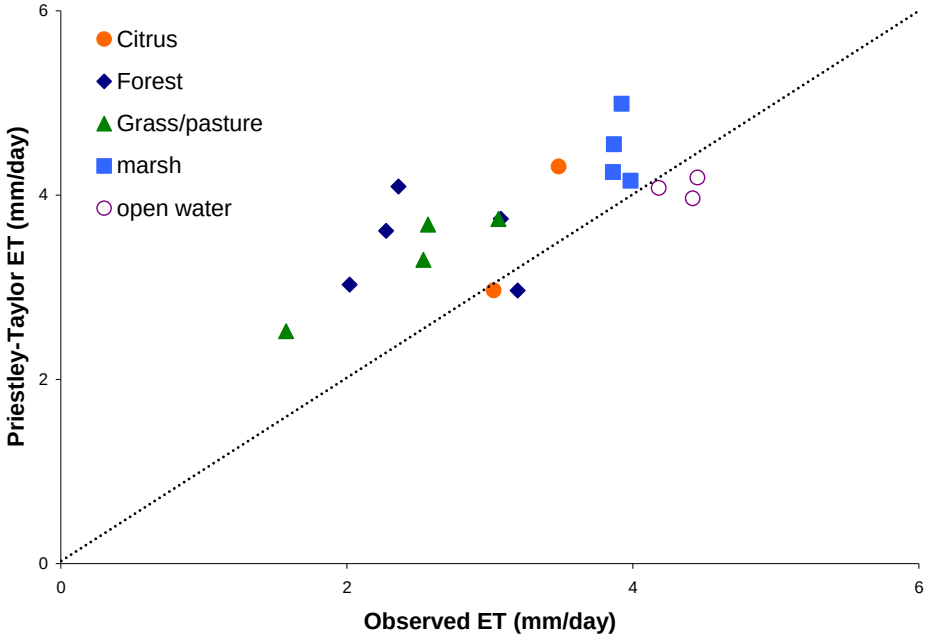

Figure 2.4a: Comparison of annual average daily Priestley-Taylor ET estimates with observations for all "good" days. Different land cover classes are distinguished by color.

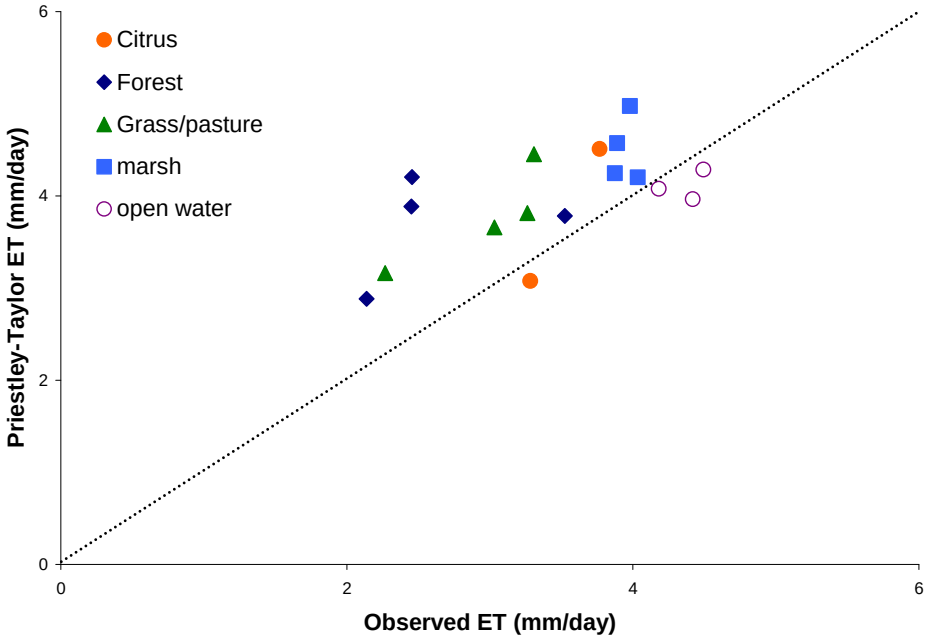

Figure 2.4b: Comparison of annual average daily Priestley-Taylor ET estimates with observations for days when $\beta \leq 1$. Different land cover classes are distinguished by color.

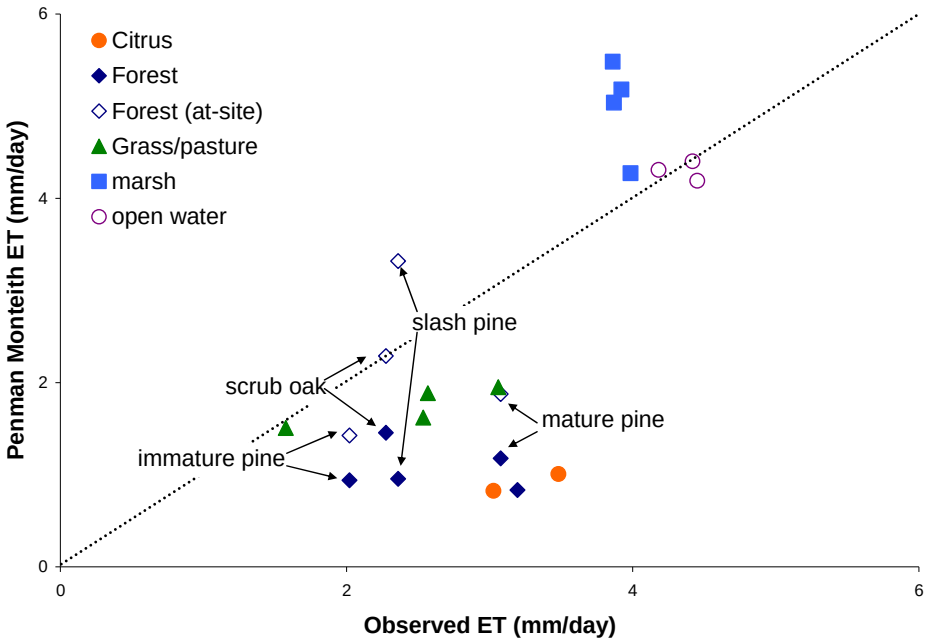

Figure 2.5a: Comparison of annual average daily Penman-Monteith estimates with observations for all "good" days. Different land cover classes are distinguished by color.

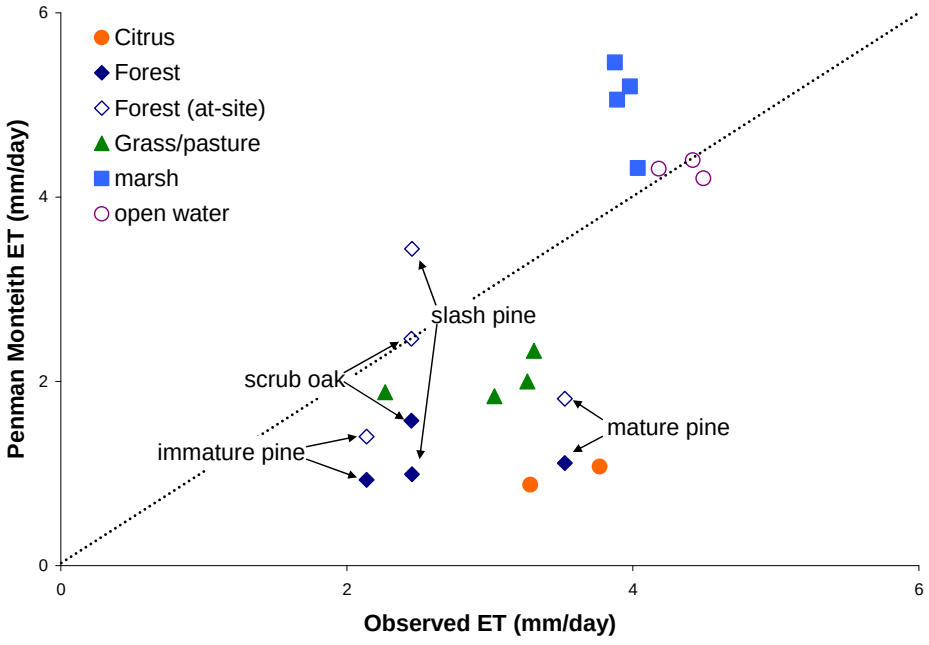

Figure 2.5b: Comparison of annual average daily Penman-Monteith ET estimates with observations for days when $\beta \leq 1$. Different land cover classes are distinguished by color.

Table 2.6: Mean daily modeled and observed evapotranspiration (ET) in mm/day for all "good" days where N is the number of daily observations, Obs are the observed value, Sp are the Simple method estimates, PT are the Priestley-Taylor method estimates, and PM are the Penman-Monteith method estimates.

	Daily average evapotranspiration (mm d^{-1})									
	all "good" days					*days when $\beta \leq 1$*				
Site	N	obs	Sp	PT	PM	N	obs	Sp	PT	PM
Alachua (immature)	1110	2.02	3.41	3.03	0.94	931	2.14	3.23	2.88	0.93
Alachua (mature)	606	3.08	4.32	3.74	1.18	320	3.52	4.64	3.78	1.11
Belleview	365	3.03	3.41	2.97	0.83	294	3.28	3.33	3.08	0.88
Blue Cypress	1001	3.98	4.13	4.16	4.27	982	4.03	4.15	4.20	4.32
Blue Springs Tract	676	3.20	3.34	2.96	0.84	0	--	--	--	--
Carlton Ranch	211	3.48	4.17	4.31	1.01	171	3.77	4.09	4.51	1.08
Disney Wilderness	559	2.53	3.77	3.30	1.62	371	3.03	3.83	3.66	1.84
Duda Farm	967	3.06	4.08	3.74	1.95	826	3.26	4.02	3.82	2.00
Everglades L1	621	3.86	3.97	4.25	5.48	613	3.87	3.95	4.25	5.46
Everglades P33	1007	3.87	4.38	4.55	5.04	996	3.89	4.39	4.57	5.06
Everglades X1.5	167	3.92	4.31	4.99	5.18	157	3.98	4.27	4.98	5.20
Ferris Farm	202	1.58	3.22	2.52	1.51	81	2.27	3.20	3.16	1.88
Indian River	680	4.45	3.67	4.19	4.19	674	4.49	3.68	4.29	4.20
KSC (scrub oak)	1189	2.27	3.54	3.61	1.46	765	2.45	3.37	3.88	1.57
KSC (slash pine)	302	2.36	--	4.09	0.96	272	2.46	--	4.20	0.99
Reedy Lake	1264	4.18	3.59	4.08	4.31	1264	4.18	3.59	4.08	4.31
Starkey	310	2.57	3.96	3.68	1.89	188	3.31	4.27	4.45	2.33
WCA	341	4.42	3.59	3.96	4.40	341	4.42	3.59	3.96	4.40
All Sites										
Median	11578	3.14	3.77	3.85	1.75	9246	3.52	3.89	4.08	2.00
Mean	11578	3.21	3.81	3.79	2.61	9246	3.43	3.85	3.99	2.80

Notes: N = number of daily observations
obs = observed daily average evapotranspiration (DAET)
Sp = DAET estimated by the Simple method
PT = DAET estimated by the Priestley-Taylor method
PM = DAET estimated by the Penman-Monteith method
-- denotes no DAET estimates

Table 2.7a: Errors and regression comparison by site (Sp=Simple, PT=Priestley-Taylor, PM=Penman-Monteith) for "good" days.

	Mean Absolute Error			*Root Mean Square Error*			*Regression Intercept*			*Regression Slope*			*Correlation coefficient, R*		
Site	Sp	PT	PM	Sp	PT	PM	Sp	PT	PM	Sp	PT	PM	Sp	PT	PM
Alachua (mature pine)	1.34	1.59	3.21	1.74	2.07	3.65	2.36	1.99	0.66	0.42	0.40	0.12	0.67	0.46	0.36
Alachua (immature pine)	1.50	1.29	1.12	1.85	1.72	1.40	2.23	1.17	0.34	0.59	0.92	0.30	0.49	0.59	0.59
Belleview	0.75	0.47	2.20	0.99	0.59	2.50	1.41	-0.06	0.09	0.66	1.00	0.24	0.80	0.93	0.81
Blue Cypress	0.53	0.51	0.77	0.69	0.67	0.93	1.36	0.17	1.88	0.71	1.02	0.61	0.88	0.91	0.79
Blue Springs Tract	0.46	0.39	2.72	0.60	0.50	2.96	0.80	-0.25	-0.04	0.80	1.01	0.25	0.94	0.96	0.88
Carlton Ranch	0.98	0.91	2.47	1.26	1.06	2.68	2.17	0.32	0.16	0.57	1.15	0.24	0.67	0.93	0.90
Disney Wilderness	1.25	0.79	0.94	1.52	1.00	1.11	1.92	0.46	0.26	0.73	1.12	0.54	0.72	0.90	0.90
Duda Farm	1.06	0.75	1.14	1.39	0.99	1.30	1.89	0.30	0.21	0.72	1.12	0.57	0.71	0.89	0.87
Everglades L1	0.60	0.77	1.65	0.80	0.98	1.92	1.24	-0.12	0.17	0.71	1.13	1.38	0.76	0.83	0.87
Everglades P33	0.80	0.97	1.24	1.01	1.17	1.47	1.53	0.43	1.11	0.74	1.07	1.02	0.75	0.81	0.81
Everglades X1.5	0.66	1.27	1.29	0.87	1.45	1.48	1.63	0.35	0.30	0.68	1.18	1.24	0.64	0.74	0.83
Ferris Farm	1.65	0.97	0.34	1.86	1.12	0.42	2.00	0.47	0.31	0.78	1.30	0.75	0.68	0.93	0.92
Indian River	1.36	1.48	1.28	1.77	1.92	1.68	2.24	2.26	2.24	0.32	0.45	0.45	0.52	0.45	0.53
KSC (scrub oak)	1.71	1.57	1.16	2.03	1.94	1.58	2.47	1.81	0.84	0.54	0.80	0.25	0.56	0.61	0.59
KSC (slash pine)	--	1.94	1.49	--	2.48	1.82	--	2.45	0.58	--	0.72	0.16	0.00	0.52	0.49
Reedy Lake	0.93	0.75	0.70	1.13	0.98	0.90	1.11	0.06	0.64	0.59	0.96	0.88	0.84	0.86	0.87
Starkey	1.40	1.12	0.74	1.61	1.22	0.87	2.00	0.64	0.34	0.76	1.18	0.60	0.77	0.95	0.95
WCA	0.88	0.63	0.53	1.03	0.85	0.67	0.41	0.07	0.80	0.72	0.88	0.81	0.94	0.89	0.91

Table 2.7a: Errors (mm/day) and regression comparison by site (Sp=Simple, PT=Priestley-Taylor, PM=Penman-Monteith) for "good" days.

	Mean Absolute Error			*Root Mean Square Error*			*Regression Intercept*			*Regression Slope*			*Correlation coefficient, R*		
Site	Sp	PT	PM	Sp	PT	PM	Sp	PT	PM	Sp	PT	PM	Sp	PT	PM
All Sites															
Median	0.98	***0.94***	1.20	1.26	***1.09***	1.48	1.89	0.39	***0.34***	0.71	***1.01***	0.55	0.71	***0.88***	0.85
Mean	1.05	***1.01***	1.39	1.30	***1.26***	1.63	1.69	0.70	***0.61***	0.65	***0.97***	0.58	0.69	***0.79***	0.77

Notes: N = number of daily observations
obs = observed daily average evapotranspiration (DAET)
Sp = DAET estimated by the Simple method
PT = DAET estimated by the Priestley-Taylor method
PM = DAET estimated by the Penman-Monteith method
-- denotes no DAET estimates

Table 2.7b: Errors (mm/day) and regression comparison by site (Sp=Simple, PT=Priestley-Taylor, PM=Penman-Monteith) for days with $\beta \leq 1$.

	Mean Absolute Error			*Root Mean Square Error*			*Regression Intercept*			*Regression Slope*			*Correlation coefficient, R*		
Site	Sp	PT	PM	Sp	PT	PM	Sp	PT	PM	Sp	PT	PM	Sp	PT	PM
Alachua (mature pine)	1.46	1.90	3.88	1.82	2.39	4.25	2.35	1.70	0.53	0.42	0.42	0.12	0.69	0.46	0.38
Alachua (immature pine)	1.21	1.06	1.22	1.47	1.44	1.48	1.70	0.63	0.22	0.71	1.05	0.33	0.64	0.69	0.63
Belleview	0.51	0.44	2.40	0.64	0.55	2.67	0.81	-0.45	0.05	0.77	1.08	0.25	0.91	0.96	0.80
Blue Cypress	0.50	0.51	0.77	0.64	0.67	0.93	1.23	0.13	1.93	0.73	1.02	0.60	0.89	0.91	0.78
Blue Springs Tract	--	--	--	--	--	--	--	--	--	--	--	--	--	--	--
Carlton Ranch	0.69	0.84	2.69	0.84	0.98	2.88	1.28	-0.14	0.15	0.75	1.24	0.25	0.82	0.95	0.90
Disney Wilderness	0.82	0.67	1.19	0.99	0.82	1.31	0.89	-0.18	0.08	0.97	1.27	0.58	0.87	0.95	0.90
Duda Farm	0.80	0.64	1.26	1.02	0.79	1.38	1.13	-0.20	-0.01	0.88	1.23	0.62	0.85	0.95	0.91
Everglades L1	0.59	0.76	1.62	0.77	0.97	1.87	1.17	-0.19	0.02	0.72	1.14	1.41	0.78	0.84	0.89
Everglades P33	0.78	0.97	1.24	0.98	1.17	1.47	1.45	0.42	1.10	0.75	1.07	1.02	0.76	0.81	0.81
Everglades X1.5	0.59	1.21	1.25	0.77	1.38	1.45	1.22	-0.13	0.00	0.77	1.28	1.31	0.71	0.78	0.85
Ferris Farm	0.94	0.95	0.41	1.13	1.10	0.51	0.41	-0.07	-0.01	1.23	1.42	0.83	0.91	0.95	0.95
Indian River	1.35	1.46	1.26	1.77	1.91	1.65	2.25	2.22	2.18	0.32	0.46	0.46	0.50	0.45	0.53
KSC (scrub oak)	1.45	1.61	1.31	1.75	1.95	1.77	2.10	1.89	0.91	0.59	0.81	0.25	0.65	0.66	0.64
KSC (slash pine)	--	1.96	1.53	--	2.50	1.87	--	2.51	0.61	--	0.71	0.16	--	0.51	0.48
Reedy Lake	0.93	0.75	0.70	1.13	0.98	0.90	1.11	0.06	0.64	0.59	0.96	0.88	0.84	0.86	0.87
Starkey	0.96	1.16	0.98	1.15	1.26	1.05	0.41	-0.13	0.17	1.17	1.38	0.65	0.85	0.95	0.93
WCA	0.88	0.63	0.53	1.03	0.85	0.67	0.41	0.07	0.80	0.72	0.88	0.81	0.94	0.89	0.91

Table 2.7b: Errors (mm/day) and regression comparison by site (Sp=Simple, PT=Priestley-Taylor, PM=Penman-Monteith) for days with $\beta \leq 1$.

	Mean Absolute Error			*Root Mean Square Error*			*Regression Intercept*			*Regression Slope*			*Correlation coefficient, R*		
Site	Sp	PT	PM	Sp	PT	PM	Sp	PT	PM	Sp	PT	PM	Sp	PT	PM
All Sites															
Median	***0.85***	0.95	1.25	***1.02***	1.10	1.47	1.19	***0.06***	0.22	0.74	***1.07***	0.60	0.83	***0.86***	0.85
Mean	***0.90***	1.03	1.43	***1.12***	1.28	1.65	1.24	***0.48***	0.55	0.76	***1.03***	0.62	0.79	***0.80***	0.77

Notes: N = number of daily observations
obs = observed daily average evapotranspiration (DAET)
Sp = DAET estimated by the Simple method
PT = DAET estimated by the Priestley-Taylor method
PM = DAET estimated by the Penman-Monteith method
-- denotes no DAET estimates

Figure 2.6: Comparison of RMSE across models and sites. Color signifies general land cover type: orange = citrus, dark blue = forest, green = grass/pasture, light blue = marsh and open symbol = open water. Shape indicates methods: circle = simple method, triangle = Penman-Monteith method, and square = Priestley-Taylor method.

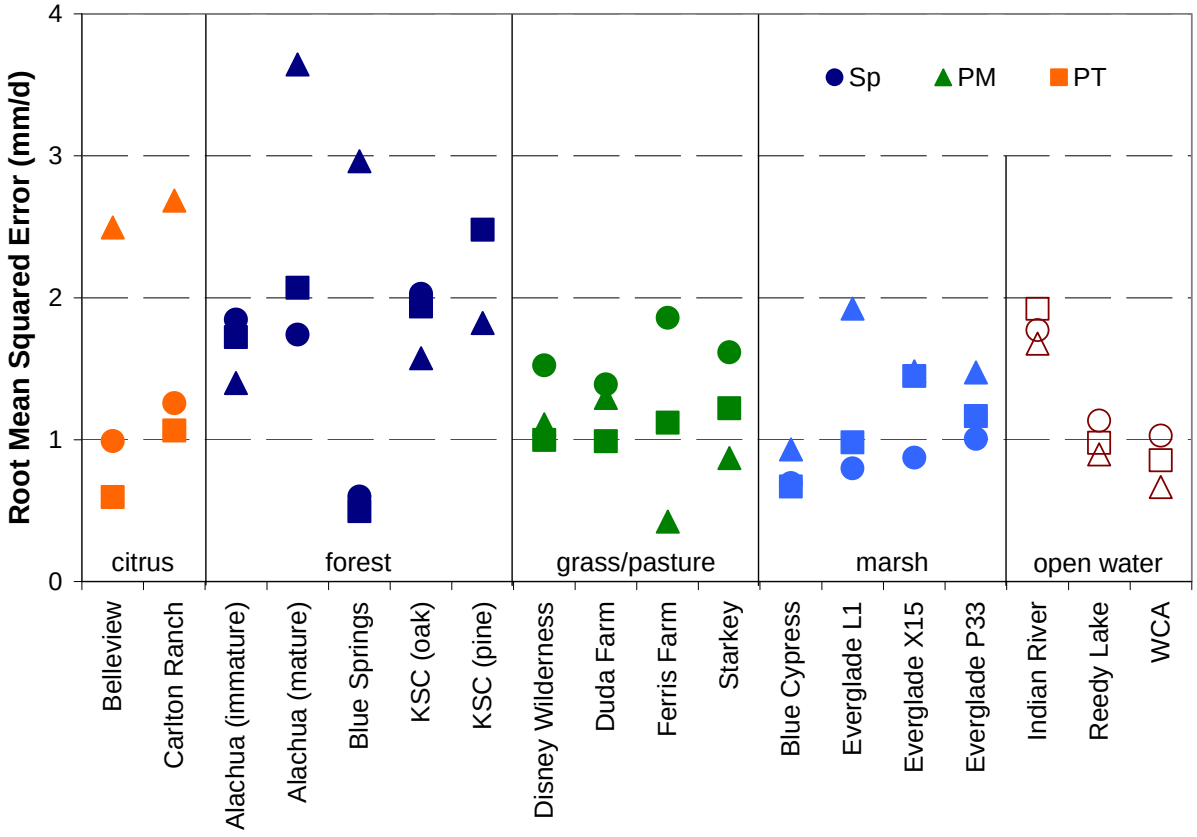

2.3.3.2 Average Daily Results

While RMSE, MAE and averages provide an indicator of a model's ability to perform on an annual basis, other metrics are more suited to identify seasonal trends. To examine the daily variations, regression analyses were conducted on the daily values by site. In addition, daily model residuals were examined as a function of daily ET and day of year.

Ideally, the regression results would have intercepts close to zero, slopes close to one, and correlation coefficients close to one. Tables 2.7a and 2.7b show relatively strong correlations between measured and modeled values for all three models. However, the Simple method typically has very high intercepts and relatively low slopes. The Penman-Monteith method has much better agreement, but with considerable variability. The Priestley-Taylor method, with the exception of the forested sites provides the best regression relationships. The overall (all sites) statistics in both tables show that the Priestley-Taylor method has slopes essentially equal to one.

Differences (residuals) between modeled and measured values PET were examined based on the day of year and the measured PET magnitude. Figures 2.7 through 2.11 show model residuals (Simple (ETsp), Priestley-Taylor (ETpr) and Penman-Monteith (ETpm)) for one site selected from each land cover type. The "wet" sites (open water and marsh) show that errors are not strongly related to time of year or ET magnitude. There is a slight tendency to underestimate the highest values and overestimate the lowest values. The residuals also indicate that the models are relatively unbiased. For the three "dry" sites (grass/pasture, forest and citrus), the Simple and PT methods tend to overestimate ET while the PM method tends to underestimate ET. A distinct seasonality can be seen in the residuals at the "dry" sites, which is less pronounced at the "wet" sites. The seasonality is particularly pronounced for the PM residuals with bias increasing with increasing ET. The slopes of the residuals versus the daily observed evapotranspiration plots given in Appendix 2.3 indicate that this behavior is consistent for most sites. While many of the sites and methods have significant trends as a function of PET magnitude, the trends are particularly strong for the PM residuals. This behavior can be explained by considering that the bulk surface resistance (r_s) is a seasonally dynamic property. However, due to limited knowledge, only a single, constant value is used in this analysis. Seasonally-varying r_s values would likely reduce this problem and improve performance. Residual plots for all sites are included in Appendix 2.2 and 2.3.

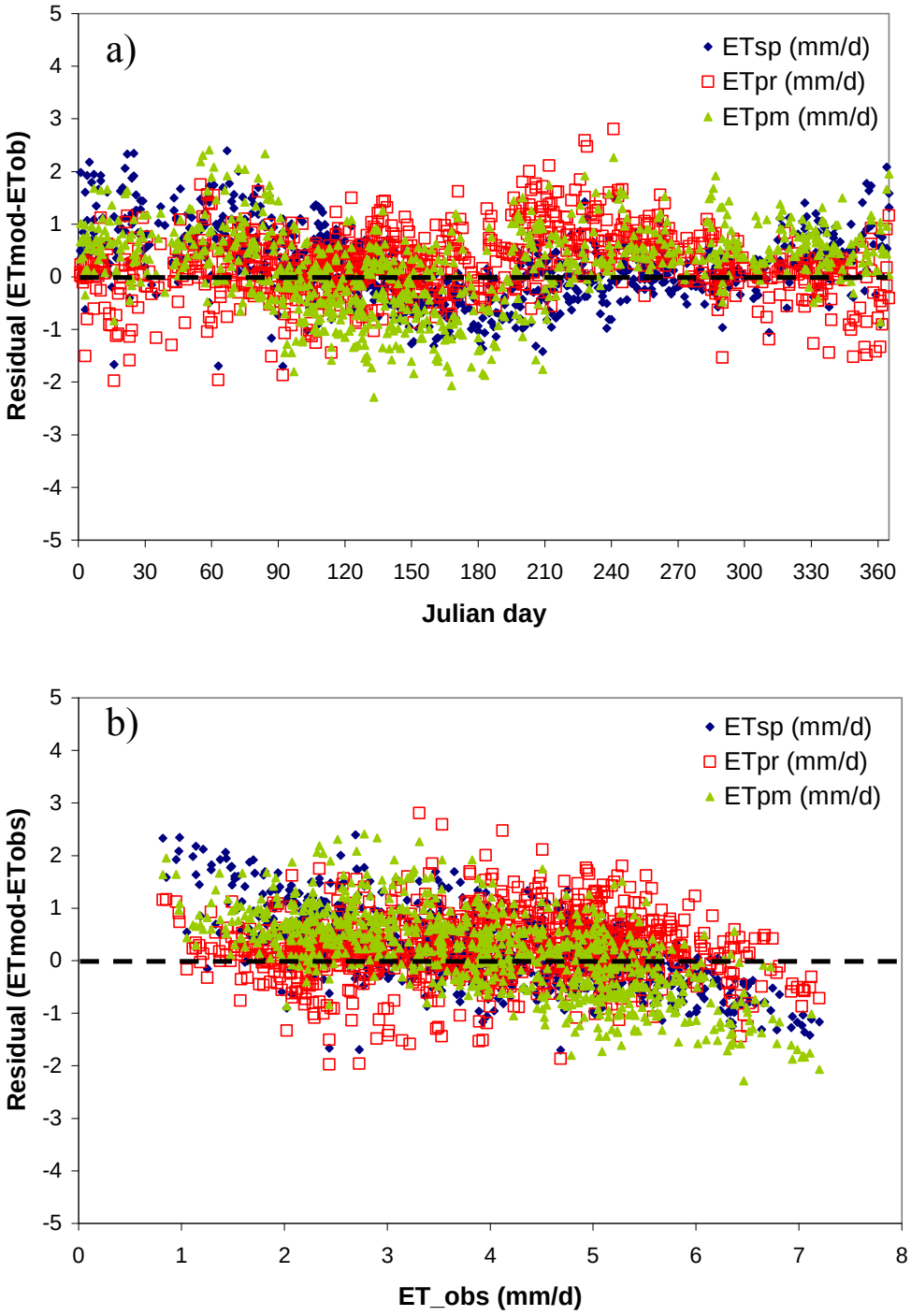

Figure 2.7: Residuals from the Simple (ETsp), Priestley-Taylor (ETpr) and Penman-Monteith (ETpm) models for Blue Cypress Marsh a) with julian day and b) with observed ET.

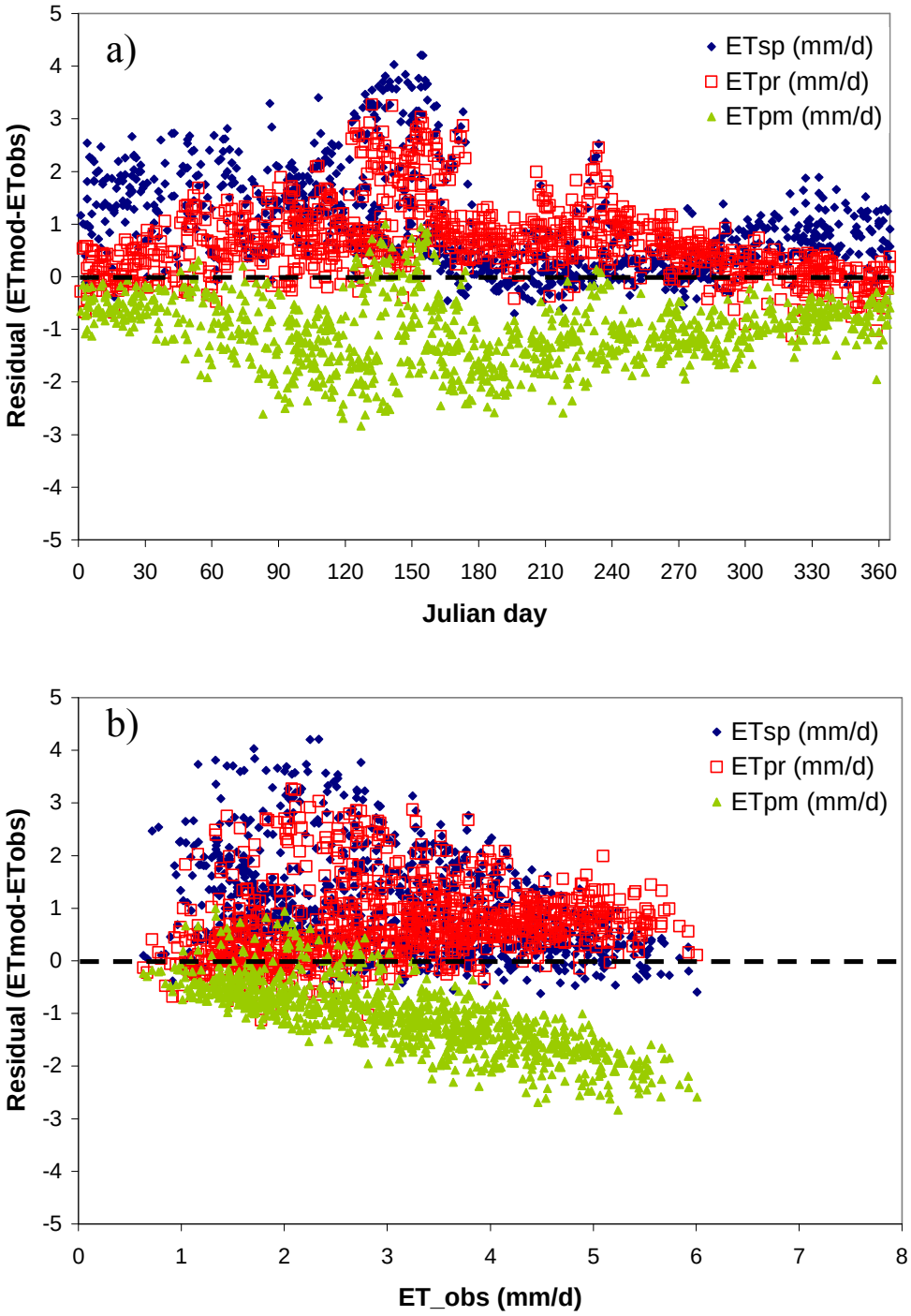

Figure 2.8: Residuals from the Simple (ETsp), Priestley-Taylor (ETpr) and Penman-Monteith (ETpm) models for Duda Farm (pasture) a) with julian day and b) with observed ET.

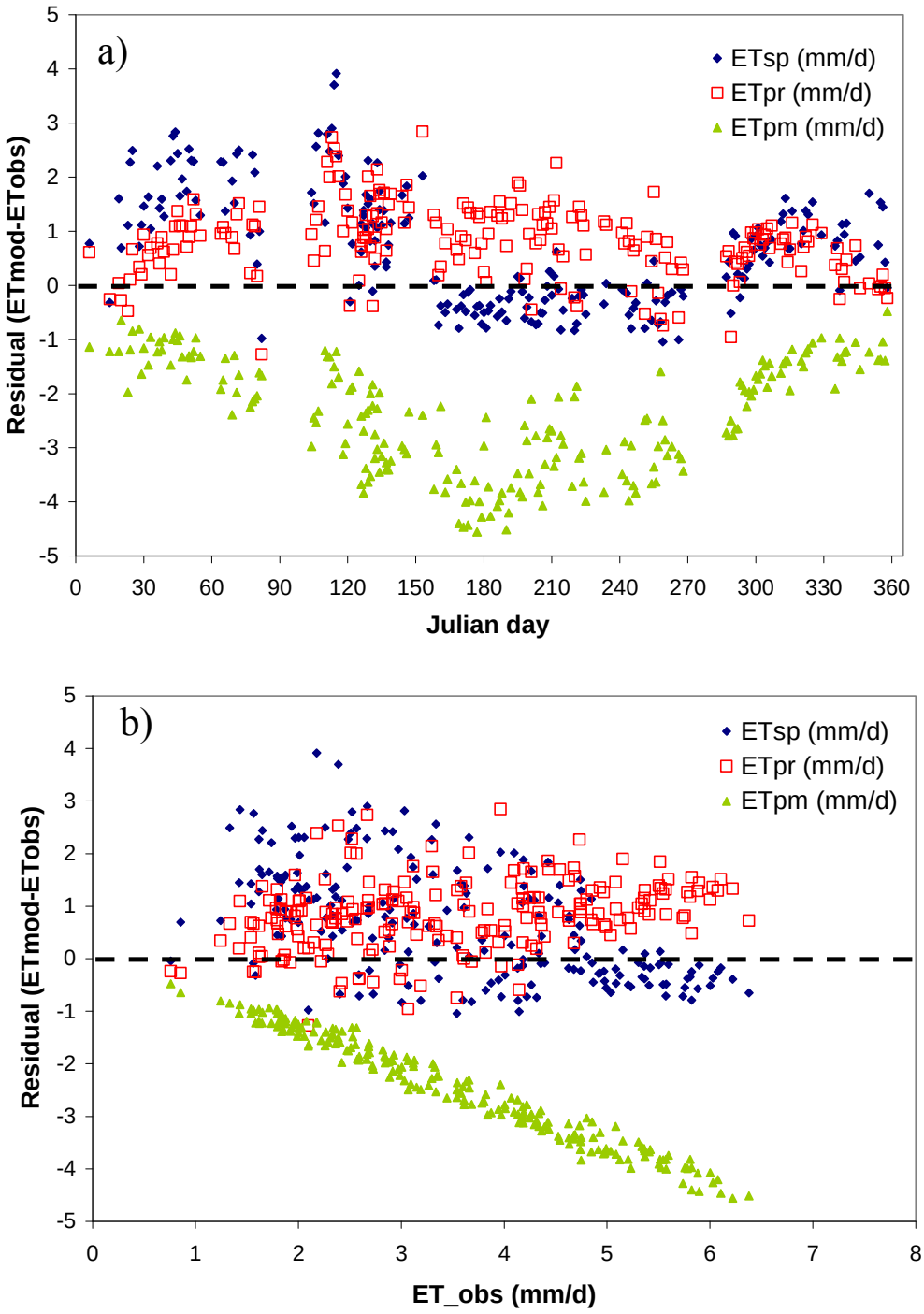

Figure 2.9: Residuals from the Simple (ETsp), Priestley-Taylor (ETpr) and Penman-Monteith (ETpm) models for Carlton Ranch (citrus) a) with julian day and b) with observed ET.

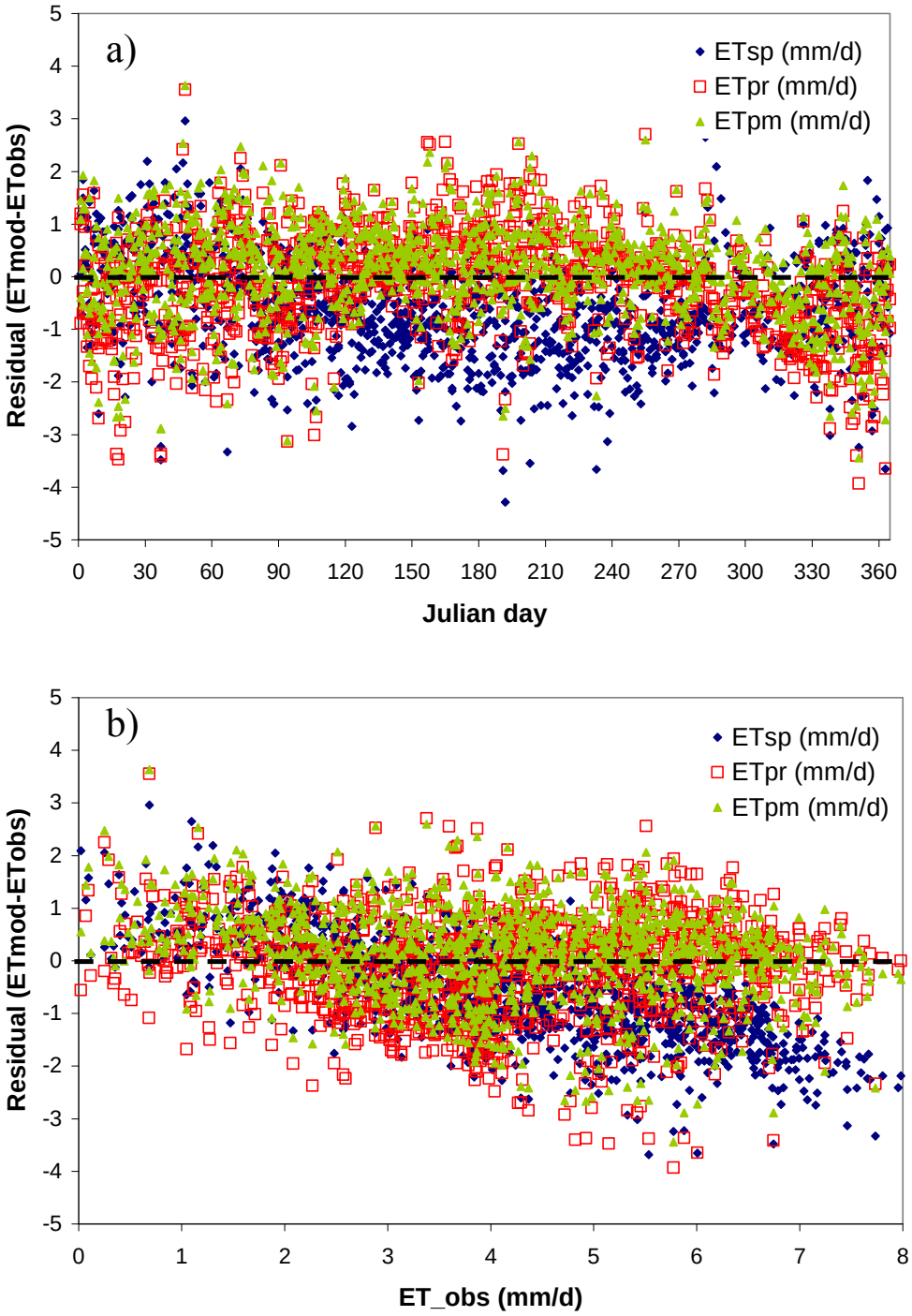

Figure 2.10: Residuals from the Simple (ETsp), Priestley-Taylor (ETpr) and Penman-Monteith (ETpm) models for Reedy Lake (open water) a) with julian day and b) with observed ET.

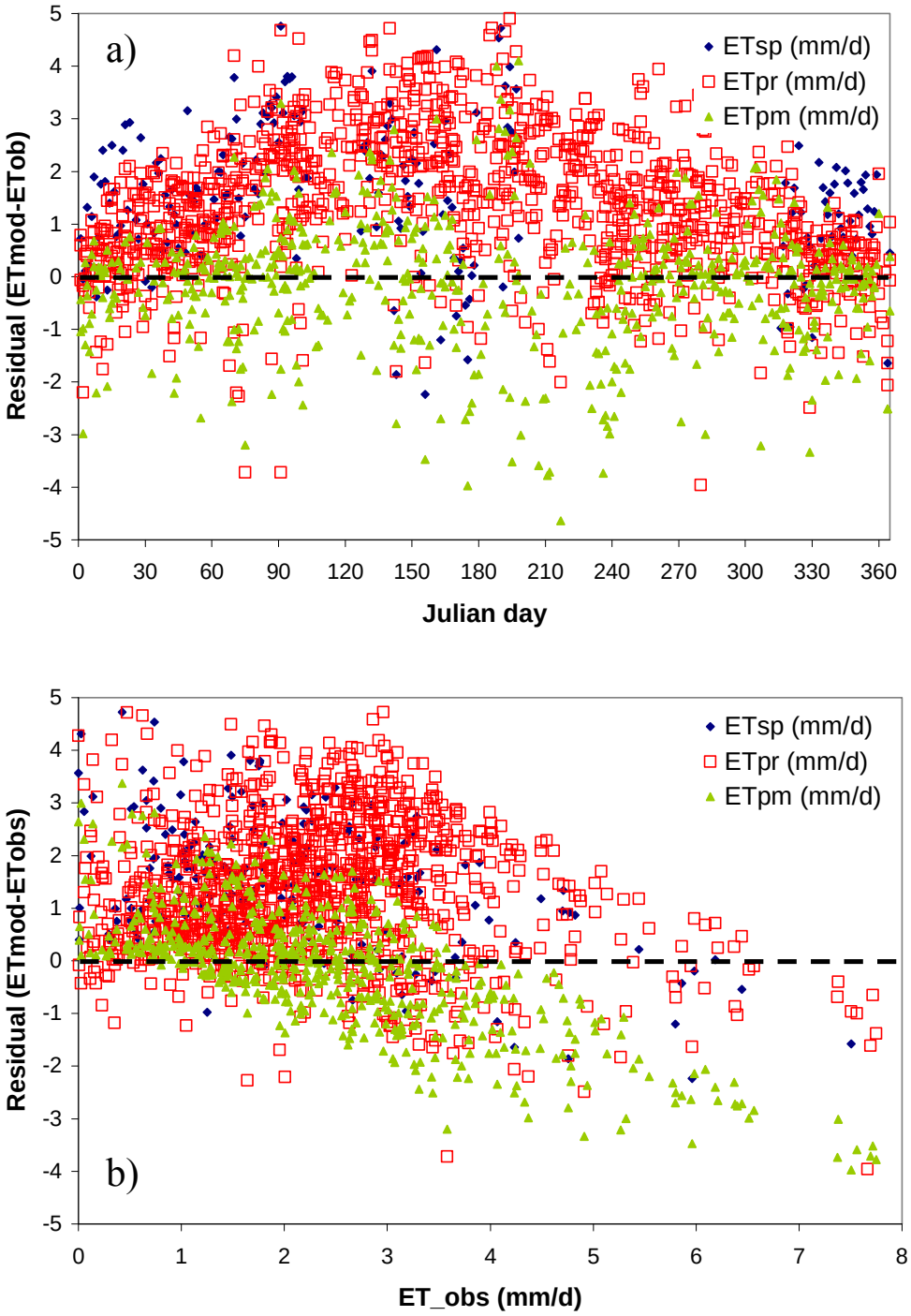

Figure 2.11: Residuals from the Simple (ETsp), Priestley-Taylor (ETpr) and Penman-Monteith (ETpm) models for Kennedy Space Center (forest) a) with julian day and b) with observed ET.

2.3.4 PET Model Selection

The summary statistics show strengths and weaknesses for each method as aggregate in Table 2.7. Figure 2.12 graphically compares these summary statistics of model performance for all "good" days (filled bars) and for days when $\beta \leq 1$ (hashed bars). The MAE is lowest for the PT method, while the Simple (Sp) and PT values are within the standard error of the mean values (Figure 2.12), indicating that there is no statistical difference between the aggregate MAE values. However, the MAE for the PM method is statistically higher than the others. As noted previously, the performance of the Simple method improves when applied to days when conditions are close to PET as shown by a decrease in both the MAE and the RMSE statistics. However, the improved Sp statistics are still not statistically different from the MAE and RMSE statistics for PT. On an aggregate annual basis, the Sp and PT methods appear to perform comparably and better than the PM method, possibly due to the sensitivity of the PM method to model parameters.

Performance at a daily time scale is indicated by the values of the regression intercept and slope and the correlation coefficient, R. If a model performs perfectly, the intercept should equal zero, and the slope and R should equal one. At a daily scale, the Sp intercept is much higher and statistically different than either the PT or PM statistics. The PT intercept statistics are closest to zero and slope and R statistics closest to one (the horizontal dashed line indicates a value of one). At a daily scale, the performance of all three methods does improve when applied to conditions close to PET. However, probably due to the lower sample size, the improved statistics are not significantly different from those computed for all "good" data. Interestingly, R values for all models are nearly identical. Figure 2.12 illustrates that, in aggregate, the Sp and PT methods perform comparably and outperform the PM. But at a daily scale, the PT performance appears to be superior to the other two. In fact, the slope and intercept show that the Sp method significantly overestimates of low ET values and underestimates high values.

A tradeoff exists between PT and PM models. The latter is more complex and can account for difference among vegetation. Hence, the PM method has the potential to be a more accurate representation of PET from vegetated surfaces, while the PT is more generalized. However, the PM model requires parameters that cannot be easily or robustly estimated from literature values. At best, fixed values may be determined for each landuse, but such parameters are difficult to defend from a biophysical perspective. The inability to characterize annual variability in plant water conductance is likely the cause of the PM residuals' seasonality (Figures 2.7 through 2.11). Also on annual scales (Figure 2.5), it is quite evident that when the literature values are used to calculate ET, results from PM are markedly different when the site specific values are used. The PT model avoids such problems and is easy to use with comparable accuracy, hence appears to be the best model for estimating PET in Florida.

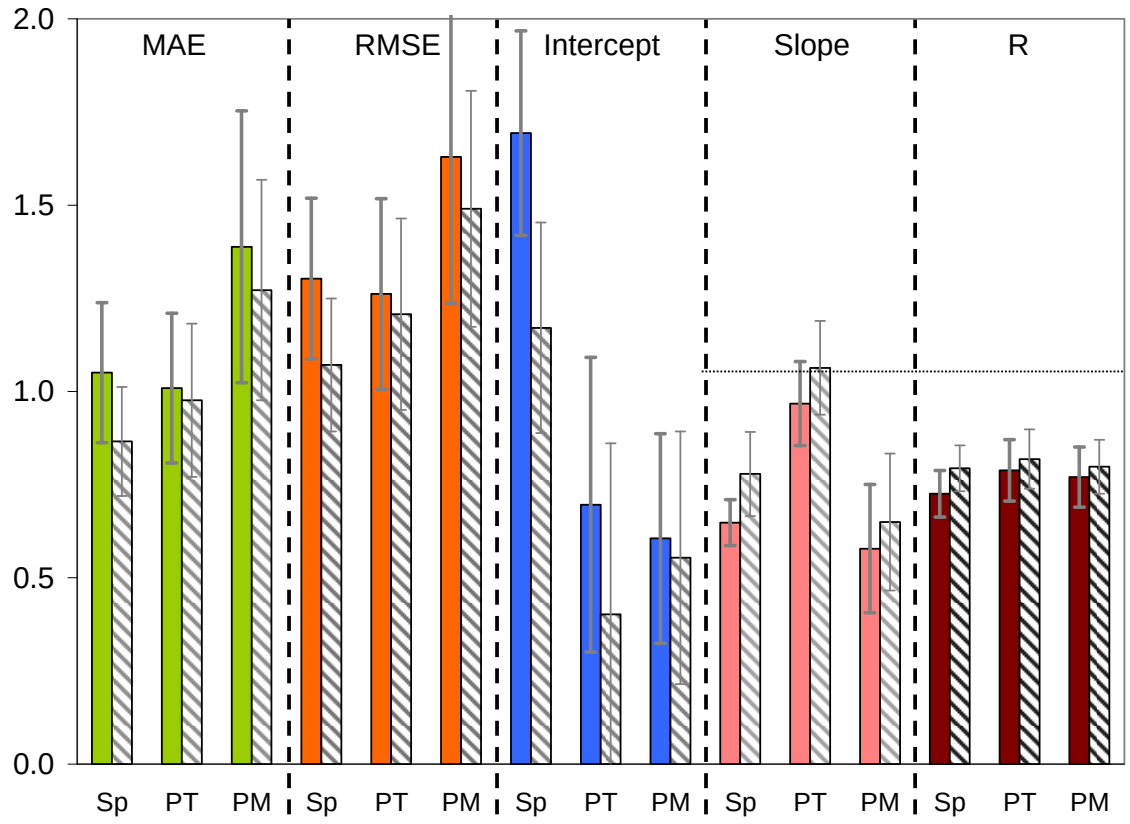

Figure 2.12: Comparison of aggregate error statistics (mm/day) and regression coefficients with standard error of the mean values (Sp=Simple method; PT= Priestley-Taylor method; PM=Penman-Monteith method). Filled bars represent statistics computed on all "good" days, hashed bars represent statistic computed for days when $\beta \leq 1$. Horizontal line represents a value of one.

In summary, the Simple method only appears to accurately estimate PET for marshland cover at a daily scale. A tradeoff exists between the PT and PM models. The PM is more accurate for small scale studies when accurate at-site parameter values are available. However, the PM model has several parameters that cannot be easily measured or estimated over large areas. In the case of open water, where there is no canopy and hence the bulk canopy resistance is zero, the PM method is superior to the other two methods. The PT method, on the other hand, is easier to use, has fewer tuning parameters, does not have a seasonal bias, and is slightly (but not statistically) more accurate over large regions. Based on our analysis, we recommend the use of the PT model.

3. Satellite-Estimated Solar Insolation

3.1. Introduction

Satellite visible data have been used for estimating solar insolation for a number of years, with methods ranging from statistical-empirical relationships such as Tarpley [1979], to physical models of varying complexity [see Gautier et al., 1980; Diak and Gautier, 1983; Gautier et al., 1984; Möser and Raschke, 1984; Pinker and Ewing, 1985; Dedieu et al., 1987; Darnell et al., 1988; Frouin and Chertock, 1992; Pinker and Laszlo, 1992; Weymouth and Le Marshall, 1999]. Studies such as Schmetz [1989] and Pinker et al. [1995] have proven the utility of satellite-estimated solar insolation methods, showing that such models produce fairly accurate results – with hourly insolation estimates within 5-10% of pyranometer data during clear-sky conditions (15-30% for all sky conditions) and daily estimates within 10-15%. Additional works such as those of Stewart et al. [1999] and Otkin et al. [2005] have further bolstered the utility of this technique. The limitations for much of this previous work have been centered around the need for information on atmospheric parameters that limit the effectiveness of these models, such as aerosols and precipitable water (PW) information. Also, problems associated with assessing the performance of these models are often fraught with issues related to scale differences between point observations and satellite pixel resolution (from ~1-4 km). Satellite sensor degradation, especially prevalent on the National Oceanic and Atmospheric Administration (NOAA) Geostationary Operational Environmental Satellite (GOES) satellite series, are often difficult to quantify, albeit it is one aspect this study attempts to address.

In this study, data from the NOAA GOES "East" series of satellites were used. GOES data were obtained from the GOES data archive at the Space Science and Engineering Center at the University of Wisconsin–Madison. Approximately 102,000 individual GOES images were processed for this effort. These data were processed using the model of Gautier et al. [1980] to produce half-hourly and daily-integrated solar insolation and 2 week running minimum surface albedo data throughout the State of Florida at 2-km horizontal spatial resolution. This high resolution was chosen to provide solar insolation observations between cumulus clouds, which comprise a significant component of Florida's cloud climatology.

The other unique aspect of this work involved an extensive model calibration activity for the insolation product, undertaken by comparing satellite-derived insolation estimates to that of ground-based pyranometers and clear-sky radiation models. This comparison provided information to tune or adjust biases in the daily-integrated insolation dataset for local environmental conditions. This was achieved via a three-step process: 1) comparison with ground-based pyranometer measurements on clear (non-cloudy) reference days, 2) correcting for a bias related to cloudiness, and 3) deriving a monthly bias correction factor. This resulted in a significant reduction in bias errors and henceforth a very robust ET product.

3.2. The Solar Insolation Model

The Gautier-Diak-Masse model developed by Gautier et al. [1980] (with modifications by Diak and Gautier, [1983] and updated application methods by Diak et al., [1996], from this point onwards referred to as the "GDM" model) employs a fairly simple physical representation of cloud and atmosphere radiative processes, yet has been shown to perform as well as, or even better than, more complex methods over a variety of land-surface and climatic conditions [Gautier et al., 1984; Diak et al., 1996; Frouin et al., 1988; Raphael and Hay, 1984; Jacobs et al., 2002; Jacobs et al., 2004; Otkin et al., 2005]. When comparing with pyranometer data, these studies reported root mean square errors in hourly and daily insolation estimates (as a percentage of the mean pyranometer observed value) from 17-28% and 9-10%, respectively. The high ends of these errors (~28% and ~10%, respectively) were reported in the study of Jacobs et al. [2002], which took place over northern-central Florida and was characterized by significant convective-cloud activity. The GDM model has also been proven in operational use, producing near-real-time insolation estimates for regional- and continental-scale land-surface carbon and water flux assessments [Mecikalski et al., 1999; Anderson et al., 2003; Anderson et al., 2004], subsurface hydrologic modeling, and the generation of agricultural forecasting products [Diak et al., 1998; Anderson et al., 2001]. A full description of the GDM model is given by Gautier et al. [1980], Diak and Gautier [1983] and Diak et al. [1996] – a basic overview is given here.

The model is based on conservation of radiant energy in the Earth-atmosphere column. The GDM model has two modes for determining solar insolation received at the Earth's surface: one for clear and one for cloudy conditions, based on satellite-inferred surface albedo data. A running 2 week minimum of this albedo data, reassessed daily, is stored for each GOES satellite visible data pixel, yielding a reference albedo grid representative of clear-sky conditions and capturing temporal changes in land-surface characteristics. This approach represents the true land-surface albedo more accurately than using the daily estimated value because the latter can be corrupted by high albedo values when clouds are present during the course of a day. [It should be noted that this minimum albedo product is wavelength-specific field, unique to the GOES visible sensor (which does in fact include contributions from the near infrared), and therefore does not represent a true surface albedo.]

For a given GOES image, the digital brightness at each image pixel is compared to that of the stored clear-sky reference albedo data for that pixel. If the brightness exceeds a given threshold (a function of the two-week running minimum noontime albedo; Diak and Gautier [1983]), the pixel is deemed cloudy, and vice versa. Based on this determination, either a clear or cloudy model of atmospheric radiation processes is used to calculate solar insolation received at the surface, for each pixel. Both the clear and cloudy models incorporate parameterizations for ozone absorption, Raleigh scattering, and water vapor absorption within the atmospheric column using simple bulk relationship. The cloudy GDM model component estimates a cloud-top albedo, and accounts for atmospheric effects above and below the cloud separately.

For the water vapor absorption parameterization, a fixed, approximate annual median value of 3.0 cm was used to estimate atmospheric column-integrated PW during the initial processing. [PW is defined as the amount of water that would precipitate out of a vertical column of the atmosphere if all the water vapor were condensed into liquid]. PW data are needed to calculate the slantwise path, and subsequently the absorption coefficients in the Gautier et al. (1980) method. Post-processing adjustments were then made to account for diurnal variations of PW (i.e. PW values greater or less than the 3.0 cm median value), given the logistical difficulty of including these data within the modeling stage. These adjustments were made by deriving diurnal adjustment factors based on daily representative PW values over Florida from numerical weather prediction model data [National Centers for Environmental Prediction (NCEP) reanalysis dataset (NOAA/OAR/ESRL PSD, Boulder, Colorado USA, www.cdc.noaa.gov)]. In many instances, daily PW values over Florida were well above 3.0 cm, certainly during summer, while wintertime values were often lower. No accounting was made for daily variations in PW considering the relatively small amount of inter-day variability that typically occurs over Florida, especially during summer, and because this would have required a reliance on forecasts from these models, which are often incorrect. We also do not account for meso-γ scale (2-25 km) scale variations in PW given this would require substantially larger amounts of model-derived data.

3.3. Data Acquisition, Processing and Quality Control

3.3.1 GOES Satellite Data

The GOES East series of satellites (the most recent additions being GOES-8 and -12) have been placed in geostationary orbit above the Earth's equator at longitude 75° W, providing continuous observations in several visible and non-visible radiation bands of much of the western hemisphere at high spatial (≥1 km) and temporal (≥15 min) resolution, making data collected by them ideal for high-resolution estimates of solar insolation. During the time period spanned by this study, the GOES-8 satellite (launched in April 1994) was decommissioned and the GOES-12 satellite took its place on 1 April, 2003. Data from both of these satellites were acquired and utilized.

Although the GOES visible sensors have a nadir (the point directly below the satellite) spatial resolution of 1 km, this resolution decreases the further from nadir the instrument scans: for the state of Florida region, the highest resolution attainable is about 1.5-2.0 km. This was the input and output resolution of the GDM MODEL model in this work. Half-hourly solar insolation values were calculated using GOES data from 15 and 45 min past the hour, and daily values were calculated by integrating the half-hourly values over the period of daylight (using the trapezoidal integration method). We use a simple method for computing sunrise and sunset times per pixels across the domain. The running 2 week minimum albedo product discussed in Section 3.2 was calculated using data at solar noon. These products were generated both in the original satellite projection, and translated to a grid identical to that used for the Statewide NEXRAD radar-derived rainfall product [Hoblit et al., 2003]. In the latter dataset, the data were interpolated in time to 00 and 30 minutes past the hour.

Potential GOES data issues include sensor degradation with time and sun glint effects (i.e. the reflection of the Sun disk from land and sea surfaces). The effects of the latter are small, and not addressed in this study due to the complexity of the phenomena. Sensor degradation is addressed and corrected for through the calibration of the product, detailed in following sections. This issue is also discussed further in Section 3.5.

In general, GOES satellite data are available on a continual basis with high reliability. Under specific conditions though, the instruments are shut down (for example when sunlight shines directly into the sensors), and other issues such as receiving-station glitches can result in the occasional loss or corruption of an image or series of images. For this reason, if more than 5 half-hourly satellite images were missing on a given day, the daily insolation value for that day (being derived from the half-hourly data) was flagged as unusable. Days with 3 to 5 missing images were designated usable, and those with zero to 2 missing images were designated as good quality data. Where there were gaps in the usable data, linear interpolation was used to fill them. [The final insolation product includes flags for data loss.]

3.3.2 Pyranometer Data

Pyranometer data used to calibrate the satellite isolation product, and subsequently assess calibration performance, were obtained from a number of weather stations networks across Florida, each maintained by a different agency as shown in Figure 3.1. Historical pyranometer data were provided by 3 of the WMDs (SFWMD, SJRWMD, and SWFWMD) and the remaining data were obtained from the University of Florida (UF) Institute of Food and Agricultural Sciences (IFAS) Florida Automated Weather Network (FAWN) web site (fawn.ifas.ufl.edu), and the U. S. Geological Survey (USGS). Datasets from 57 stations were used, divided into three groups, referred to in this work as "Group 1," "Group 2" and "Group 3". Group 2 and 3 data were used for calibration purposes while Group 1 data were used for GDM model performance assessment. The locations and details of each of the stations in these groups are shown in Figure 3.1 and Table 3.1. For performance assessment (Group 1), we used 9 stations - 2 from each WMD region (except NWFWMD, only 1 quality station available) so that each region would be represented; these stations had good data quality over the longest available data records. For the other 2 groups (Group 2 and 3), used for the calibration coefficient derivations, high-quality data were needed, which meant using many different stations over the 10-year period as a means of having enough quality information.

Each weather station network used the LI-COR 200 pyranometer produced by LI-COR, Inc. (Lincoln, NE). This is a silicon cell device that has a quoted accuracy of 5%, with re-calibration necessary every 1-2 years. Pyranometer site locations varied from open fields to water bodies (lakes and bays), but the latter were avoided whenever possible to minimize issues such as salt deposit contamination of the sensors. Temporal resolution of the pyranometer data ranged from 15 min to 1 hr averages, (see Table 1) and daily-integrated insolation values were calculated using the midpoint integration method.

A practical issue to be considered for the calibration activity was choosing good quality data. Most of the data were provided with quality assurance and quality control (QA/QC) flags, but these flags were not infallible. For example, some stations consistently underestimate clear-sky insolation in comparison with empirical estimates. As a result, an additional method for screening the data, developed by the American Society of Civil Engineers (ASCE), was employed [see Allen et al., 2005, Appendix D]. This method involved comparing daily-integrated insolation data with estimated clear-sky radiation, R_{so} [MJ m^{-2} day^{-1}], estimated as a function of station elevation (z) and extraterrestrial radiation (R_a: short-wave solar radiation in the absence of an atmosphere) over a 24-hour period by

$$R_{so} = (0.75 + 2 \times 10^{-5} z) R_a , \qquad (1)$$

where R_a is a function of day of year, solar constant, solar declination, and latitude, given by

$$Ra = \frac{24}{\pi} G_{sc} d_r [\omega_s \sin(\varphi) \sin(\delta) + \cos(\varphi) \cos(\delta) \sin(\omega_s)] . \qquad (2)$$

Here, G_{sc} is the solar constant (4.92 MJ m^{-2} h^{-1}), d_r is the inverse relative distance factor (squared) for the earth-sun (unitless), ω_s is the sunset hour angle (radians), φ is latitude (radians), and δ is the solar declination (radians) [see Duffie and Beckman, 1980, Allen 1996; Allen et al., 2005, Appendix D for further details].

The assumption is that measured daily insolation should be close to estimated clear-sky values on at least some days during the year – those days being considered as cloud-free. When examining annual bell curve plots of this comparison, it was possible to identify when a station had significant data quality issues not indicated by QA/QC flags; specifically, under complete sunshine, quality pyranometer measurements should be near the R_{so} values. For pyranometer data not provided with any QA/QC information, the above method was employed as an initial filter, following that, data greater than 105% of the estimated clear-sky value were removed [Allen et al., 2005]. These methods eliminated stations, or periods of the data record, that appeared erroneous.

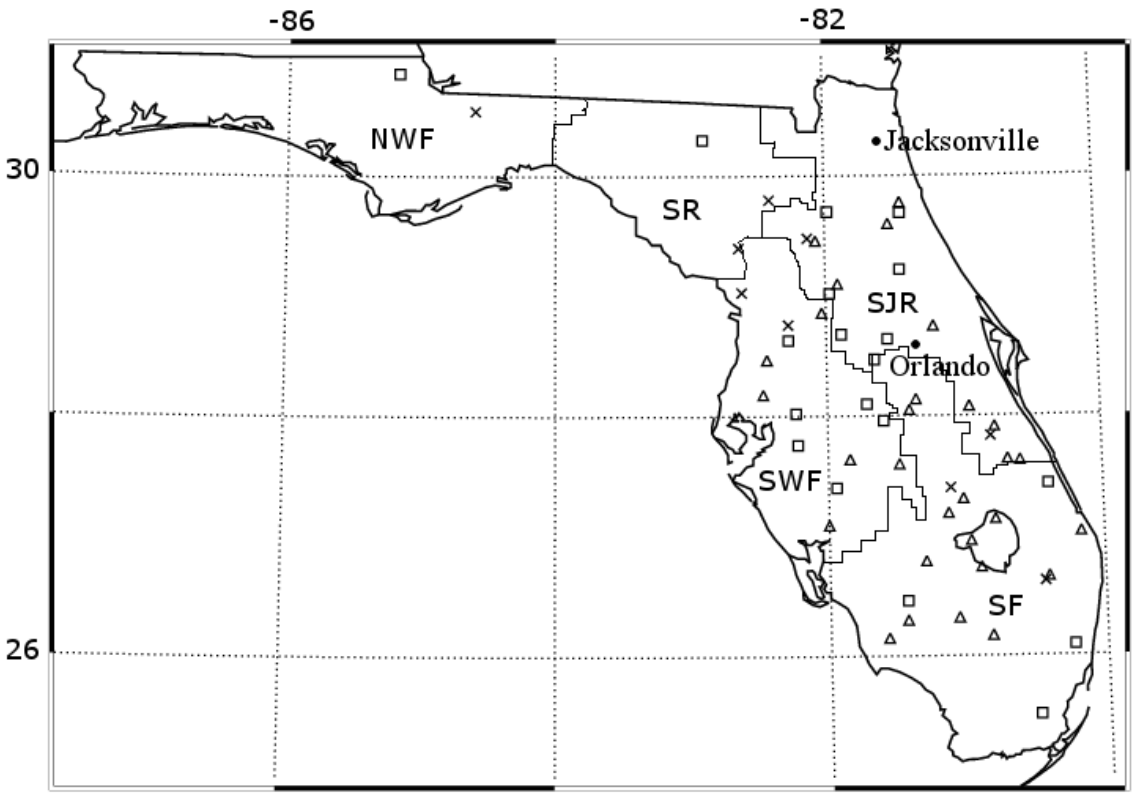

Figure 3.1: Locations of pyranometer stations used in the study. Group 1, 2 and 3 datasets are denoted by crosses, triangles, and squares, respectively. State boundaries and WMD region boundaries are thick and thin black lines, respectively. WMD acronyms are shown. Latitudes are given on the left side and longitudes at the top. Lake Okeechobee can be seen in the southeast part of the state.

Table 3.1. Pyranometer dataset information[a].

Stn No.	Group	Network	Station	County	Lat (°)	Lon (°)	Date	Days	Resolution
1	1	FAWN	Alachua	Alachua	29.80	82.41	16-Oct-99	1191	15 min
2	1	FAWN	Bronson	Levy	29.40	82.59	26-Sep-02	794	15 min
3	1	FAWN	Quincy	Gadsden	30.54	84.60	13-Sep-02	460	15 min
4	1	SF WMD	ENR308	Palm Beach	26.62	80.44	1-Jun-95	2187	30 min[c]
5	1	SF WMD	S65CW	Okeechobee	27.40	81.11	1-Sep-99	1833	30 min[c]
6	1	SJR WMD	Orange Lake	Alachua	29.48	82.13	14-Feb-97	689	30 min[c]
7	1	SJR WMD	Tucker	Brevard	27.83	80.81	1-Sep-96	838	30 min[c]
8	1	SWF WMD	Floral City	Citrus	28.76	82.28	1-Jun-95	3209	60 min
9	1	SWF WMD	Inglis	Levy	29.03	82.62	1-Jun-95	3196	60 min
10	2	SF WMD	BCSI	Hendry	26.32	81.07	N/A[b]	2	30 min[c]
11	2	SF WMD	CFSW	Hendry	26.74	80.90	N/A[b]	2	30 min[c]
12	2	SF WMD	ENR105	Palm Beach	26.66	80.41	N/A[b]	3	30 min[c]
13	2	SF WMD	JDWX	Martin	27.03	80.17	N/A[b]	1	30 min[c]
14	2	SF WMD	L001	Okeechobee	27.14	80.79	N/A[b]	6	30 min[c]
15	2	SF WMD	L005	Glades	26.96	80.97	N/A[b]	1	30 min[c]
16	2	SF WMD	S61W	Osceola	28.14	81.35	N/A[b]	2	30 min[c]
17	2	SF WMD	S65DWX	Okeechobee	27.31	81.02	N/A[b]	7	30 min[c]
18	2	SF WMD	S75WX	Glades	27.19	81.13	N/A[b]	1	30 min[c]
19	2	SF WMD	S78W	Glades	26.79	81.30	N/A[b]	1	30 min[c]
20	2	SF WMD	S140W	Broward	26.17	80.83	N/A[b]	3	30 min[c]
21	2	SF WMD	SGGEWX	Collier	26.15	81.58	N/A[b]	1	30 min[c]
22	2	SF WMD	SILVER	Collier	26.30	81.44	N/A[b]	1	30 min[c]
23	2	SF WMD	WRWX	Polk	28.05	81.40	N/A[b]	5	30 min[c]
24	2	SJR WMD	Bull Creek	Osceola	28.08	80.96	N/A[b]	1	30 min
25	2	SJR WMD	Elkton	St. Johns	29.78	81.44	N/A[b]	4	60 min
26	2	SJR WMD	Ft Drum	Indian River	27.59	80.69	N/A[b]	3	30 min[c]
27	2	SJR WMD	Hell Cat Bay	Putnam	29.60	81.53	N/A[b]	4	60 min
28	2	SJR WMD	Lake Jessup	Seminole	28.75	81.21	N/A[b]	1	30 min[c]
29	2	SJR WMD	Lindsey Citrus	Indian River	27.58	80.60	N/A[b]	2	30 min
30	2	SJR WMD	Mulberry Marsh	Brevard	27.91	80.78	N/A[b]	1	30 min
31	2	SJR WMD	Ocklawaha Prairie	Marion	29.10	81.91	N/A[b]	2	30 min
32	2	SJR WMD	Orange Creek	Alachua	29.46	82.07	N/A[b]	3	30 min
33	2	SWF WMD	Avon Park	Highlands	27.60	81.48	N/A[b]	1	60 min
34	2	SWF WMD	Bowling Green	Hardee	27.64	81.84	N/A[b]	4	60 min
35	2	SWF WMD	Headquarters	Hernando	28.47	82.44	N/A[b]	8	60 min
36	2	SWF WMD	Lake Como	Pasco	28.18	82.47	N/A[b]	7	60 min
37	2	SWF WMD	Peace River	Desoto	27.09	82.00	N/A[b]	1	60 min
38	2	SWF WMD	Wildwood	Sumter	28.86	82.03	N/A[b]	5	60 min
39	3	FAWN	Apoka	Orange	28.64	81.55	1-Jan-98	2424	15 min
40	3	FAWN	Avalon	Orange	28.47	81.65	13-Mar-99	1993	15 min
41	3	FAWN	Balm	Hillsborough	27.76	82.22	17-Dec-03	361	15 min
42	3	FAWN	Brooksville	Hernando	28.63	82.28	25-Apr-00	1658	15 min
43	3	FAWN	Dover	Hillsborough	28.02	82.23	15-Aug-98	2242	15 min
44	3	FAWN	Ft. Lauderdale	Broward	26.09	80.24	25-Jan-01	1387	15 min
45	3	FAWN	Ft. Pierce	St Lucie	27.43	80.40	10-Jul-98	2275	15 min
46	3	FAWN	Hastings	St Johns	29.69	81.44	5-Aug-99	1919	15 min
47	3	FAWN	Homestead	Dade	25.51	80.50	1-Jan-98	2463	15 min
48	3	FAWN	Immokalee	Collier	26.46	81.44	1-Jan-98	2442	15 min
49	3	FAWN	Lake Alfred	Polk	28.10	81.71	1-Jan-98	2456	15 min
50	3	FAWN	Live Oak	Suwanee	30.30	82.90	18-Sep-02	804	15 min
51	3	FAWN	Marianna	Jackson	30.85	85.17	12-Sep-02	809	15 min
52	3	FAWN	Ocklawaha	Marion	29.02	81.97	23-Mar-99	2041	15 min
53	3	FAWN	Okahumpka	Lake	28.68	81.89	2-Feb-99	1976	15 min
54	3	FAWN	Ona	Hardee	27.40	81.94	11-Mar-98	2395	15 min
55	3	FAWN	Pierson	Volusia	29.22	81.45	24-May-99	1975	15 min
56	3	FAWN	Putnam Hill	Putnam	29.70	81.98	25-Jan-01	1323	15 min
57	3	USGS	Lake Starr	Polk	27.96	81.59	21-Jul-96	2973	60 min

a Pyranometer station: dataset group number, network agency, name, location, begin date of data record used, number of data days used, and temporal resolution (also data averaging period unless otherwise noted).

[b] Dates are individual days, refer to Table 3.3.

[c] 15 minute averaging period, every second data record used.

3.3.3 Satellite-Pyranometer Data Differences

There are inherent differences between satellite-estimated and pyranometer-measured solar insolation data. At the pixel level, satellite data provide a snapshot at a given time, with each pixel in the snapshot having a single value, that being the spatial average over the horizontal surface pixel area. Pyranometer data, on the other hand, are generally time-averaged. So in the case of the satellite instrument, insolation data are spatially smoothed, whereas pyranometer data are temporally smoothed. Additionally, even though a pyranometer is located at a point, the instrument observes solar insolation over an upward-staring hemispherical solid angle that is actually much larger than that observed on the pixel level by the GOES visible satellite instrument [Otkin et al., 2005]. These differences do not cause significant data disparities under cloud-free conditions (when solar insolation is homogeneous over a given region) but become an increasing issue as cloud cover variability and data temporal resolution increase. Both the use of high-resolution satellite data and temporal averaging blurs these disparities, the latter being demonstrated via the differences in hourly versus daily-integrated insolation errors quoted in Sections 3.1 and 3.2.

3.4. Model Calibration

As discussed in Section 3.2, the GDM model performs well over a variety of land-surface and climatic conditions, as well as spatial and temporal resolutions. In the current study, daily-integrated GOES-estimated insolation data were further fine-tuned through a cumulative three-step process via comparison with ground-based pyranometer data (hereafter referred to as "calibration"). First, the initial insolation data estimated via the GDM model (referred to as "DAILY_A") were compared with pyranometer observations on a series of clear (non-cloudy) reference days resulting in a set of calibration coefficients, the application of which produced the "DAILY_B" dataset. Secondly, a "cloudiness" bias correction was derived from, and applied to, the DAILY_B data, resulting in the "DAILY_C" dataset. Lastly, a monthly correction factor was calculated from, and applied to the DAILY_C data, yielding the final dataset "DAILY_D". These steps are discussed in detail in the sections below. For each calibration step, the GOES-estimated and pyranometer insolation data were matched spatially by choosing the satellite data pixel that each pyranometer station was located "within."

For GDM model performance assessment, each of the above datasets are compared to pyranometer data from the "Group 1" dataset, consisting of nine calibration-independent surface stations located across Florida as detailed in Figure 3.1 and Table 3.1. The results, showing the calibration progression, are shown for the entire data period and each of the nine station locations in Figure 3.2. Statistics used for this comparison (quoted on each plot) are the Root Mean Square Error (RMSE, also expressed as a percentage of the mean pyranometer observed value), the Mean Bias Error (MBE), and the coefficient of determination (R^2). Table 3.2 and Figure 3.3a present station-averaged statistics and seasonal-station averaged model MBE, respectively. Note that the number of stations in the averaged statistics (Figure 3.3b) varies from 2 to 7, subject to the data record length of each station and the necessity for quality data for comparison.

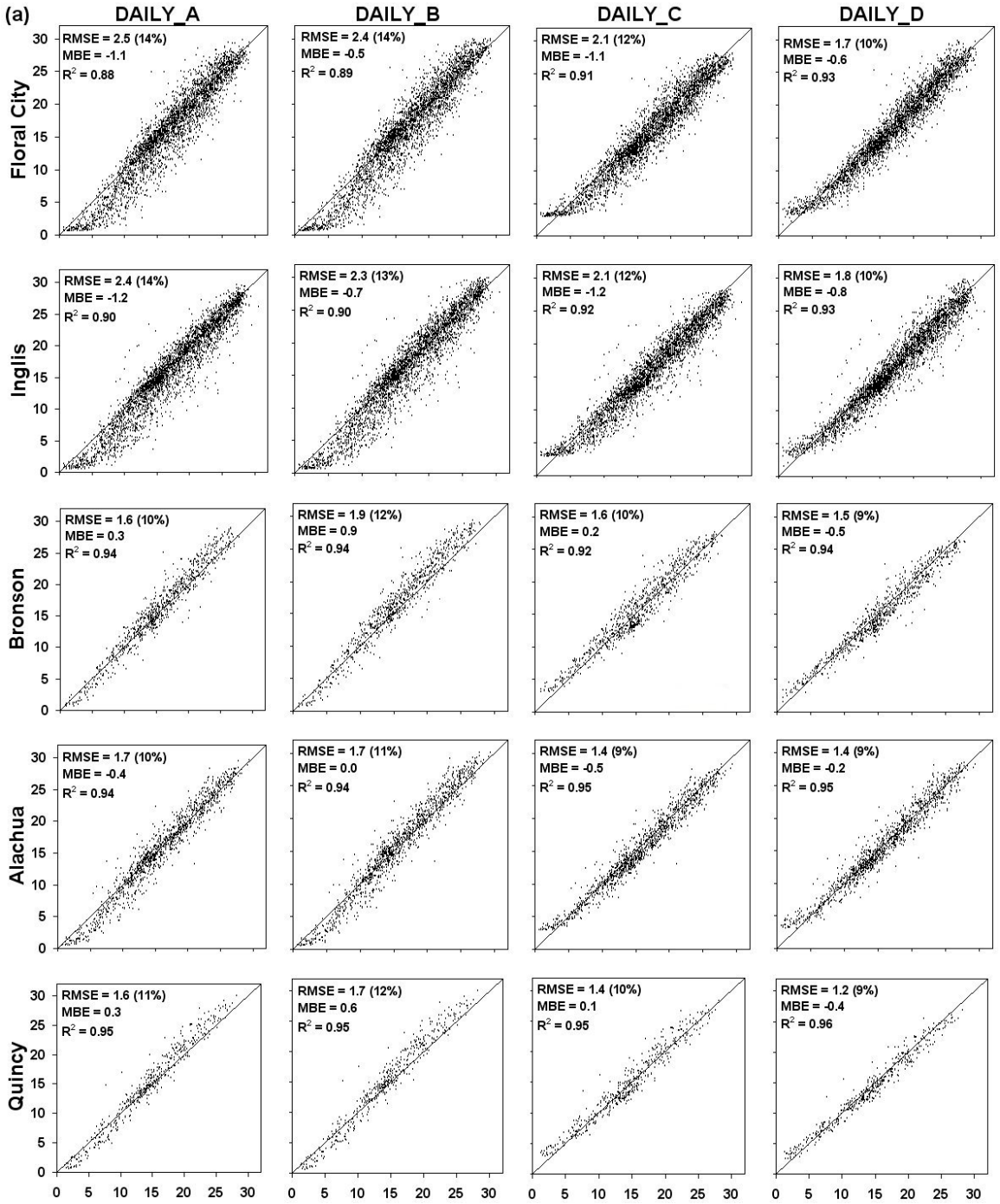

Figure 3.2: Comparison of satellite-estimated (ordinate) and pyranometer-measured (abscissa) daily integrated insolation [MJ m^{-2} day^{-1}] for the 9 model performance assessment locations. Station names are given along the left-side, and comparison satellite-estimated dataset names are indicated at the top. RMSE values [MJ m^{-2} day^{-1}] and as a percentage of the mean observed value (in parentheses), MBE [MJ m^{-2} day^{-1}], and coefficient of determination for each station and dataset are quoted for each comparison.

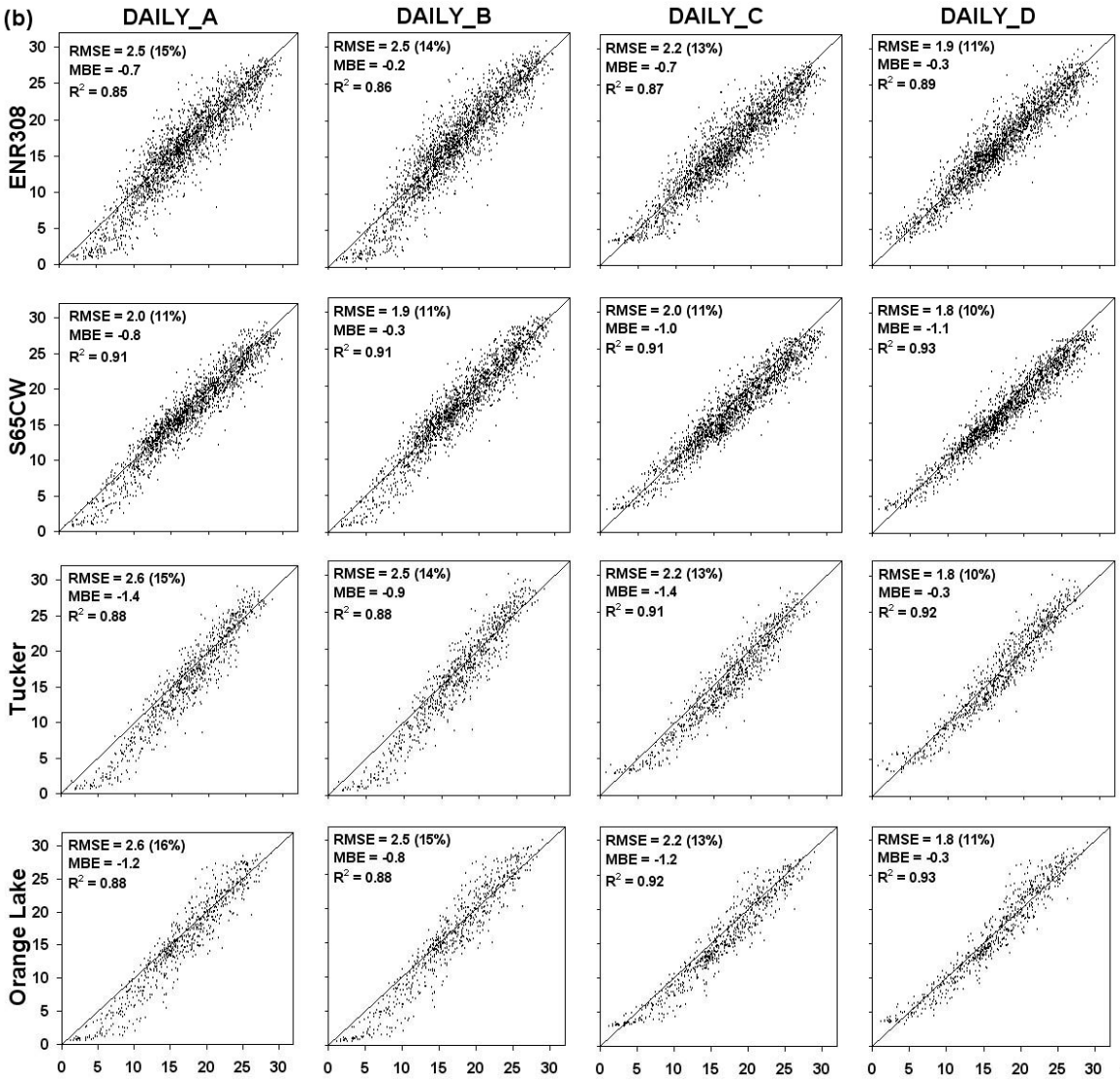

Figure 3.2. (Continued)

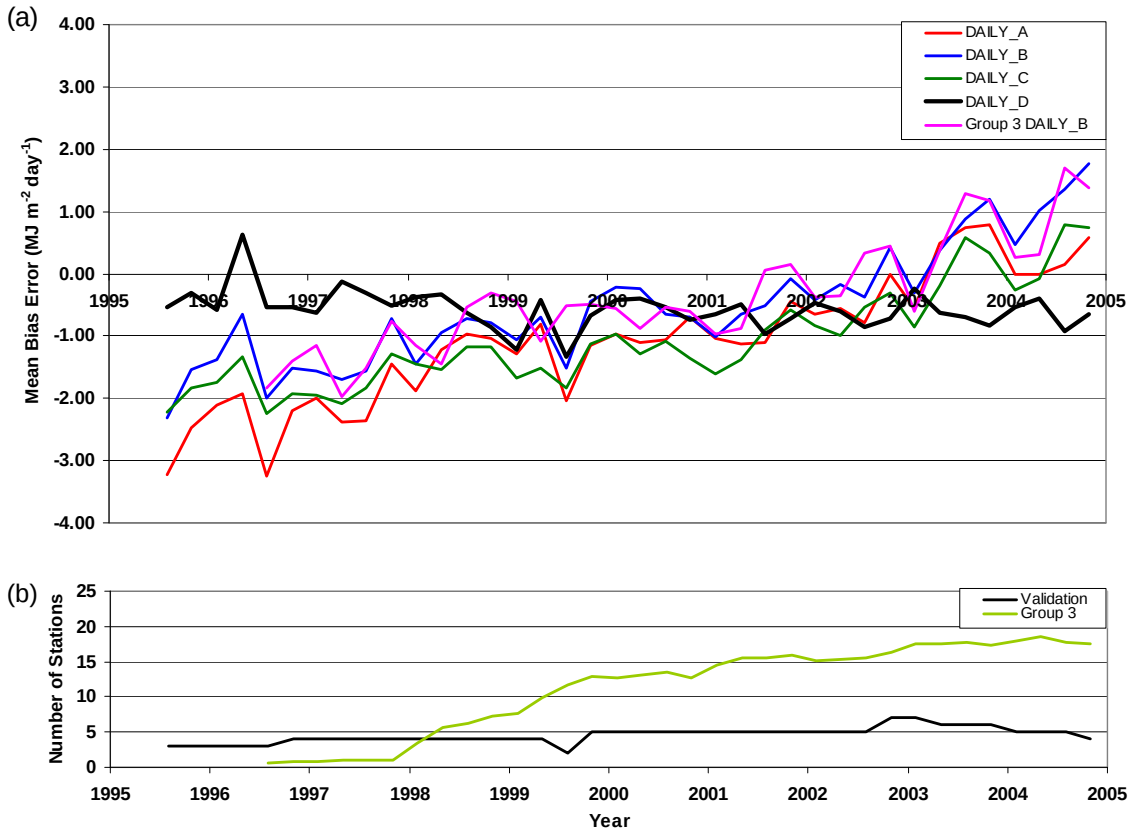

Figure 3.3: (a) Season and station averaged daily integrated solar insolation MBE, and (b) number of stations in the average at any given time. "Group 3" dataset is included in both (a) and (b) for comparison as discussed in Section 3.4.1. Season months are December to February (winter), March to May (spring), etc.

Table 3.2. Calibration and comparison station-averaged statistics for data period[a].

	DAILY_A	DAILY_B	DAILY_C	DAILY_D
RMSE MJ m^{-2} day^{-1} (%)	2.2 (13%)	2.2 (13%)	1.9 (11%)	1.7 (10%)
MBE MJ m^{-2} day^{-1}	-0.7	-0.2	-0.8	-0.5
R^2	0.90	0.91	0.92	0.93
[a]RMSE as percentage of mean observed value given in parentheses.				

3.4.1 Initial Results

Station averaged calibration statistics from the initial dataset (DAILY_A: Figures 3.2 and 3.3 and Table 3.2) are as follows: coefficient of determination 0.90, MBE –0.7 MJ m^{-2} day^{-1}, and RMSE 2.2 MJ m^{-2} day^{-1} (13% of the mean observed value). These statistics indicates performance slightly poorer than previous studies using the GDM model, which generally had RMSE values of about 10% of the mean observed value for daily integrated insolation comparisons (see Section 3.2). Figure 3.3a shows a predominantly negative bias in model-estimated daily insolation values, gradually increasing to a slight positive

bias beyond mid-2003, with about a 4 MJ m^{-2} day^{-1} difference from the beginning to the end of the ten year historical data period. A seasonal bias oscillation on the order of ±0.5 MJ m^{-2} day^{-1} is also present, with MBE values tending to be more positive during the summer and autumn seasons. This trend is clearer in the latter years of the data period (2001 onward), with increasing numbers of stations in the average (see Figure 3.3b). Due to the larger number of stations, this seasonal trend is more evident when comparing with the pyranometer data of the "Group 3" dataset (see Section 3.2) – the station average MBE, which is also plotted in Figure 3.3a ("Group 3 DAILY_B"). These observations are discussed further in Section 3.5.

The scatter plots of Figure 3.2 reveal an over- and under-estimation of insolation by the GDM model under clear and cloudy conditions, respectively – with the latter being most prevalent. The occasional data point where pyranometer data were significantly underestimating insolation is also observed, which may be due to the so-called "bird effect" – when birds use the pyranometer as a perch and shade the sensor (personal communication with USGS staff). The approach we use to fine-tune and correct the data for some of these observations are described in the following sections.

3.4.2 Clear Day Comparison

On a clear day, disparities between satellite-estimated and pyranometer-measured insolation should be minimized, since without clouds solar insolation received at the surface will locally be spatially homogeneous, providing reference conditions for the comparison of the two datasets. This "clear day comparison" was made on a day as free of cloud as possible over Florida every 6 months – one day in each summer and winter season (or as close as possible). Clear days over the entire state of Florida are rare, and therefore many times the comparison was limited to available cloud-free regions. Additionally, due to factors such as site decommissioning, periods of missing data, instrument issues and variations in data quality, it was not possible to use a single set of pyranometer stations for the entire 10-year study period, but continuity was maintained as much as possible.

For each clear day, the half-hourly satellite insolation product was compared with "Group 2" pyranometer data for up to three stations within each of the SF, SJR and SWF WMD regions (no data were available for NWF or SR for this analysis). Pyranometer data time-stamps were adjusted to the middle of their data-averaging period and GOES data times were used unmodified. For each WMD region, the satellite and corresponding pyranometer datasets were averaged (across the selected stations), resulting in two datasets (GOES satellite and pyranometer). These two averaged datasets were then plotted, and the satellite data calibration coefficient for each WMD was determined by multiplying the averaged satellite data by a factor necessary for its diurnal insolation curve to align with the averaged pyranometer data curve as closely as possible. This factor was manually determined as a means of correcting for the satellite–pyranometer differences. Subsequently, the average of all available WMD correction factors were taken to obtain a calibration coefficient for that particular day for application over the entire state of Florida. This process was carried out for the entire observation period, resulting in a set of 20 approximately bi-annual calibration coefficients spanning the 10-

year data record, as shown in Table 3.3. The individual coefficients, obtained only on days when pyranometer data were available, were then interpolated in time to obtain a calibration coefficient set that could be applied to each day across the data record.

As a check for potential issues, calibration factors using the above method were obtained for three consecutive clear days (6-8 March 2001, results not shown in Table 3.3). During these days weather conditions remained consistent over Florida, implying that if the application of the GDM model in this study was successful, the same should be the case of the three calibration factors. This was the case: the calibration coefficient of each day had a value of 1.09.

For the model calibration, these coefficients were applied to the initial (DAILY_A) data, yielding the DAILY_B dataset. The results of this calibration are shown in Figures 3.2 and 3.3 and Table 3.2. The station averaged RMSE remained the same as that of the initial dataset, the coefficient of determination increased to 0.91, and the average MBE decreased in magnitude from –0.7 to –0.2 MJ m^{-2} day^{-1} (Table 3.2). Figure 3.3 reveals that although the MBE has been reduced on average, the temporal trend of MBE (positive shift with time) is still present, with a similar range (from dataset beginning to end) as the initial dataset. The seasonal MBE oscillation is also still present, as is the cloudiness-related bias (see Figure 3.2). The following sections address these remaining issues.

Table 3.3. Calibration Coefficients Determined by Clear-Day Comparison of Satellite-Estimated and Pyranometer-Measured Solar Insolation[a].

Date	SF	SJR	SWF	Average
14-Jun-95	1.05 (11,20)	N/A[b]	N/A[b]	1.05
22-Nov-95	1.12 (20)	1.14 (25,27)	1.12 (35,36)	1.13
28-Jul-96	1.03 (19,20)	N/A[b]	N/A[b]	1.03
14-Dec-96	1.11 (12)	1.10 (25,27)	1.08 (36)	1.10
4-May-97	N/A[b]	1.06 (25,27)	1.06 (38)	1.06
17-Dec-97	1.08 (12)	1.14 (28)	1.10 (38)	1.11
13-May-98	1.03 (12,13)	1.03 (26)	1.04 (38)	1.03
16-Dec-98	N/A[b]	1.06 (25,27)	1.08 (36)	1.07
13-Apr-99	1.06 (11,14,15)	1.07 (26)	1.04 (35,36)	1.06
24-Dec-99	1.10 (16)	1.12 (26)	1.07 (35,36)	1.10
20-May-00	1.04 (10,14)	N/A[b]	1.04 (35,36)	1.04
30-Nov-00	1.06 (14,17)	N/A[b]	1.05 (36)	1.05
17-May-01	1.05 (10,17)	N/A[b]	1.01 (33,34)	1.03
21-Dec-01	1.08 (14,17,22)	N/A[b]	1.07 (35)	1.08
3-May-02	1.06 (16,17,23)	N/A[b]	1.01 (34,37)	1.04
29-Dec-02	1.12 (14,17,23)	N/A[b]	1.07 (35)	1.10
13-Apr-03	1.03 (21,23)	N/A[b]	1.01 (34,35)	1.02
20-Dec-03	1.11 (17,23)	1.10 (24,30,32)	1.07 (34,35)	1.09
28-Apr-04	1.08 (17)	1.07 (29,31,32)	1.04 (38)	1.06
12-Dec-04	1.12 (14,18,23)	1.12 (29,31,32)	1.09 (38)	1.11

[a]Clear-day date, average coefficient for each WMD region, and average of all regions. Numbers in parentheses indicate stations used in the analysis (see Table 1).

[b]Comparison not possible due to lack of data or cloud cover.

3.4.3 Cloudiness Bias Correction

In an effort to correct for the cloudiness-related bias in model data, a "cloudiness" bias correction was developed using the DAILY_B satellite-estimated insolation dataset (the product of the clear-day calibration). These data were compared with pyranometer data from the "Group 3" dataset with model bias values calculated for each individual station and data day combined (but not averaged), and plotted versus "cloudiness index" (Figure 3.4). Cloudiness index is defined here as the ratio of the Daily_B satellite-estimated insolation and estimated daily clear-sky solar insolation, R_{so}.

Examination of Figure 3.4 reveals a model bias [MJ m^{-2} day^{-1}] approximated as linearly related to cloudiness by

$$Cloudiness\_bias = 4.44[Cloudiness\_index] - 2.55 \qquad (3)$$

The cloudiness bias given by Equation 3 was calculated for each comparison station and day and subtracted from the DAILY_B data, resulting in the DAILY_C dataset. Examination of this dataset revealed that the bias related to cloudiness was then found to be negligible, reflected by an increase in the coefficient of determination to 0.92 and decrease in the average RMSE from 2.2 to 1.9 MJ m^{-2} day^{-1} (Table 3.2). This improvement is also evident in Fig. 3.2: although the low end of the model data has been somewhat "raised", this affects only a small percentage of the data, and for the ultimate purpose of this dataset (the estimation of ET), this is not considered to be a significant issue since the component of ET due to solar insolation will be small on these cloudy (and/or rainy) days.

Table 3.2 reveals that with this bias correction the station and time-averaged MBE became more negative, increasing in magnitude from –0.2 to –0.8 MJ m^{-2} day^{-1}. Figure 3.3 indicates that the issues of predominantly negative model data bias, positive shift of MBE with time and seasonal MBE oscillation still remain. These issues were addressed with the next calibration step.

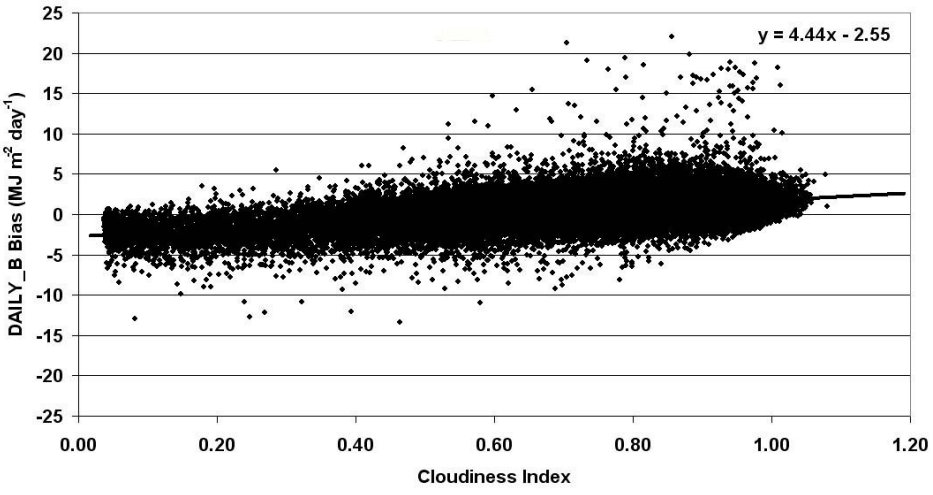

Figure 3.4: Model bias versus cloudiness index for DAILY_B dataset.

3.4.4 Monthly Bias Correction and Final Data Product

The final calibration step was the development of a monthly bias correction. DAILY_C model and "Group 3" pyranometer data were averaged over all calibration stations for each data month. The latter were then subtracted from the former, resulting in a set of monthly bias correction coefficients spanning the data period. (Note: due to data availability and time constraints, June 1996 through June 1997 coefficients were used for the June 1995 through June 1996 period. This was deemed acceptable as the most important bias features (for example the seasonal oscillation) were captured by this surrogate set of coefficients). These bias corrections were then subtracted from the DAILY_C data, giving us the final dataset, "DAILY_D". The results of this adjustment are presented in Figures 3.2 and 3.3 and Table 3.2.

The result of this procedure is that the station-averaged statistics all improved. The average RMSE and MBE values decreased in magnitude to 1.7 (10% of the mean observed value) and –0.5 MJ m^{-2} day^{-1}, respectively, and the coefficient of determination increased to 0.93. In comparison with the initial dataset (DAILY_A), the RMSE and MBE decreased in magnitude by 0.5 and 0.2 MJ m^{-2} day^{-1}, respectively, and the coefficient of determination rose by 0.03. Although the average MBE is still negative and of greater magnitude than the result of the DAILY_B calibration, Figure 3.3 shows that the effect of this calibration step was the removal of both the seasonal oscillation and the positive shift of MBE with time, with the station average ranging between about –1 to 0 MJ m^{-2} day^{-1} across the data record period.

3.5 Discussion of Calibration Issues

3.5.1 Change in Model Bias with Time

Although the gains made by this calibration work may be seen as minimal compared to the effort invested, it may have been worthwhile just to have discovered and removed the GDM model's positive shift of MBE with time as this temporal bias likely would introduce a spurious trend into computed ET. The cause of this trend is unclear. It is not a function of the number of calibration stations in the statistical average (which also generally increased with time, see Figure 3.3b) as it is also evident in single station MBE analyses. When comparing the initial dataset (DAILY_A) station-averaged MBE with that of the Otkin et al. [2005] GOES East satellite analysis over the 15 month period of their work (December 2002 to February 2004), essentially the same result is found (0.3 and 0.4 MJ m^{-2} day^{-1}, respectively), with the GDM model tending to slightly overestimate daily insolation values in both cases. Although the short length of this comparison period and the averaging of statistics are not sufficient to make any qualified conclusions, the indication, given the range of comparison site characteristics and climates of the two studies, is that something independent of these is causing this effect. It is possible that issues pertaining to the GOES satellite data may be responsible, for example sensor degradation caused by dust accumulating on the visible sensors lens itself. It is believed that in both studies, this one and that of Otkin et al. [2005], the expected effects were to see signs of the GOES-8 visible sensor's degradation with the aging of the satellite, but this was not clearly apparent. Additionally, on April 1, 2003, the GOES-12 satellite took

over operations from the GOES-8 satellite. With the fresh sensors on board the new spacecraft, we expected to see a sudden change in the model data bias, but again this was not evident in the data. It is believed that in both cases, the expected effects are not clearly seen because they are masked by the inherent limitations of the GDM model and this particular application of it. Although this issue of satellite sensor degradation has not been directly addressed, the effects of it have been indirectly corrected for through the calibration process of this work.

3.5.2 Seasonal Bias Oscillation

With regard to the seasonal oscillation observed in the model data MBE, both Pinker et al. [2003] and Otkin et al. [2005] observed such an oscillation over the 1 to 2 year periods of their analyses, with the MBE generally being more positive in the summer months. Comparing the initial dataset with the GOES East satellite analysis of Otkin et al. [2005] for the time period of their work, but now on a seasonal basis, similar station-averaged MBE values were found. As for the increase in model bias trend with time, the reason for this seasonal trend is also unclear; it is not due to cloudier conditions during the Florida summer, as (discussed in Section 3.4.3) the GDM model tends to under-estimate rather than over-estimate insolation under cloudy conditions. It may simply be due to inherent limitations of the model algorithm, for example seasonal sun-angle effects that are not accounted for. Fortunately, and regardless of the cause, this bias oscillation was estimated to be small, even in the initial dataset.

3.5.3 Comparison with Previous Studies

The RMSE of 10% of the mean observed value for the final dataset is comparable with the (un-calibrated) results of previous studies. We believe this is may be due to the complex and prevalent cloud conditions of Florida relative to previous study areas, leading to a particularly challenging application of the model. Previous studies have found that as cloudiness increased GDM model performance decreased. Gu et al. [1999] found coefficient of determination values of 0.96, 0.77 and 0.59 for half-hourly observations during clear, partly cloudy and cloudy conditions, respectively over forested regions of central Canada. Otkin et al. [2005] found similar results, with lower coefficients of determination and higher RMSE values in the complex cumulus cloud environments of summer months. The study of Jacobs et al. [2002] over northern central Florida reported a similar conclusion in comparison with studies over less convective-cloud-prone locations and seasons.

3.6. Summary

GOES satellite estimates of incoming solar radiation (insolation) for the state of Florida have been made using the model of Gautier et al. [1980] (the "GDM model") for the 10 year study period (1995 to 2004). The dataset has been produced with 2 km spatial, and half-hour and daily temporal resolution. In addition, a two-week running minimum surface albedo product was generated, also at 2 km resolution. Through comparison with ground-based pyranometer data, a series of cumulative calibration steps were developed to de-bias and fine-tune the daily-integrated insolation product.

It was found that the initial ("uncalibrated") GDM model product ("DAILY_A") performed well, but slightly poorer than previous studies, with a calibration station averaged value of the coefficient of determination of 0.90, MBE of –0.7 MJ m^{-2} day^{-1}, and RMSE of 2.2 MJ m^{-2} day^{-1} (13% of the mean observed value). The model data had a predominantly negative bias that became increasingly positive with time over the data record period. A seasonal bias oscillation was also discovered, with MBE values tending to be more positive in the summer and autumn seasons. Additionally, the model was found to over- and under-estimate solar insolation under clear and cloudy conditions, respectively, with the latter being most evident.

Following the three calibration steps, the final product ("DAILY_D") showed improvements in comparison with the initial dataset, with the station-averaged coefficient of determination increasing to 0.93, and MBE and RMSE values decreasing in magnitude to –0.5 and 1.7 MJ m^{-2} day^{-1}, respectively. Perhaps the most significant effect of this calibration effort was to remove both the positive shift of model bias with time and the seasonal bias oscillation. The final dataset RMSE (10% of the mean observed value) is comparable with the (un-calibrated) results of previous studies. We believe this may be due to the cloudy conditions of Florida relative to previous study areas, leading to a particularly challenging application of the model.

4. Net Radiation Methods

4.1 Introduction

In this particular section, we determine the net radiation and albedo estimation methods to be used to estimate PET and RET. In Section 2, the Priestley-Taylor method was selected to estimate PET. As with most standardized methods, including the Priestley-Taylor method, net radiation is one of the most important forcing data. Net radiation (RN) is defined as the difference between incoming and outgoing radiation of both short and long wavelengths where

$$RN = R_s(1-\alpha) + R_{ld} - R_{lu} \tag{4.1}$$

where R_s is the daily incoming solar radiation (W m^{-2}), α is the surface albedo, R_{ld} is the downwelling longwave radiation and R_{lu} is the upwelling longwave radiation. Measured RN is frequently not available or not accurate. Instead, net radiation is normally determined from measured or estimated solar radiation, estimates of surface albedo, and modeled longwave radiation values from ancillary meteorological data. For this project, the GOES solar radiation product was provided by University of Alabama, Huntsville as documented in section 3.

To identify a robust method to calculate net radiation, a range of methods were evaluated. Validation uses radiation measurements from eleven locations including urban, agricultural, rangeland, forest, wetland, and open water land types in central Florida. The results identify the most appropriate method to estimate net radiation and quantify the respective net radiation and potential ET error estimates by method. To estimate the 2 km albedo, existing albedo estimates by land use were identified and MODIS and GOES remotely sensed data were reviewed. This report documents the comparison of net radiation and albedo estimation methods and provides a recommendation for the most appropriate model for Florida based on these comparisons.

4.2. Study Sites

Figure 4.1 shows the eleven sites in central Florida used in the net radiation analysis (Table 4.1). The sites were installed and maintained by St. Johns River Water Management District (SJRWMD). Each site has a Kipp & Zonen CNR1 four channel radiometer installed approximately 2 meters above the canopy surfaces. The CNR1s measure incoming and outgoing shortwave and longwave radiation at 15 min intervals. Albedo and effective ground temperature values are calculated over the same time intervals. The time series data were averaged to provide daily average values. Daily average albedo was determined from the ratio of the average daily outgoing to incoming shortwave radiation. Two years of data, January 1, 2004 to December 31, 2005, were available for this analysis. Daily temperature and relative humidity data were obtained from nearby Florida Automated Weather Network (FAWN) meteorological stations.

For the albedo analyses, two additional stations operated by the U.S. Geological Survey, Blue Cypress and Duda Farms, were also included. Blue Cypress is a marsh located at longitude -80.71^{o} W, latitude 27.70 ^{o} N. Duda Farms is a grass site located at longitude -80.78^{o} W, latitude 28.27 ^{o} N. Both stations had measured climate, solar radiation, and net radiation data.

Table 4.1. Net radiometer study sites, locations, and land use.

Site	Land Use	Lat	Long	Ave. Daily Net Radiation (W/m^2)
Lake Washington	Water	28.1	-80.7	115.2
Lake Apopka	Water	28.6	-81.6	128.4
Mulberry Marsh	Wetland	27.9	-80.8	112.1
Ocklawaha Prairie	Wetland	29.1	-81.9	108.4
Jarboe Park	Urban	30.3	-81.4	107.1
Deland STP	Urban	29.0	-81.3	102.0
Bull Creek	Rangeland	28.1	-81.0	109.1
Orange Creek Restoration	Rangeland	29.5	-82.1	97.7
Denver Rd	Forest	29.4	-81.6	117.9
Hastings IFAS[1]	Agriculture	29.7	-81.4	N/A
Lindsey Citrus	Agriculture	27.6	-80.6	117.3

[1]Partial Years

4.3. Net Radiation

Two approaches are considered to estimate net radiation. The first approach uses simplified radiation based equations where net radiation is estimated from shortwave radiation through the use of linear regressions (Pinker et al., 1995). The second approach determines each of the four components of net radiation as well as surface albedo. Solar radiation is provided by the GOES product. Surface albedo, and modeled longwave radiation values are estimated using ancillary meteorological data as discussed in Section 4.3.2. This section compares results using both approaches.

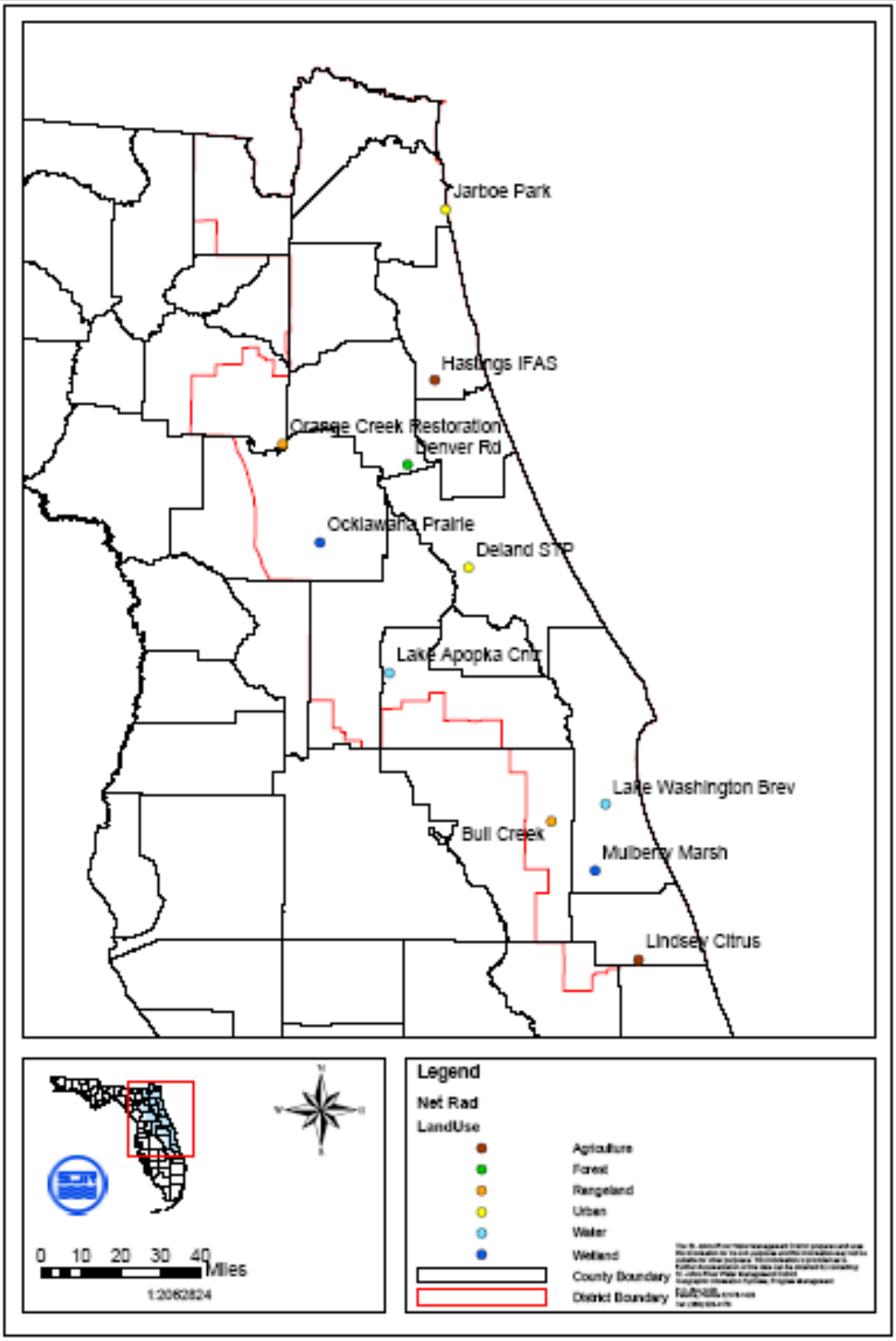

Figure 4.1. Eleven net radiation experimental sites run by SJRWMD.

4.3.1 Solar Radiation Regression

The most commonly used forms of simplified radiation based equations, net radiation estimated from shortwave radiation through the use of linear regressions, are:

$$RN = a_1 R_s + b_1 \text{ and} \tag{4.2}$$

$$RN = a_2 R_s (1 - \alpha) + b_2 \tag{4.3}$$

where a_1, a_2, b_1, and b_2 are regression coefficients. This type of regression ignores the effect of net longwave radiation, which may vary considerably with cloud cover. While studies have shown that cloud cover has little effect on net radiation or evapotranspiration estimates in arid terrain (Llasat and Snyder, 1998), this is not the case in humid climates, where cloud cover is much more varied. The empirical regression equations (4.2) and (4.3) were used to estimate daily values of net radiation. The 2004 data were used to calibrate the empirical parameters. The 2005 dataset was used to validate these relationships. Table 4.2 shows that the slopes are fairly similar while the intercepts vary somewhat. Both empirical models do a reasonable job estimating net radiation using site specific parameters. RMSE values are typically on the order of 20% of the average daily, but can exceed 30% for the open water sites.

Table 4.2. Daily net radiation and incoming solar radiation data predicted using equations (4.2) and (4.3). Parameters were fit with 2004 data. 2005 data were used to determine RMSE (W/m^2).

Site	a_1	b_1	R^2	RMSE	a_2	b_2	R^2	RMSE
Lake Washington	0.674	-16.38	0.841	29.8	0.814	-28.76	0.861	27.4
Lake Apopka	0.687	-16.82	0.860	31.9	0.810	-27.00	0.867	28.8
Mulberry Marsh	0.669	-17.25	0.818	22.3	0.730	-19.79	0.820	22.4
Ocklawaha Prairie	0.609	-10.52	0.845	20.1	0.670	-14.71	0.840	20.5
Jarboe Park	0.650	-21.05	0.836	23.5	0.695	-21.85	0.840	23.1
Deland STP	0.610	-9.57	0.821	21.2	0.681	-12.36	0.823	21.0
Bull Creek	0.620	-11.32	0.812	20.7	0.757	-16.17	0.838	20.5
Orange Creek	0.602	-13.53	0.781	24.6	0.664	-20.25	0.780	23.6
Denver Rd	0.646	-11.86	0.863	27.3	0.735	-17.35	0.861	26.6
Hastings IFAS[1]	0.580	-8.35	0.879	19.0	0.625	-9.24	0.895	17.8
Lindsey Citrus	0.619	-9.04	0.844	24.1	0.687	-12.66	0.843	23.6
Average			0.836	24.0			0.843	23.2

[1]Partial Years

4.3.2 Four Component Approach

To estimate net radiation using the four component approach, incoming solar radiation, surface albedo, and upwelling and downwelling longwave radiation must be measured or estimated. Because solar radiation is provided separately, as stated earlier, only the longwave radiation values and the surface albedo values are required. This section reviews methods available to estimate each of the three components and provides a recommendation for net radiation calculation.

Net radiation is or can be strongly affected by net longwave radiation in overcast conditions (Offerle et al., 2003). Thus, direct computation of longwave radiation may provide improved net radiation estimates. Net longwave radiation (R_l) refers to the thermal emissions with wavelengths greater than 4 μm. R_l has two components, the upwelling longwave thermal radiation emitted from the earth (R_{lu}) and the longwave downwards thermal radiation emitted by the atmosphere (R_{ld}). Under clear-sky conditions at the earth's surface, net longwave radiation should be the difference between the downwelling and the upwelling radiation.

Upwelling Longwave Radiation

Longwave upwards radiation can be directly measured by a pyrgeometer with an downwards-facing black horizontal suface. It can also be calculated using surface measurements of emissivity and temperature:

$$R_{lu} = \varepsilon_s \sigma T_s^4 \qquad (4.4)$$

where ε_s is the surface emissivity, σ is the Stefan-Boltzmann constant, and T_s is the surface temperature. In practice, for daily estimates T_a is used in eqs. (4.4) instead of T_s (Brutsaert, 1982). For typical surfaces, the surface emissivity is approximately 0.97. Daily values of upwelling longwave radiation were calculated using equation (4.4) for each of the study locations. Table 4.3 shows that there is fairly good overall agreement with a small bias.

Downwelling Longwave Radiation

Longwave downwards radiation can be directly measured by a pyrgeometer with an upwards-facing black horizontal surface or estimated using atmospheric temperature and emissivity. Vertical profile soundings of humidity provide the most accurate methods to determine atmospheric emissivity. Lacking these data, R_{ld} can also be calculated using screen height measurements of vapor pressure and temperature.

Downwelling longwave radiation requires two steps; 1) estimate the clear sky radiation and 2) correct for cloud cover. This section compares methods that are available for each step.

Table 4.3. Daily clear sky upwelling longwave radiation estimated using eqn (4.4).

Site	Land Use	Measured (W/m^2)	Calculated (W/m^2)	R^2	RMSE (W/m^2)	Ratio of the Calculated to Measured
Lake Washington K&Z	Water	435.6	417.4	0.92	15.9	0.96
Lake Apopka K&Z	Water	430.7	417.7	0.74	21.1	0.97
Mulberry Marsh	Wetland	424.3	417.3	0.71	19.9	0.98
Ocklawaha Prairie	Wetland	419.9	414.3	0.96	8.9	0.99
Jarboe Park	Urban	424.8	407.9	0.94	19.5	0.96
Deland STP	Urban	418.6	411.1	0.78	18.7	0.98
Bull Creek	Rangeland	424.9	417.4	0.95	10.9	0.98
Orange Creek Restoration	Rangeland	418.4	412.2	0.97	8.8	0.99
Denver Rd	Forest	419.9	412.3	0.70	13.8	0.98
Hastings IFAS1	Agriculture	428.9	405.1	0.88	16.3	0.94
Lindsey Citrus	Agriculture	424.4	420.5	0.94	7.9	0.99
Average		424.6	413.9	0.86	14.7	0.97

Table 4.4. Methods for calculating clear sky R_{ldc} Note: e_a [mb], Temp [k]

Clear-Sky Longwave Radiation	Eqn	Variables	Source
$R_{ldc} = (a_1+a_2 e_a^{1/2})\ \sigma T_a^4$	4.6	a_1 =0.605 a_2 = 0.048	Sellers (1965)
$R_{ldc} = c_1\ (e_a/T_a)^{1/7} \sigma T_a^4$	4.7	c_1=1.24	Brutsaert (1975)
$R_{ldc} = (1\text{-}c\ \exp[-d(273\text{-}T_a)^2])\ \sigma T_a^4$	4.8	c=0.261 d=7.77X10^{-4}	Idso and Jackson (1969)
$R_{ldc} = \{a_4(1\text{-}\exp[-e_a^{(Ta/b4)}])\}\ \sigma T_a^4$	4.9	a_4 = 1.08 b_4 = 2016	Satterlund (1979)
$R_{ldc} = \varepsilon_a \sigma\ T_a^4$ $\varepsilon_a = \{1\text{-}[1+c_1(e_a/T_a)]\exp[-(c_2+c_1c_3(e_a/T_a))^{1/2}]\}$	4.10	c_1=46.5 c_2=1.20 c_3=3.0	Prata (1996)

1) Estimate clear sky radiation
The typical form of the clear sky downwelling longwave radiation relationship is

$$R_{ldc}=\varepsilon_a \sigma T_a^4 \quad (4.5)$$

where R_{ldc} is the clear sky downwelling longwave radiation (W m^{-2}), ε_a the atmospheric emissivity, σ is the Stefan-Boltzman constant (W m^{-2} K^4), and T_a is the air temperature (K). Five methods available to estimate atmospheric emissivity and clear sky downwelling longwave are listed in Table 4.4.

The clear sky analysis requires the site data to be screened to identify clear sky conditions. For clear sky downwelling longwave radiation estimation, fractional cloud cover (C) may be observed by a human or estimated by from the incoming solar radiation (Crawford and Duchon, 1999) as

$$c = 1- R_s/R_{so} \quad (4.11)$$

where R_s is the incoming solar radiation at the surface and R_{so} is the theoretical clear sky downward solar radiation. Here R_s values were obtained from site measurements. R_{so} was calculated based on day of year and latitude using the method described in FAO56 (Allen et al., 1998). For each of the study sites, we identified clear sky days as those days that had c less than 0.05.

The clear sky downwelling longwave radiation methods were analyzed using only the clear sky days and the results appear in Table 4.5. All equations overestimated measured clear sky R_{ldc}. Based on the Table 4.5 statistics, the Sellers' equations was selected as the best equation for clear sky R_{ldc} estimation. Then, we calibrated the parameters (a_1 and a_2) of the Sellers' equations using the site specific data to provide parameter estimates for the local conditions. For our 11 sites, average values of the parameters were 0.575 and 0.054, respectively. These values are quite similar to Seller's original values (0.605 and 0.048).

2) Correct for Cloud Cover
Having identified Sellers' method using local parameterizations as the preferred approach to estimate clear sky downwelling longwave radiation estimation, the next step is to correct for cloud cover. Table 4.6 reviews seven different cloudy sky correction methods. The cloudy sky analysis uses the complete set of downwelling longwave radiation measurements (01/01/2004 to 12/31/2005) which includes both clear and cloudy days. The seven methods listed in Table 4.6 were analyzed and the results appear in Table 4.7. Note that R_{ldc} was computed using Seller's equation with the site specific parameters. Table 4.7 indicates that the parameterizations of Jacobs, Crawford and Duchon, and Duarte et al. (2006) eqn (22) provided better statistics, smaller RMSE and higher R^2 than other parameterizations. Of these, Crawford and Duchon provides the best overall results The remaining three selected cloudy sky parameterizations tend to overestimate measured data.

Table 4.6. Empirical methods for calculating cloudy sky R_{ldc} Note: c is the fractional cloud cover

Cloudy-Sky Longwave Radiation	Equation	Source
$Rld = R_{ldc}(1 + 0.26c)$	12	Jacobs (1978)
$Rld = R_{ldc}(1 + 0.22c^{2.75})$	13	Maykut and Church (1973)
$Rld = R_{ldc}(1 + 0.0496c^{2.45})$	14	Sugita and Brutsaert (1993)
$Rld = R_{ldc}(1 - c^4) + 0.952c^4\sigma T_a^4$	15	Konzelmann et al. (1994)
$Rld = R_{ldc}(1 - c) + c\sigma T_a^4$	16	Crawford and Duchon (1999)
$Rld = R_{ldc}(1 + 0.242c^{0.583})$	17	Duarte et al.'s (2006) eqn (21)
$Rld = R_{ldc}(1 - c^{0.671}) + 0.990c^{0.671}\sigma T_a^4$	18	Duarte et al.'s (2006) eqn (22)

The next step was to calculate net radiation using the best performing longwave methods. Here, three clear sky methods (Sellers – eqn 4.6, Brutsaert – eqn 4.7, and Idso and Jackson – eqn 4.8) are included to show the value of the cloud cover correction. Three downwelling longwave radiation cloudy sky methods (Jacobs (1978), Crawford and Duchon (1999), and Duarte et al. (2006) eqn (22)) are analyzed. Finally, the FAO Penman approach of net radiation described in the FAO No.58 report using the site specific albedo is included. The goal of this analysis is to examination the effect of longwave calculations on net radiation predictions. Thus, site specific measured daily albedo and solar radiation are used in the calculation.

The results in Table 4.8 show that the net radiation estimations using any of the three cloudy sky parameterizations give better results than the using only the clear sky approaches. As expected, clear sky net radiation estimations tend to underestimate measured data, while cloudy sky net radiation tend to overestimate measured data. Based on these results, the recommended approach to calculate downwelling longwave radiation is to use the Seller's equation with the parameters $a_1 = 0.575$and $a_2 = 0.054$ to estimate the clear sky radiation and the Crawford and Duchon (1999) method to correct for cloudy conditions.

Albedo

The final step in the four component calculation of net radiation is to identify a means to estimate surface albedo. Ultimately, each 2 km grid cell will require an albedo estimate. To estimate the 2 km albedo, three approaches were considered including estimating albedo by land use, using measured albedo values to provide estimates, and using MODIS or GOES remotely sensed data.

A review of the site specific daily albedo measurements provides some insight as to typical albedo values across Florida land uses. Average daily albedo values calculated by site are listed in Table 4.9. Lake Washington was removed from this analysis due to sampling problems (personal communication with G. Robinson, SJRWMD). These

values were typically between 0.10 and 0.20. A much lower value, 0.062 was observed for the open water site. The largest average value was found for Orange Creek, a rangeland site. Albedo values were sometimes similar for comparable land uses. Some land uses (rangeland and urban) had large differences between sites. This likely reflects the highly heterogeneous nature of some land uses.

Most sites exhibited an annual cycle. The highest albedo values are in December and the lowest values in July (Figure 4.2). Differences between the low and high values were on the order of 0.05. The annual cycle was less pronounced for the citrus and forest sites. Apart from the annual cycle, day to day values are fairly consistent. Exceptions include the Mulberry wetland site and the Hasting agricultural site. The wetland variation may be due to dynamic water levels that change the relative portion of water and vegetation at the surface. The agricultural site is likely influenced by crop growth and harvest.

The first approach considered to estimate albedo was to use look-up tables populated with literature values. The available values typically were reasonable in light of the observations and were consistent with the relatively lower albedo for water. However, literature values typically included a range of values (0.10 to 0.15) that exceeded the entire range observed across sites (excluding water). Given the wide range of values, the existing measurements were considered a better estimate of Florida conditions.

The second approach was to use the site specific measurements. Because albedo values do not differ greatly across sites and no consistent values could be distinguished by landuse, constant albedo values were considered to be reasonable estimates. Two constant albedo approaches were examined. The first uses a single average albedo value determined from the measured values (0.141). The second uses two albedo values determined from the measured values for land (0.149) and for water (0.062).

The final approach was to use remote sensing albedo products. MODIS and GOES remotely sensed data were reviewed to determine their ability to provide albedo values for net radiation calculations. The MODIS products (Terra, Aqua, and Terra/Aqua combination products) are available from 2002 to present for Aqua and from 2000 to present for Terra. The time resolution is 16-day compositions for MODIS. To estimate real albedo (blue sky albedo) using MODIS black and white sky albedo, solar zenith angle and optical depth information is required. The solar zenith angle can be obtained using existing equations or MODIS products. The optical depth can be obtained by MODIS atmospheric product (MOD 04 aerosol product that has four or five values by each date). However, we found that intensive pre-processing and post-processing efforts was required to obtain MODIS albedo products and that ongoing efforts are required (personnel communication, researchers at University of California Berkley and Tufts University). Thus we concluded that no consistent, reliable MODIS solution can be expected in the near future.

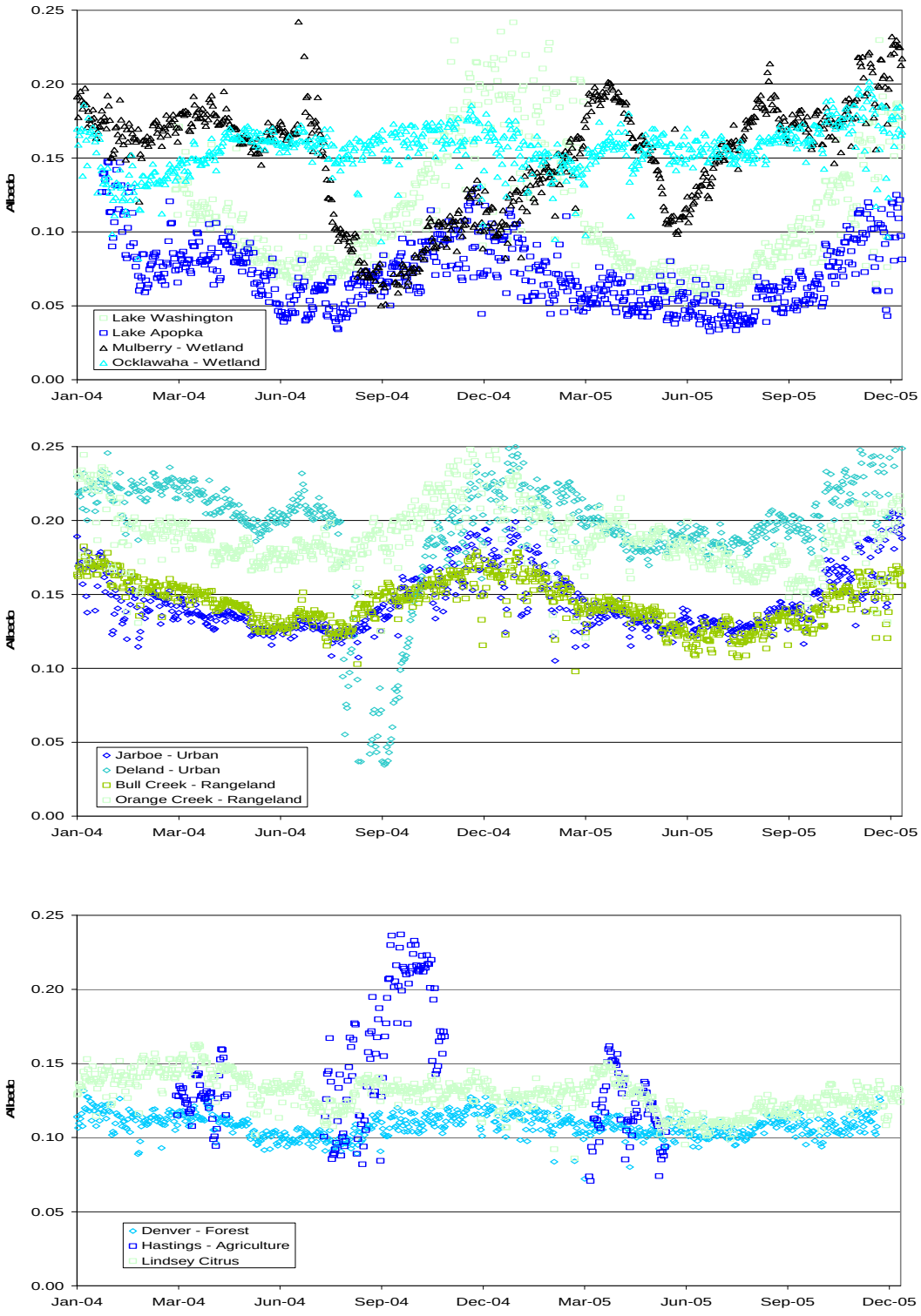

Figure 4.2. Daily albedo values by site.

Table 4.9. Annual average measured albedo values

Site	Land Use	Mean Albedo
Lake Apopka K&Z	Water	0.062
Mulberry Marsh	Wetland	0.162
Ocklawaha Prairie	Wetland	0.160
Jarboe Park	Urban	0.144
Deland STP	Urban	0.202
Bull Creek	Rangeland	0.139
Orange Creek Restoration	Rangeland	0.186
Denver Rd	Forest	0.107
Hastings IFAS1	Agriculture	0.122
Lindsey Citrus	Agriculture	0.124
Average with water		0.141
Average without water		0.149

The GOES albedo is an intermediate product produced to generate the GOES solar radiation product by University of Alabama at Huntsville. After examining satellite images of all the net radiation sites, we identified the three sites that have relatively homogeneous land cover conditions over at least a 2 km footprint (Bull Creek, Denver, and Lindsey). These sites were used to compare the GOES and measured albedo. The remaining sites were not considered viable because the 2 km albedo and the local measured albedo represent different land uses. We found the GOES products consistently underestimate albedo compared to observed albedo. However, the seasonal patterns appeared to be consistent. Thus, we conducted the regional statistical method using measured values from the three sites and estimated scaled GOES albedo for 2005. A linear correction was determined by regressing the original GOES and the measured albedo scaled GOES. We found that the original GOES albedo product can be improved by average regression equation ($y = 0.634x+0.0679$ where y = scaled GOES albedo, x = original GOES albedo where R^2 values were less than 0.2). Figures 4.3 to 4.5 show the measured albedo values, the original GOES and the corrected GOES albedo values (yellow points).

Of the two remotely sensed products, the GOES albedo product appear to be viable. It is straight forward to obtain and, once corrected, appears to reasonably track the measured albedo values. Because it uses the same satellite and instrument to make measurements as the GOES solar radiation product, the albedo product was produced for the entire period of the study, at the same resolution as the solar radiation, and the satellite/instrument will have an identical lifetime. In addition, there will be no additional continuing support effort required to work with a GOES albedo product. In contrast, the MODIS albedo appears to be an active topic of research that is not ready for routine applications. Thus, only the GOES albedo products were considered for calculating net radiation.

To summarize, three approaches were considered viable means to estimate albedo; the corrected GOES albedo product, a single average albedo value determined from the measured values (0.141), and two albedo values determined from the measured values for land (0.149) and for water (0.062). Each of the three methods used in the RN calculations to determine expected error with results shown in Tables 4.10, 4.11, and 4.12. Tables 4.10, 4.11, and 4.12 calculate RN identically to Table 4.7, except the albedo values differ.

Based on these results, the Crawford and Duchon (1999) method is consistently the best method. Regarding albedo, the results indicate that all estimation approaches provide reasonable R^2 values with little difference among the methods. The RMSE values favor the use of either a single or two albedo values with a slight improvement using the latter. The GOES albedo tends to create a 6% positive bias, while the other methods slightly underestimate the measured net radiation values. Overall, the constant albedo values provided better net radiation estimates than the GOES albedo. The results for the three methods may also be considered in light of the results obtained using the at site albedo (varying by day) given in Table 4.7. Table 4.7 results indicate that the estimates that could be achieved if site specific albedo values were available would have on average R^2 = 0.93, RMSE = 14.8 W m^{-2}, and a 1% positive bias. The two albedo approach gives the same R^2 = 0.93, RMSE = 16.0 W m^{-2}, and a 2% negative bias suggesting a very minor reduction in performance using a constant albedo rather than site specific values. Overall, a modest improvement in performance is evident when using two albedos as compared to one. However, both the literature and the Lake Apopka results indicate a lower albedo for water as compared to land which in turn will effectively increase net radiation and potential ET. Based on these results, the two albedo approach that distinguishes between the land albedo (0.149) and the water albedo (0.062) is recommended for use in net radiation calculations for Florida.

4.3.3 Net Radiation Recommendation

The two net radiation approaches examined in sections 4.3.1 and 4.3.2 suggest that the inherently more complicated four component method yields decidedly better results than the regression approach. Based on these results, the Crawford and Duchon (1999) method using the two albedo values determined from the measured values for land (0.149) and for water (0.062) is recommended for use in Florida net radiation calculations. This recommendation is based on model parsimony, estimation uncertainty, ease of use, availability of data. While albedo from satellite is a promising approach, further research is needed before it can be reasonably applied for operational purposes.

Table 4.5. Daily clear sky downwelling longwave radiation estimation using five equations in Table 4.4 and local calibration for Sellers' equation

Rldc Clear Sky		Sellers local calibration		R^2						Ratio of the Calculated to Measured					
Site	Land Use	a1	a2	Seller	Brutsaert	Idso	satterlund	Prata	Local	Seller	Brutsaert	Idso	satterlund	Prata	Local
Lake Washington K&Z	Water	0.578	0.057	0.926	0.928	0.905	0.919	0.926	0.927	0.996	1.013	1.017	1.058	1.022	1.000
Lake Apopka K&Z	Water	0.632	0.041	0.875	0.875	0.850	0.865	0.876	0.873	0.993	1.008	1.018	1.059	1.019	1.000
Mulberry Marsh	Wetland	0.560	0.055	0.910	0.911	0.894	0.904	0.911	0.912	1.031	1.046	1.057	1.099	1.058	1.000
Ocklawaha Prairie	Wetland	0.588	0.049	0.801	0.806	0.776	0.795	0.802	0.802	1.016	1.032	1.042	1.082	1.043	1.000
Jarboe Park	Urban	0.565	0.057	0.900	0.904	0.880	0.898	0.900	0.901	1.012	1.028	1.028	1.077	1.039	1.000
Deland STP	Urban	0.624	0.047	0.854	0.857	0.825	0.847	0.855	0.853	0.981	0.994	1.004	1.047	1.006	1.000
Bull Creek	Rangeland	0.585	0.047	0.793	0.800	0.758	0.788	0.794	0.793	1.034	1.047	1.061	1.106	1.061	1.000
Orange Creek Restoration	Rangeland	0.530	0.064	0.867	0.877	0.820	0.857	0.868	0.874	1.037	1.047	1.067	1.110	1.064	1.000
Denver Rd	Forest	0.573	0.058	0.927	0.932	0.898	0.920	0.929	0.930	0.999	1.013	1.022	1.065	1.025	1.000
Hastings IFAS1	Agriculture	0.553	0.057	0.810	0.811	0.831	0.834	0.813	0.803	1.025	1.047	1.040	1.086	1.052	1.000
Lindsey Citrus	Agriculture	0.540	0.060	0.878	0.880	0.845	0.869	0.879	0.882	1.032	1.049	1.055	1.100	1.059	1.000
Average		0.575	0.054	0.867	0.871	0.844	0.863	0.868	0.868	1.014	1.029	1.037	1.081	1.041	1.000

			RMSE						Calculated Rldc					
Site	Land Use	Measured	Seller	Brutsaert	Idso	satterlund	Prata	Local	Seller	Brutsaert	Idso	satterlund	Prata	Local
Lake Washington K&Z	Water	306.9	8.9	9.8	11.5	20.4	11.1	8.6	305.6	311.0	312.2	324.7	313.6	306.7
Lake Apopka K&Z	Water	300.6	10.8	11.9	12.7	20.7	12.1	10.5	298.6	303.0	306.0	318.2	306.4	300.6
Mulberry Marsh	Wetland	288.9	12.7	16.2	19.4	30.3	19.0	9.0	297.8	302.0	305.5	317.6	305.5	288.9
Ocklawaha Prairie	Wetland	295.8	16.1	18.3	20.5	28.9	19.9	15.3	300.6	305.1	308.3	320.1	308.5	295.7
Jarboe Park	Urban	291.6	10.7	13.0	13.9	24.8	15.1	10.0	295.0	299.8	299.6	313.9	302.9	291.6
Deland STP	Urban	297.1	12.5	11.7	12.1	18.0	11.2	11.1	291.3	295.2	298.1	311.1	299.0	297.1
Bull Creek	Rangeland	281.7	13.5	16.7	20.1	31.4	19.7	9.5	291.3	295.0	299.0	311.7	298.9	281.9
Orange Creek Restoration	Rangeland	277.4	14.5	16.5	22.0	32.4	20.5	10.0	287.7	290.6	295.9	308.0	295.2	277.5
Denver Rd	Forest	296.1	9.1	9.7	12.6	21.5	11.6	8.9	295.7	300.0	302.6	315.2	303.5	296.2
Hastings IFAS1	Agriculture	303.1	14.0	18.2	16.9	28.7	19.6	11.8	310.7	317.3	315.4	329.3	318.9	303.0
Lindsey Citrus	Agriculture	290.8	12.5	16.5	18.5	30.3	19.0	8.2	300.0	305.0	306.7	319.8	307.9	290.8
Average		293.6	12.3	14.4	16.4	26.1	16.3	10.3	297.6	302.2	304.5	317.2	305.5	293.6

Table 4.7. Daily cloudy sky downwelling longwave radiation estimation using seven parameterizations in Table 4.3

Rldc Cloudy Sky			R^2							Ratio of the Calculated to Measured						
Site	Land Use		Jacobs	May&Chu	Sug&Bru	Konzel	Cra&Duc	Duarte (21)	Duarte (22)	Jacobs	May&Chu	Sug&Bru	Konzel	Cra&Duc	Duarte (21)	Duarte (22)
Lake Washington K&Z	Water		0.809	0.783	0.753	0.763	0.817	0.825	0.827	1.040	0.985	0.953	0.972	1.022	1.067	1.035
Lake Apopka K&Z	Water		0.678	0.661	0.633	0.651	0.688	0.694	0.698	1.018	0.965	0.949	0.961	1.013	1.050	1.032
Mulberry Marsh	Wetland		0.711	0.673	0.666	0.671	0.732	0.726	0.745	1.010	0.956	0.942	0.946	1.002	1.043	1.024
Ocklawaha Prairie	Wetland		0.900	0.869	0.801	0.849	0.912	0.898	0.909	1.034	0.977	0.962	0.967	1.025	1.066	1.046
Jarboe Park	Urban		0.946	0.930	0.878	0.912	0.957	0.949	0.957	1.038	0.983	0.968	0.972	1.023	1.070	1.041
Deland STP	Urban		0.799	0.766	0.740	0.764	0.822	0.809	0.823	1.044	0.984	0.966	0.969	1.022	1.075	1.039
Bull Creek	Rangeland		0.888	0.849	0.798	0.829	0.899	0.890	0.903	1.007	0.949	0.936	0.939	1.003	1.039	1.027
Orange Creek Restoration	Rangeland		0.940	0.910	0.850	0.892	0.956	0.936	0.954	1.044	0.986	0.971	0.975	1.031	1.076	1.051
Denver Rd	Forest		0.751	0.728	0.731	0.733	0.769	0.769	0.776	1.052	0.992	0.975	0.978	1.030	1.084	1.047
Hastings IFAS1	Agriculture		0.912	0.864	0.802	0.837	0.927	0.917	0.931	1.035	0.981	0.967	0.970	1.023	1.067	1.043
Lindsey Citrus	Agriculture		0.903	0.880	0.840	0.862	0.922	0.910	0.924	1.038	0.978	0.965	0.967	1.023	1.072	1.044
Average			0.840	0.810	0.772	0.797	0.855	0.847	0.859	1.033	0.976	0.959	0.965	1.020	1.064	1.039
			RMSE							Calculated Rldc						
Site	Land Use	Measured	Jacobs	May&Chu	Sug&Bru	Konzel	Cra&Duc	Duarte (21)	Duarte (22)	Jacobs	May&Chu	Sug&Bru	Konzel	Cra&Duc	Duarte (21)	Duarte (22)
Lake Washington K&Z	Water	380.4	26.8	22.3	25.9	24.6	18.6	34.4	20.0	395.7	374.8	362.6	369.9	388.7	405.7	393.8
Lake Apopka K&Z	Water	372.4	27.6	29.1	32.5	31.2	24.2	32.2	24.6	379.2	359.4	353.4	358.0	377.1	390.9	384.1
Mulberry Marsh	Wetland	368.9	28.2	32.7	35.3	34.4	24.8	31.4	24.9	372.7	352.6	347.6	348.9	369.7	384.6	377.9
Ocklawaha Prairie	Wetland	363.8	17.3	21.5	27.7	24.8	13.1	24.8	16.5	376.2	355.4	350.1	351.6	372.9	387.9	380.6
Jarboe Park	Urban	363.2	16.6	18.1	24.6	21.7	9.7	24.6	12.3	377.0	357.0	351.4	353.0	371.4	388.5	378.0
Deland STP	Urban	369.6	25.4	25.0	28.9	27.4	19.2	32.2	20.7	385.7	363.6	357.1	358.2	377.6	397.3	383.9
Bull Creek	Rangeland	367.6	16.6	27.3	32.7	30.7	14.3	20.7	15.7	370.0	348.8	344.0	345.3	368.6	381.9	377.5
Orange Creek Restoration	Rangeland	359.3	21.1	18.0	24.2	20.7	13.0	30.3	18.0	375.0	354.1	348.8	350.3	370.4	386.6	377.8
Denver Rd	Forest	367.7	30.4	26.5	28.5	27.7	23.5	37.1	25.2	386.9	364.8	358.6	359.7	378.7	398.6	385.0
Hastings IFAS1	Agriculture	363.4	16.4	18.8	24.1	22.3	10.8	24.1	14.1	376.2	356.3	351.4	352.3	371.6	387.9	379.1
Lindsey Citrus	Agriculture	371.2	20.1	18.9	23.4	22.0	12.7	28.8	16.7	385.3	363.1	358.2	358.9	379.7	397.8	387.5
Average		368.0	22.4	23.5	28.0	26.1	16.7	29.1	19.0	380.0	359.1	353.0	355.1	375.1	391.6	382.3

Table 4.8. Daily net radiation estimates calculated using albedo measured at sites. Methods include clear sky (Eqn 4.6, .7, and 4.8), cloudy sky parameterizations of Jacobs (1978), Crawford and Duchon (1999), and Duarte et al. (2006) eqn (22), and ASCE method.

		RN			R^2				RMSE							Ratio of the Calculated to Measured						
Site	Land Use	Eq 6	Eq 7	Eq 8	Jacobs	Cra&Duc	Duarte (22)	ASCE	Eq 6	Eq 7	Eq 8	Jacobs	Cra&Duc	Duarte (22)	ASCE	Eq 6	Eq 7	Eq 8	Jacobs	Cra&Duc	Duarte (22)	ASCE
Lake Washington K&Z	Water	0.94	0.95	0.93	0.91	0.93	0.93	0.96	27.4	21.8	28.1	25.7	19.8	23.0	22.6	0.85	0.93	0.87	1.14	1.07	1.12	1.16
Lake Apopka K&Z	Water	0.93	0.94	0.91	0.86	0.86	0.87	0.95	27.0	22.0	28.1	26.2	24.9	26.9	22.3	0.87	0.94	0.89	1.07	1.04	1.09	1.14
Mulberry Marsh	Wetland	0.91	0.92	0.89	0.86	0.87	0.87	0.95	28.6	22.5	28.8	21.0	20.7	21.2	19.8	0.81	0.89	0.83	1.00	0.97	1.05	1.14
Ocklawaha Prairie	Wetland	0.92	0.93	0.90	0.93	0.95	0.95	0.95	29.6	24.1	30.5	14.5	12.3	12.8	20.1	0.81	0.89	0.83	1.01	0.98	1.04	1.15
Jarboe Park	Urban	0.93	0.94	0.91	0.96	0.98	0.98	0.97	26.4	23.3	29.2	19.7	12.8	17.5	24.4	0.88	0.96	0.87	1.12	1.07	1.13	1.21
Deland STP	Urban	0.94	0.95	0.92	0.94	0.97	0.97	0.97	32.9	26.0	33.6	14.7	9.1	10.5	13.9	0.73	0.82	0.74	1.07	0.99	1.05	1.10
Bull Creek	Rangeland	0.91	0.92	0.89	0.89	0.89	0.89	0.95	27.5	22.0	28.4	18.3	18.2	18.8	21.9	0.86	0.95	0.88	0.98	0.97	1.05	1.17
Orange Creek Restoration	Rangeland	0.91	0.93	0.89	0.94	0.97	0.97	0.97	28.2	23.5	29.8	17.3	10.7	14.1	22.1	0.82	0.91	0.84	1.07	1.03	1.10	1.20
Denver Rd	Forest	0.94	0.95	0.92	0.95	0.98	0.98	0.97	30.8	24.2	32.2	16.9	9.2	12.2	16.5	0.80	0.87	0.81	1.08	1.01	1.06	1.12
Hastings IFAS1	Agriculture	0.91	0.91	0.90	0.95	0.96	0.96	0.95	24.6	21.8	26.9	15.3	11.7	16.5	27.3	0.92	1.00	0.92	1.06	1.02	1.08	1.20
Lindsey Citrus	Agriculture	0.94	0.95	0.91	0.92	0.94	0.94	0.97	27.4	20.7	28.6	15.6	13.7	14.7	18.1	0.82	0.90	0.83	1.03	0.98	1.05	1.13
Average		0.92	0.94	0.91	0.92	0.93	0.94	0.96	28.2	22.9	29.5	18.7	14.8	17.1	20.8	0.84	0.92	0.85	1.06	1.01	1.08	1.16

Table 4.10. Daily net radiation estimates calculated using GOES albedo. Methods include clear sky (Eq 4.6, 4.7, and 4.8), cloudy sky parameterizations of Jacobs (1978), Crawford and Duchon (1999), and Duarte et al. (2006) eqn (22), and ASCE method.

RN		R^2							RMSE							Ratio of the Calculated to Measured						
Site	Land Use	Eq 6	Eq 7	Eq 8	Jacobs	Cra&Duc	Duarte (22)	ASCE	Eq 6	Eq 7	Eq 8	Jacobs	Cra&Duc	Duarte (22)	ASCE	Eq 6	Eq 7	Eq 8	Jacobs	Cra&Duc	Duarte (22)	ASCE
Lake Washington K&Z	Water	0.92	0.93	0.90	0.91	0.92	0.92	0.94	27.2	21.9	28.5	25.5	20.2	24.1	25.3	0.87	0.95	0.89	1.15	1.09	1.14	1.18
Lake Apopka K&Z	Water	0.91	0.92	0.89	0.85	0.85	0.85	0.94	29.9	23.8	30.9	25.7	25.3	26.2	20.5	0.84	0.91	0.86	1.04	1.01	1.06	1.11
Mulberry Marsh	Wetland	0.90	0.92	0.89	0.88	0.88	0.88	0.94	26.2	24.1	27.9	24.7	23.1	27.3	30.9	0.91	0.99	0.92	1.10	1.07	1.14	1.24
Ocklawaha Prairie	Wetland	0.91	0.92	0.89	0.93	0.94	0.94	0.94	28.2	26.3	30.3	21.3	17.4	22.0	31.3	0.91	0.99	0.93	1.10	1.07	1.14	1.25
Jarboe Park	Urban	0.91	0.92	0.89	0.95	0.96	0.96	0.96	28.7	28.9	31.3	28.9	22.4	28.2	35.7	0.98	1.06	0.96	1.21	1.16	1.22	1.30
Deland STP	Urban	0.92	0.93	0.90	0.94	0.96	0.96	0.95	27.9	25.5	30.3	28.0	21.1	26.3	30.8	0.89	0.97	0.90	1.22	1.15	1.21	1.26
Bull Creek	Rangeland	0.90	0.91	0.88	0.90	0.89	0.89	0.94	26.4	23.6	28.2	20.2	19.8	23.5	29.9	0.93	1.02	0.95	1.05	1.04	1.11	1.24
Orange Creek Restoration	Rangeland	0.89	0.91	0.86	0.95	0.96	0.96	0.95	29.7	30.3	33.0	31.0	24.9	30.9	39.9	1.00	1.08	1.01	1.24	1.20	1.27	1.37
Denver Rd	Forest	0.93	0.94	0.91	0.94	0.96	0.96	0.96	31.0	25.1	32.6	19.5	12.4	15.5	19.6	0.81	0.89	0.82	1.10	1.03	1.08	1.13
Hastings IFAS1	Agriculture	0.83	0.84	0.84	0.88	0.89	0.89	0.88	29.2	30.2	30.7	26.8	23.4	28.9	39.6	1.01	1.08	1.01	1.14	1.10	1.16	1.28
BlueCypress	Sawgrass	0.92	0.93	0.89	0.90	0.91	0.91	0.93	28.3	23.4	29.8	20.5	18.2	20.5	24.6	0.86	0.94	0.86	1.06	1.02	1.08	1.16
DudaFarm	Pasture	0.98	0.98	0.97	0.95	0.96	0.97	0.97	39.7	32.1	38.0	18.4	17.4	10.1	9.8	0.63	0.69	0.65	0.80	0.79	0.86	0.92
Lindsey Citrus	Agriculture	0.95	0.96	0.95	0.93	0.94	0.95	0.95	28.6	25.2	28.8	16.7	14.5	17.2	24.1	0.90	0.96	0.91	1.02	1.01	1.07	1.17
Average		0.91	0.92	0.90	0.92	0.93	0.93	0.94	29.3	26.2	30.8	23.6	20.0	23.1	27.9	0.89	0.96	0.90	1.10	1.06	1.12	1.20

Table 4.11. Daily net radiation estimates calculated using a constant annual average albedo (With water albedo = 0.141). Methods include clear sky (Eq 4.6, 4.7, and 4.8), cloudy sky parameterizations of Jacobs (1978), Crawford and Duchon (1999), and Duarte et al. (2006) eqn (22), and ASCE method.

		RN			R^2				RMSE							Ratio of the Calculated to Measured						
Site	Land Use	Eq 6	Eq 7	Eq 8	Jacobs	Cra&Duc	Duarte (22)	ASCE	Eq 6	Eq 7	Eq 8	Jacobs	Cra&Duc	Duarte (22)	ASCE	Eq 6	Eq 7	Eq 8	Jacobs	Cra&Duc	Duarte (22)	ASCE
Lake Apopka K&Z	Water	0.91	0.93	0.90	0.84	0.84	0.84	0.95	36.9	28.9	36.8	26.6	28.0	25.7	15.9	0.76	0.83	0.77	0.96	0.92	0.98	1.03
Mulberry Marsh	Wetland	0.90	0.91	0.88	0.88	0.87	0.87	0.94	27.8	22.4	28.5	20.4	19.9	21.5	22.3	0.83	0.91	0.85	1.02	1.00	1.07	1.16
Ocklawaha Prairie	Wetland	0.91	0.93	0.89	0.93	0.95	0.95	0.95	28.5	23.8	29.8	15.1	12.0	14.4	22.9	0.84	0.92	0.86	1.03	1.00	1.07	1.18
Jarboe Park	Urban	0.91	0.93	0.89	0.96	0.98	0.97	0.97	26.8	23.5	29.8	18.5	12.2	17.2	24.6	0.88	0.97	0.87	1.12	1.07	1.13	1.21
Deland STP	Urban	0.91	0.92	0.89	0.94	0.96	0.96	0.96	28.3	23.6	30.2	21.1	14.3	19.2	23.7	0.83	0.91	0.84	1.16	1.09	1.15	1.20
Bull Creek	Rangeland	0.90	0.91	0.88	0.90	0.89	0.89	0.95	27.7	22.1	28.8	17.4	17.7	18.6	22.2	0.86	0.95	0.88	0.98	0.97	1.05	1.17
Orange Creek Restoration	Rangeland	0.89	0.91	0.86	0.95	0.97	0.96	0.95	27.0	25.1	29.9	22.5	16.1	22.0	31.4	0.92	1.00	0.94	1.17	1.12	1.19	1.29
Denver Rd	Forest	0.93	0.95	0.91	0.94	0.97	0.97	0.97	35.2	27.6	36.2	14.2	10.2	9.3	12.2	0.75	0.82	0.76	1.03	0.96	1.01	1.06
Hastings IFAS1	Agriculture	0.85	0.86	0.85	0.91	0.92	0.92	0.91	27.0	24.4	28.7	18.4	15.7	19.6	29.0	0.92	1.00	0.92	1.06	1.02	1.08	1.20
Lindsey Citrus	Agriculture	0.92	0.94	0.90	0.92	0.93	0.93	0.96	29.4	22.2	30.6	15.1	14.6	14.5	17.0	0.81	0.89	0.81	1.01	0.97	1.03	1.11
BlueCypress	Sawgrass	0.98	0.98	0.97	0.95	0.97	0.98	0.97	43.8	35.9	41.8	22.1	21.5	13.2	9.2	0.59	0.65	0.61	0.76	0.76	0.82	0.89
DudaFarm	Pasture	0.95	0.96	0.95	0.93	0.95	0.95	0.95	30.3	25.1	30.1	15.1	13.4	13.0	18.0	0.84	0.91	0.86	0.97	0.96	1.02	1.12
Average		0.91	0.93	0.90	0.92	0.93	0.93	0.95	30.7	25.4	31.8	18.9	16.3	17.3	20.7	0.82	0.90	0.83	1.02	0.99	1.05	1.14

Table 4.12. Daily net radiation estimates calculated using a constant annual average albedo for water (0.062) and land (0.149). Methods include clear sky (Eq 4.6, 4.7, and 4.8), cloudy sky parameterizations of Jacobs (1978), Crawford and Duchon (1999), and Duarte et al. (2006) eqn (22), and ASCE method.

		RN			R^2				RMSE							Ratio of the Calculated to Measured						
Site	Land Use	Eq 6	Eq 7	Eq 8	Jacobs	Cra&Duc	Duarte (22)	ASCE	Eq 6	Eq 7	Eq 8	Jacobs	Cra&Duc	Duarte (22)	ASCE	Eq 6	Eq 7	Eq 8	Jacobs	Cra&Duc	Duarte (22)	ASCE
Lake Apopka K&Z	Water	0.91	0.92	0.89	0.86	0.86	0.86	0.95	27.0	22.2	28.5	26.3	25.1	27.4	23.8	0.75	0.81	0.76	1.08	1.05	1.10	1.01
Mulberry Marsh	Wetland	0.90	0.91	0.88	0.87	0.87	0.87	0.94	28.5	22.7	29.0	20.3	20.0	20.9	21.0	0.82	0.90	0.83	1.01	0.98	1.05	1.15
Ocklawaha Prairie	Wetland	0.91	0.93	0.89	0.93	0.95	0.95	0.95	29.0	24.0	30.2	14.7	12.0	13.4	21.5	0.83	0.91	0.85	1.02	0.99	1.06	1.16
Jarboe Park	Urban	0.92	0.93	0.89	0.96	0.98	0.97	0.97	27.2	23.3	30.1	17.3	11.1	15.8	23.1	0.87	0.95	0.86	1.11	1.06	1.12	1.19
Deland STP	Urban	0.91	0.92	0.89	0.94	0.96	0.96	0.96	28.9	23.8	30.6	19.8	13.2	17.8	22.3	0.81	0.89	0.82	1.15	1.08	1.14	1.19
Bull Creek	Rangeland	0.90	0.91	0.88	0.89	0.89	0.89	0.95	28.5	22.4	29.4	17.5	18.0	18.1	20.7	0.85	0.93	0.87	0.97	0.96	1.03	1.16
Orange Creek Restoration	Rangeland	0.89	0.91	0.86	0.95	0.97	0.96	0.95	27.1	24.6	29.8	21.2	14.8	20.5	29.8	0.90	0.99	0.92	1.15	1.11	1.18	1.28
Denver Rd	Forest	0.93	0.95	0.91	0.94	0.97	0.97	0.97	36.3	28.5	37.1	14.1	11.0	9.2	11.4	0.73	0.81	0.74	1.01	0.95	1.00	1.05
Hastings IFAS1	Agriculture	0.85	0.86	0.85	0.91	0.92	0.92	0.91	27.3	24.1	28.9	17.7	15.2	18.5	27.5	0.91	0.99	0.91	1.04	1.01	1.07	1.19
Lindsey Citrus	Agriculture	0.92	0.94	0.90	0.92	0.93	0.93	0.96	30.4	22.9	31.4	15.1	15.1	14.1	15.7	0.79	0.87	0.80	1.00	0.95	1.02	1.10
BlueCypress	Sawgrass	0.98	0.98	0.97	0.95	0.97	0.98	0.97	45.2	37.2	43.1	23.6	23.0	14.5	9.8	0.58	0.64	0.60	0.75	0.75	0.81	0.88
DudaFarm	Pasture	0.95	0.96	0.95	0.93	0.95	0.95	0.95	31.2	25.6	30.8	15.4	13.9	12.5	16.6	0.83	0.90	0.85	0.95	0.94	1.01	1.11
Average		0.91	0.93	0.90	0.92	0.93	0.93	0.95	30.5	25.1	31.6	18.6	16.0	16.9	20.3	0.81	0.88	0.82	1.02	0.98	1.05	1.12

Figure 4.3 Annual albedo cycles at Lindsey, Denver and Bull Creek. sites including the average daily measured albedo values (hollow blue), the measured albedo value at noon (hollow red), the original GOES (solid blue) and the corrected GOES albedo values (solid orange).

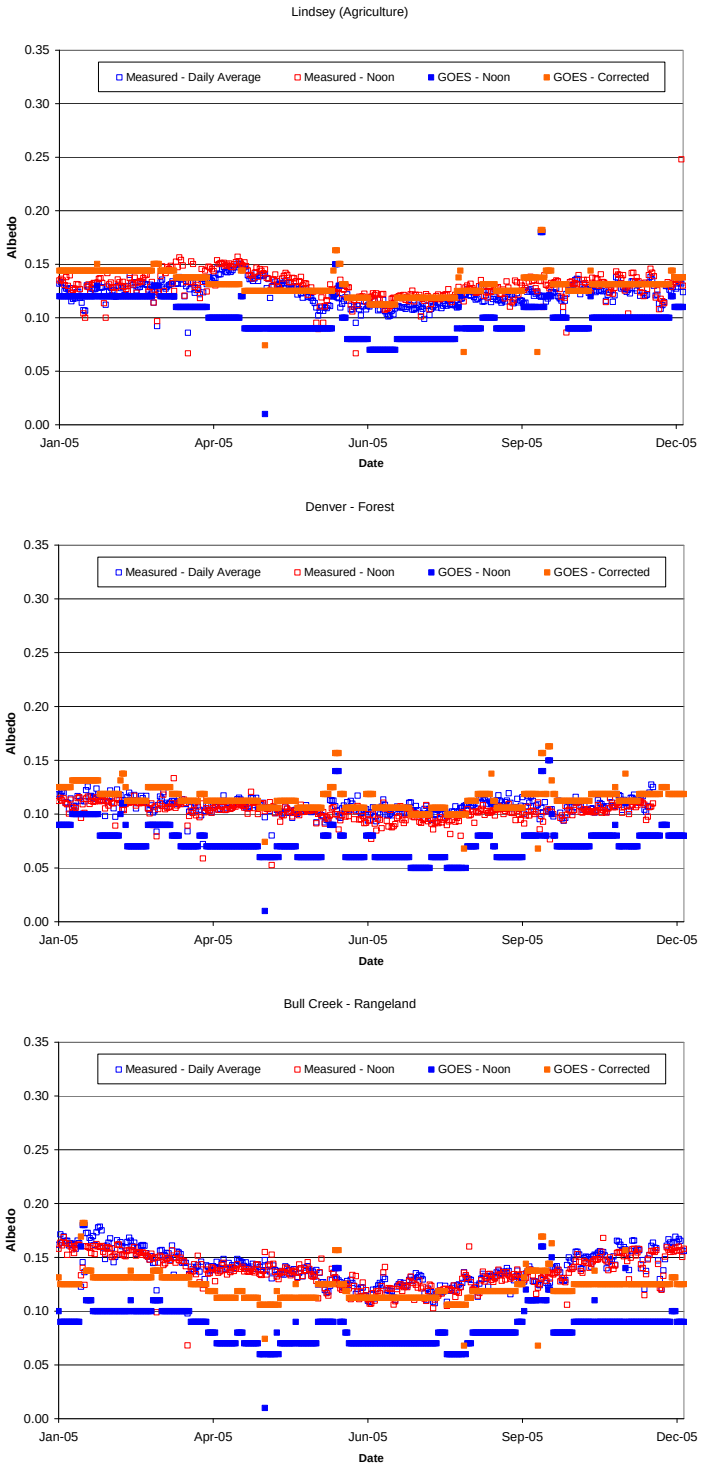

5. Daily PET and Reference ET Calculations

5.1. Introduction

This section documents the methods and datasets used to calculate PET and RET. The method selection processes are documented in earlier sections. This section is organized into two sections. Section 5.2 describes the methodologies used to calculate evapotranspiration in a general format. Section 5.2 includes the equations and references used to calculate PET and RET. It also documents the required meteorological and albedo data required to perform the PET calculations including the data source, quality assurance checks, intermediate calculations, and the interpolation algorithm. Section 5.3 includes the technical documentation of the datasets and software codes used to calculate the 10-year dataset. This section provides details on the specific input files, Fortran codes, and output files used to generate the gridded meteorological data as well as the PET and the RET values. The complete set of datasets and software codes were provided to USGS on a backup drive. Appendix 5.1 provides the directory structure and a brief description of the backup drive.

5.2. Methodology

5.2.1 PET Calculation Method

For this project the Priestley-Taylor (PT) method (Priestly and Taylor, 1972) model was selected to calculate PET (Section 2). This selection resulted from the comparison of three PET models, the SFWMD Simple method (Abtew, 1995; 1996), the Priestley-Taylor method and the Penman-Monteith (PM) method (Penman, 1948; Monteith, 1965). In summary, the Simple method only accurately estimates PET for marshland cover at a daily scale. A tradeoff exists between the PT and PM models. The PM is more accurate for small scale studies when accurate at-site parameter values are available. However, the PM model has several parameters that cannot easily be measured or estimated over large areas. In the case of open water, where there is no canopy and hence the bulk canopy resistance is zero, the PM method is superior to the other two methods. The PT method, on the other hand, is easier to use, has fewer tuning parameters, does not have a seasonal bias, and is slightly (but not statistically) more accurate over large regions. Based on these findings, the PT model was selected to calculate PET.

The Priestley-Taylor method uses the concept of the theoretical lower limit of evaporation from a wet surface as the "equilibrium" evaporation to estimate PET where

$$ET_o = \frac{1000}{\lambda \rho_w}\left[\alpha \frac{\Delta}{\Delta + \gamma}\left(R_n - G\right)\right] \qquad (5.1)$$

where ET_o is the potential evapotranspiration, mm day^{-1}, λ the latent heat of vaporization, MJ kg^{-1}, ρ_w the density of water (1000 kg m^{-3}), α the Priestley-Taylor constant (1.26), Δ the slope of the saturation vapor pressure temperature curve, kPa $^oC^{-1}$, γ the psychrometric constant (0.06737 kPa $^oC^{-1}$), R_n the net radiation, MJ m^{-2} day^{-1}, and G

the soil heat flux, MJ m^{-2} day^{-1}. Here G is assumed to equal zero over the course of a day. 1000 in the numerator on the right hand side is the conversion from m day^{-1} to mm day^{-1}.

The climate variables, solar radiation (r_s), MJ m^{-2} day^{-1}, maximum and minimum daily temperature (T_{max} and T_{min}), ºC, and maximum and minimum daily relative humidity (RH_{max} and RH_{min}), %, are used directly and indirectly in the PET equation. The average temperature (T) is computed as the average of T_{max} and T_{min}.

The parameter Δ was computed as

$$\Delta = \frac{4098 e_s}{(237.3 + T)^2} \tag{5.2}$$

where e_s is the saturated vapor pressure, kPa, computed as

$$e_s = 0.6108 \exp\left(\frac{17.27T}{237.3 + T} \right). \tag{5.3}$$

The latent heat of vaporization, MJ kg^{-1}, is determined as

$$\lambda = 1000(2.501 - 0.002361T). \tag{5.4}$$

Section 4 documented the comparisons conducted to identify a robust method to calculate net radiation. The recommended method uses the four component approach: incoming solar radiation, surface albedo, and upwelling and downwelling longwave radiation must be measured or estimated. Net radiation is the difference between incoming and outgoing radiation of both short and long wavelengths where

$$R_n = R_s(1 - \alpha) + 0.0864 \varepsilon_s R_{ld} - 0.0864 R_{lu} \tag{5.5}$$

where R_s is the daily incoming solar radiation, MJ m^{-2} day^{-1}, α is the surface albedo, ε_s is the surface emissivity, R_{ld} is the downwelling longwave radiation, W m^{-2}, R_{lu} is the upwelling longwave radiation, W m^{-2}, and 0.0864 is the conversion between W m^{-2} and MJ m^{-2} day^{-1}. Thus, net radiation is determined from measured or estimated solar radiation, estimates of surface albedo, and modeled longwave radiation values from ancillary meteorological data. For this project, the GOES solar radiation product, documented in Section 3, is used to estimate solar radiation. Constant albedo values are used for land (0.149) and for water (0.062). G. Robinson, SJRWMD in collaboration with SFWMD and USGS identified all the 2 km grid pixels as either land or water (Figure 5.1). Inland pixels were identified as water if 75% or more of the pixel contained water. Note: the Atlantic, Gulf, lagoons and bays were not identified as water in the albedo map and are coded as land. The calculated values use a land albedo for these regions.

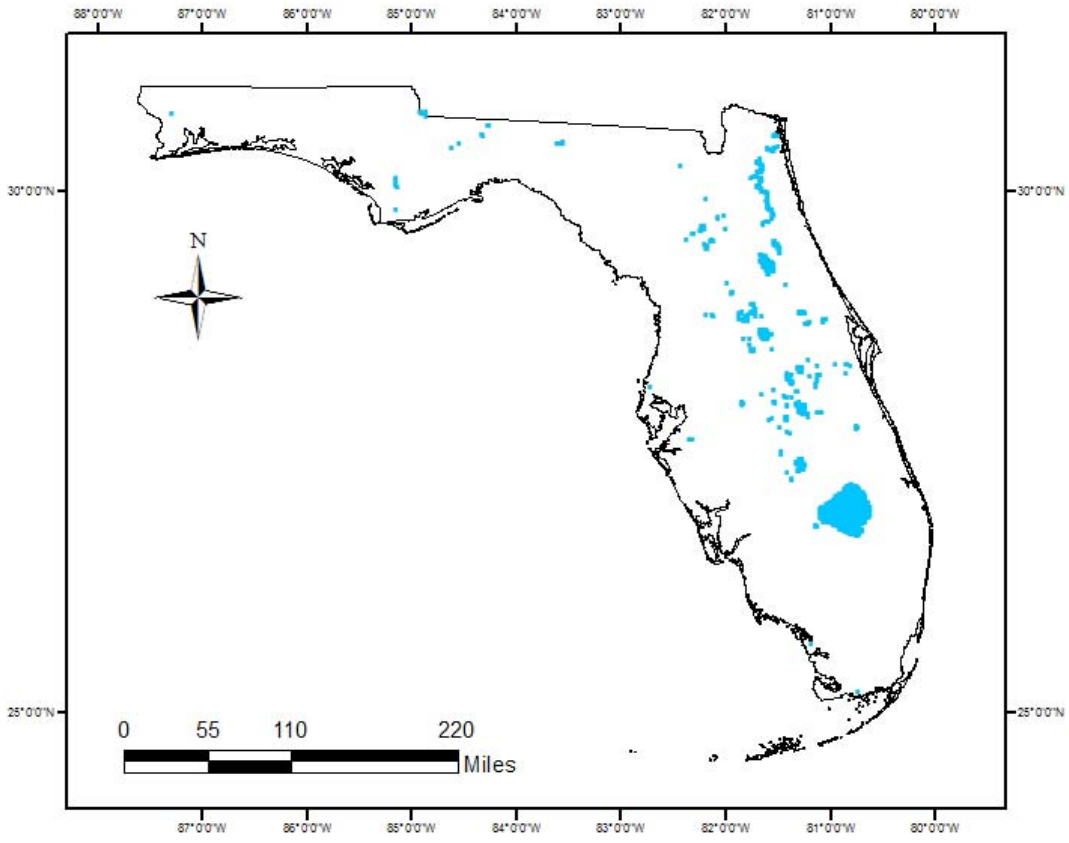

Figure 5.1. Florida inland water bodies.

Downwelling longwave radiation requires two steps; 1) estimate the clear sky radiation and 2) correct for cloud cover. The clear sky downwelling longwave radiation is determined as

$$R_{ldc} = (a_1 + a_2 e_a^{1/2}) \sigma T^4 \qquad (5.6)$$

where R_{ldc} is the clear sky downwelling longwave radiation, W m^{-2}, parameters a_1 and a_2 are 0.575 and 0.054, respectively, e_a is the atmospheric vapor pressure, mb, σ is the Stefan-Boltzman constant, W m^{-2} K^4, and T is the average air temperature, K. This equation calculates the atmospheric emissivity using Sellers' (1965) equation and Florida specific parameters.

The vapor pressure, kPa, required the saturation vapor pressure equation

$$e_o(T) = 0.6108 \exp\left(\frac{17.27T}{T + 237.3}\right). \quad (5.7)$$

Using this equation, the mean actual vapor pressure, kPa, was calculated as

$$e_a = \frac{e_o(T_{\max})\frac{RH_{\min}}{100} + e_o(T_{\min})\frac{RH_{\max}}{100}}{2}. \quad (5.8)$$

and converted from kPa to mb using a multiplier of 10.

R_{ldc} is corrected for cloud cover using the Crawford and Duchon (1999) method where

$$R_{ld} = R_{ldc}(1 - c) + c\sigma T^4 \quad (5.9)$$

where c is fractional cloud cover estimated from the incoming solar radiation (Crawford and Duchon, 1999) as

$$c = 1 - R_s/R_{so} \quad (5.10)$$

where R_s is the GOES-estimated incoming solar radiation at the surface and R_{so} is the theoretical clear sky downward solar radiation. R_{so} is calculated based on the day of year and latitude using the method described in FAO56 (Allen et al. 1998) as described in the following section.

Longwave upwards radiation is calculated using surface measurements of emissivity and temperature:

$$R_{lu} = \varepsilon_s \sigma T_s^4 \quad (5.11)$$

where ε_s is the surface emissivity, σ is the Stefan-Boltzmann constant, and T_s is the surface temperature. In practice, for daily estimates average daily T is used in eq. (5.11) instead of T_s (Brutsaert, 1982). For typical surfaces, the surface emissivity is approximately 0.97.

5.2.2 Reference ET Calculation Method

The ASCE Evapotranspiration in Irrigation and Hydrology Committee (ASCE-ET) recommends, for the intended purpose of establishing uniform evapotranspiration (ET) estimates and transferable crop coefficients, two standardized reference evapotranspiration surfaces: (1) a short crop (similar to grass) and (2) a tall crop (similar to alfalfa), and one standardized reference evapotranspiration equation based on the Penman-Monteith equation (Allen et al., 1998). As a part of the standardization, the "full" form of the Penman-Monteith equation and associated equations for calculating aerodynamic and bulk surface resistance were combined and reduced to a single equation having two constants. The derivation of equation (10) appears in Allen et al. (1998).

The standardized method used in this project is the short crop or grass reference on a daily basis. This surface has an assumed height of 0.12 m, a fixed surface resistance r_s of 70 s m^{-1}, and an albedo of 0.23. The zero plane displacement height and roughness lengths are estimated as a function of the assumed crop height, so that r_a becomes a function of only the measured wind speed. The height for the temperature, humidity, and wind measurements is assumed to be 2 m. The latent heat of vaporization (λ) is assigned a constant value of 2.45 MJ kg^{-1}.

For a grass reference on a daily basis, the reference ET method is given as

$$ET_o = \frac{0.408\,\Delta\,(R_n - G) + \gamma \frac{900}{T + 273} u_2\,(e_s - e_a)}{\Delta + \gamma\,(1 + 0.34\,u_2)} \tag{5.12}$$

where ET_o is the reference evapotranspiration, mm day^{-1}, Δ the slope of the saturation vapor pressure temperature relationship, KPa $^oC^{-1}$, γ the psychrometric constant, KPa $^oC^{-1}$ (0.06737 KPa $^oC^{-1}$), R_n the net radiation, MJ m^{-2} day^{-1}, G the soil heat flux, MJ m^{-2} day^{-1} (generally very small at daily resolution and assumed to be zero), T the average air temperature, ^oC, u_2 the wind speed at 2 m, m s^{-1}, e_s the saturation vapor pressure, KPa, and e_a the actual vapor pressure, KPa, and e_s-e_a the saturation vapor pressure deficit, KPa.

The climate variables, solar radiation (r_s), MJ m^{-2} day^{-1}, maximum and minimum daily temperature (T_{max} and T_{min}), ºC, maximum and minimum daily relative humidity (RH_{max} and RH_{min}), %, and wind speed (u), m s^{-1}, are used directly and indirectly in the RET equation. The average temperature (T) is the average of T_{max} and T_{min}.

The slope of the saturation vapor pressure temperature (Δ), KPa $^oC^{-1}$, is given by

$$\Delta = \frac{4098\left[0.6108\exp\left(\frac{17.27T}{T+237.3}\right)\right]}{(T+237.3)^2} \tag{5.13}$$

Wind speed values were converted to the 2-m prior to calculating RET using the standard procedures outlined in the Food and Agriculture Organization of the United Nations Irrigation and Drainage Paper No.56 (FAO56; Allen et al., 1998) according to the following equation:

$$u_2 = u_x \frac{4.87}{\ln(67.8z - 5.42)} \tag{5.14}$$

where u_2 is the wind speed at 2-m above ground surface (m s^{-1}), u_z is the measured wind speed at z-m above ground surface (m s^{-1}), and z is the height of measurement above ground surface (m).

The vapor pressure deficit requires the saturation vapor pressure equation

$$e_o(T) = 0.6108 \exp\left(\frac{17.27T}{T + 237.3}\right). \tag{5.15}$$

Using this equation, the mean saturation vapor pressure, KPa, is calculated as

$$e_s = \frac{e_o(T_{\max}) + e_o(T_{\min})}{2} \tag{5.16}$$

and the mean actual vapor pressure, KPa, is calculated as

$$e_a = \frac{e_o(T_{\max})\frac{RH_{\min}}{100} + e_o(T_{\min})\frac{RH_{\max}}{100}}{2}. \tag{5.17}$$

R_n is the difference between absorbed incoming shortwave solar radiation (R_{ns}) and net outgoing long-wave radiation (R_{nl}).

$$R_n = R_{ns} - R_{nl} \tag{5.18}$$

Net shortwave radiation, R_{ns} is calculated as:

$$R_{ns} = (1 - \alpha)R_s \tag{5.19}$$

where α (0.23) is the defined the albedo of grass and R_s, MJ m^{-2} day^{-1}, is the measured net radiation.

The R_{nl} calculation is somewhat more involved. The variables used to estimate R_{nl} on a daily basis are shown below. Extraterrestrial radiation, R_a is calculated as

$$R_a = \frac{24(60)}{\pi} G_{sc} d_r \left[(\omega_s)\sin(\varphi)\sin(\delta) + \cos(\varphi)\cos(\delta)\sin(\omega_s)\right] \tag{5.20}$$

where G_{sc} (0.0820 MJ m^{-2} day^{-1}) is the solar constant, d_r is the inverse relative distance between the earth and sun, φ (rad) is the solar declination, and ω_s (rad) is the sunset hour angle. These calculations require the julian day and the latitude.

Outgoing solar radiation, R_{so} is calculated as:

$$R_{so} = 0.75R_a \tag{5.21}$$

Finally, R_{nl} is calculated as

$$R_{nl} = \sigma\left[\frac{\left(T_{\max,K}\right)^4 + \left(T_{\min,K}\right)^4}{2}\right]\left(0.34 - 0.14\sqrt{e_a}\right)\left(1.35\frac{R_s}{R_{so}} - 0.35\right)$$

where σ is the Stefan-Boltzmann constant (4.903×10^{-9} MJ K^{-4} m^{-2} day^{-1}), and $T_{max,K}$ and $T_{min,K}$ are the maximum and minimum absolute temperatures (K) during the 24-hour period.

5.2.3 Meteorological Data

The reference ET and the potential ET calculations require daily meteorological data. Tables 5.1 and 5.2 summarize the required data and their sources. A quality assurance procedure was applied to measured data. A threshold analysis was applied to limit the maximum relative humidity to 100%. Temperature, relative humidity, and wind speed were assessed using graphical tools. The short periods having erroneous or missing values were replaced with an average of the previous and next day's values. Longer periods having erroneous or missing values were replaced with average recorded values using the remaining years' observations for that site and day.

5.3. Calculation Approach

Using the methods described in Section 5.2, the daily RET and PET values were calculated on an annual basis. These calculations are divided into two major steps 1) meteorological data creation and 2) evapotranspiration calculation. The meteorological data are created, then used in the evapotranspiration calculations. The complete datasets are maintained in a backup drive that includes the Fortran source code, required input files, and output files for each of these steps.

Table 5.1. Summary table of required input data sources by method.

Model Input	PT	REF ET	Source
Solar Radiation (mean)	X	X	GOES
Air Temperature (min and max)	X	X	NOAA/NCDC, FAWN
Relative Humidity (min and max)	X	X	NOAA/NCDC, WMDs, FAWN
Wind Speed (mean)		X	NOAA/NCDC, WMDs, FAWN
Incoming Longwave Radiation	X		Calculated using Air Temperature, RH, and incoming solar radiation
Outgoing Longwave Radiation	X		Calculated using Air Temperature
Albedo	X		SJRWMD RN Network Values
Land or Water	X		GIS Landcover Analysis

Table 5.2. Summary table of sources web addresses (effective November, 2007).

Source	Full Name	Source
NOAA/NCDC	National Oceanic and Atmospheric Administration (NOAA) National Climate Data Center	http://www.ncdc.noaa.gov/oa/ncdc.html
FAWN	Florida Automated Weather Network	http://fawn.ifas.ufl.edu/data/reports/
SJRWMD	St. Johns River Water Management District	http://sjr.state.fl.us/data.html
SWFWMD	Southwest Florida Water Management District	http://www.swfwmd.state.fl.us/data/
SFWMD	South Florida Water Management District: DBHydro	http://my.sfwmd.gov/

5.3.1 Meteorological Data Interpolation

The gridded meteorological data are created from point station data. The inverse distance weighting interpolation method is used to interpolate daily point (station) meteorological data to a 2 km grid scale on an annual basis for each meteorological variable. The five meteorological variables, wind speed, minimum temperature, maximum temperature, minimum relative humidity, and maximum relative humidity, each require a separate interpolation.

For each year, all available data sources documented in section 5.2 were reviewed to identify meteorological stations having a reasonably complete record for the year and one or more meteorological variables. Table 2 lists the meteorological web sites reviewed. Available data were downloaded from the source website into an Excel spreadsheet. The data QA/QC process was performed in Excel. Stations having large periods of missing or bad data were not used for that year. However, if some of the station meteorological data were considered good quality for one variable (e.g., temperature), but another variable had poor quality data (e.g., relative humidity), the good quality data from that station were still used.

Because there was a robust network of temperature stations available from NOAA NCDC and the FAWN network, no WMD temperature data were used. Temperature data were obtained from NCDC, graphically reviewed, and a data quality flag was assigned to the dataset. The data quality flag was left blank if no data were available from the station, X if the year's data were good. Flags 991, 992, …, 999 were used to indicate that data were available, but that there were some data problems. The flag value indicated the extent of the data's problems. A 991 flag indicated minor problems while a 999 flag indicated major problems. No data having 991 to 999 flags were used. The stations and data quality flags appear in the data archive (station_t_all.xls) as well as Appendix 5.1.

In addition to the NOAA NCDC data and the FAWN network data, WMD stations were used to obtain wind speed and relative humidity data. WMD data tend to be sporadic and somewhat problematic. Relatively few WMD stations were available to supplement the relative humidity and wind speed data. In some years, few relative humidity stations were available with both the maximum and minimum values, but instead recorded the average relative humidity. For these years, the maximum relative humidity was estimated as 1 except where the average was less than 0.65 in which case the maximum relative humidity was estimated as 0.9. The estimated maximum relative humidity values and the average measured relative humidity values were used to calculate the minimum relative humidity. Appendix 5.2 lists all of the meteorological stations having relative humidity data and wind speed data and the data availability by year. The station lists also are in the data archive (station_RH_all.xls and station_W_all.xls).

Figure 5.2 shows the files required to interpolate a year of meteorological data for each meteorological variable. These files are input to the appropriate Fortran Source code. The code outputs one meteorological file for each day of the year. All files are placed in a single directory.

Figure 5.2. Flow Diagram for Meteorological Interpolation

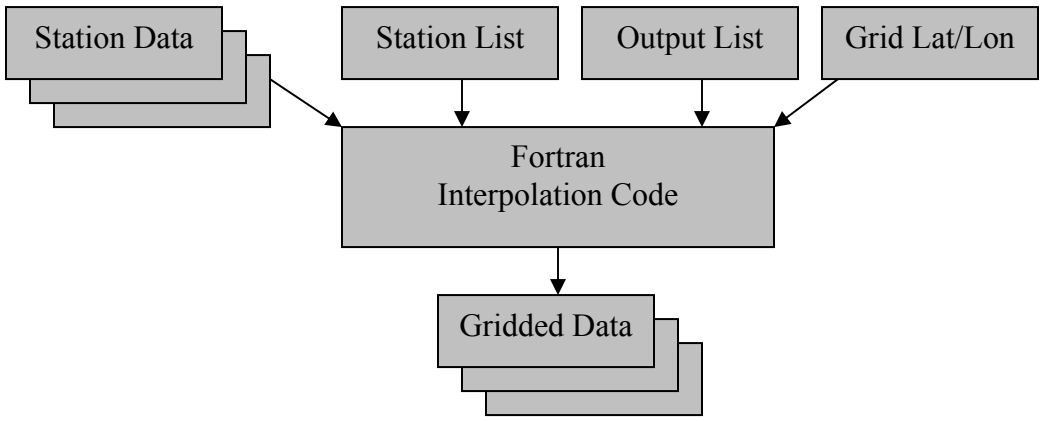

Input Files

Station Data Files: For each meteorological station, a separate file was created for the temperature data, the relative humidity data, and the wind speed data. Files are ONLY created for stations having a full year data for the meteorological variable. The temperature data files were named #_#_yearT where #_# is the station identifier and year is the data's year (e.g., 80211_112832_1995T). The file has a series of 365 or 366 rows, each having two columns of numbers with one decimal place. The first column is the maximum temperature in ^{o}C. The second column is the minimum temperature in ^{o}C. A similar convention was followed for relative humidity where the file name is #_#_yearRH and each file contains the maximum and minimum relative humidity rounded to the nearest %. For wind speed, the file name is #_#_yearW and each file

contains the average daily wind speed to one decimal place (m/s) corrected to a 2 m height (see equation 5.14).

Station List: A station list file, *Year*T_Stations, *Year*_StationsRH, or *Year*_StationsW, contains a list of the meteorological stations for temperature, relative humidity, and wind speed data, respectively. A separate row is used for each station and contains the file name, the latitude, longitude, and name. The name is not used in any calculations and appears in the file to help debugging if there is a processing error.

Output File List: The output file contains a list of all the output files to be generated (one for each day of the year). The files are named List_RHmax, List_RHmin, List_Tmax, List_Tmin, or List_Wind. The file contains one row for each day of the year with the variablename.yearjday (e.g., RHmax.2002001 references the maximum relatively humidity for Julian Day 001 for 2002). This list provides the naming convention for all output files.

Grid Lat/Lon: The file 2km_grid.txt contains the latitude and longitude for each of the 2 km grid pixels. The order of this file is critical because it matches the order of the GOES solar radiation data set and all other meteorological and ET data sets. The file has a header row followed by a series of rows (one for each 2 km grid point), each having two columns of numbers with three decimal places. The first column is the latitude and the second column is the longitude.

Processing Files
The files Interpolation_IDW_3, Interpolation_IDW_3_RH, Interpolation_IDW_3_Wind contain the processing code for the temperature, relative humidity, and wind datasets, respectively. Each file contains the Fortran code necessary to interpolate the meteorological data. The codes are nearly identical with the wind code having only one variable while the codes for temperature and relative humidity interpolation have two variables (max and min). In addition, the output file name differ differs for the temperature, relative humidity, and wind datasets.

A copy of the interpolation is placed in the folders corresponding to each year. There are three code modifications required when the year or the available meteorological data sets change: 1. The number of days in the year is set to either 365 or 366 (ln 15), 2. the number of meteorological stations (ln 16) and 3. the file name containing the site list (ln 46). Each of these lines is preceded and following by a comment line (!----------).

Output Files
One output file is created for each day. The files are named using the convention in the output file list; variablename.yearjday (e.g., RHmax.2002001). Again, the order of this file is critical because it matches the order of the GOES solar radiation data set and all other meteorological and ET data sets. The file has a header row followed by a series of rows (one for each 2 km grid point), each having three columns of numbers with three decimal places. The first column is the latitude, the second column is the longitude, and the third column is the meteorological variable.

Backup Folder Structure

Interpolation data (Meteorological data in 2 km grid)

- Folder name: Interpolation\climate
- Subfolders: Temp, RH, Wind

Each subfolder contains 10 subfolders, one for each year from 1995 to 2004

Each subfolder contains

Input files:

2km_grid.txt (Latitude and Longitude for all pixels)
list_climatemax.dat (list of output files)
list_climatemin.dat (list of output files)
year_StationsRH.txt (list of local meteorological stations)
#_#_yearRH.txt (max, min for each pixel by stations)

Fortran source code, i.e., Interpolation_IDW_3_Temp.f90

Output files: One for each day of year (variablename.yearjday)

5.3.2 Evapotranspiration Calculations

There are two types of ET calculations; reference ET and potential ET. Both calculations follow a nearly identical process. The primary difference is that reference ET does not require an albedo dataset whereas the potential ET dataset does. Note: For 1995, GOES solar radiation was available from DOY 152 to DOY 365. As a matter of convenience and in order to not modify source code to account for the limited days, a dummy set of solar radiation data was used from DOY 1 to DOY 151 (1996 GOES solar radiation was used). PET output files for DOY 1 to 151 are labeled as ETo.YearDOY_dummy. Valid result files for reference ET and PET are available from DOY 152.

Input Files

Meteorological Data Files: For each meteorological variable, there are daily files containing all the 2 km gridded data (365 or 366 for leap years). These files are the same output files created during the meteorological interpolation. They are copied from the meteorological interpolation folder to the appropriate ET calculation folder. The files are named using the convention variablename.yearjday (e.g., RHmax.2002001). Again, the order of the data in this file is critical because it matches the order of the GOES solar radiation data set and all other meteorological and ET data sets. The file has a header row followed by a series of rows (one for each 2 km grid point), each having three columns of numbers with three decimal places. The first column is the latitude, the second column is the longitude, and the third column is the meteorological variable.

Meteorological Data List: There are six files that list the file names for each day and meteorological variable. Each file contains one row for each day of the year with a filename appearing each row.

The six files are:
list_GOES_RS.dat for the GOES solar radiation daily data file list,
list_Tmax.dat for the maximum temperature daily data file list,
list_Tmin.dat for the minimum temperature daily data file list,
list_RHmax.dat for the maximum relative humidity daily data file list,

list_RHmin.dat for the minimum relative humidity daily data file list, and list_wind.dat for the wind daily data file list.

Grid Lat/Lon: The latitude and longitude for each of the 2 km grid pixels is contained in two separate files; longitude.dat and latitude.dat. Again, the order of this file is critical because it matches the order of the GOES solar radiation data set and all other meteorological and ET data sets. The file has a header row containing either the word latitude or longitude followed by a series of rows (one for each 2 km grid point). Each row has one column of numbers with three decimal places. The column is either the latitude or the longitude.

Julian DOY: The file Julian.dat contains a list of the Julian days for the year. The file has a header row containing the words Julian day followed by a series of rows that list the DOY from 1 to 365 (or 366) for leap years.

Albedo: The file LAT_LON_Albedo_FL.dat contains a list of the albedo values for each of the 2 km grid pixels. The file has a header row followed by a series of rows, each having three columns of numbers with three decimal places. The first column is the latitude, the second column is the longitude, and the third column is the albedo. The albedo values are either 0.149 or 0.062 for water or land, respectively. This file is only used in the PET calculation.

Output File List: The output file contains a list of all the output files to be generated (one for each day of the year). The files are named List_ETo_out.dat or List_PET_out.dat. The file contains one row for each day of the year with the ETo.yearjday or PET.yearjday (e.g., ETo.2002001). This list provides the naming convention for all output files.

Processing Files

The files ETo_only.f90 and PET_only.f90 contain the processing code for the reference ET and the Potential ET calculations, respectively. Each file contains the Fortran code necessary to calculate ET. This is the only code modifications required when the year changes: change the year in the code (ln 10). This line is preceded and following by a comment line (!----------).

Output Files

One output file is created for each day. The files are named using the convention in the output file list; ETo.yearjday or PET.yearjday (e.g., ETo.2002001). Again, the order of this file follows the order of the GOES solar radiation data set and the longitude and latitude files. The file has a header row followed by a series of rows (one for each 2 km grid point), each having three columns of numbers with three decimal places. The first column is the latitude, the second column is the longitude, and the third column is the ETo value in mm/day. Values of -9999.900 indicate that the GOES solar radiation data are not available for the cell.

Backup Folder Structure

Interpolation data (Meteorological data in 2 km grid)

- Folder name: ET_com (contains subfolders for reference ETo and PET analysis)
- Subfolders: ETo_2004, ETo_2003, etc.
- Input data required: 6 list files, 4 input files, 6 types of meteorological data files (365 or 366 each)

  List files
  list_GOES_RS.dat (list for GOES insolation files)
  list_Tmax.dat (list for max. temperature files)
  list_Tmin.dat (list for min. temperature files)
  list_RHmax.dat (list for max. humidity files)
  list_RHmin.data (list for min. humidity files)
  list_wind.dat (list for wind files)

  Input files
  Julian.dat (DOY for year)
  Longitude.dat (longitude for each pixel)
  Latitude.dat (latitude for each pixel)
  LAT_LON_Albedo_FL.txt (Albedo value for land and water for each pixel)

  Meteorological data files
  GOES-Dsolar_UAH-TIRGCL_**cal**.date.Q#
  Tmax.yearjday
  Tmin.yearjday
  RHmax.yearjday
  RHmin.yearjday
  Wind.yearjday

- Fortran source code 6 list files, 4 input files, 6 types of meteorological data files (365 or 366 each)
  For reference ET (ETo_only.f90)
  For PET (PET_only.f90)

- Output Files: 365 or 366 each
  For reference ET: ETo.yearjday (-9999.900 is missing by GOES solar radiation)

  For PET: PET.yearjday (-9999.900 is missing by GOES solar radiation)

6. Suggested Future Directions

The development of new methods and the availability of PET and RET datasets provides a great opportunity for the Florida water resources community. This is the first time that a statewide evapotranspiration dataset exists for the community. This readily available product will provide a consistent means to force models across WMD and watershed boundaries. This section describes future opportunities to leverage the recent activities and developments. In addition, the process of developing these datasets has led to a heightened awareness of analysis and data needs. This section documents key steps that would enhance current data sets and support future investigations.

6.1 Outreach to User Community

The five WMDs have invested considerable resources developing a community data set. This dataset is easy to obtain via the USGS web portal in a readily accessible format. There is a large potential user community (e.g., WMDs, State Agencies, Consultants, Non-Profit and Academic) who will likely benefit from the data for a broad range of applications. Several activities are recommended to enhance the product dissemination and use.

- Active and Broad Promotion of Datasets – As compared to the potential user community, only a relatively small number of individuals participated in the dataset development. The active promotion will greatly enhance the value of the datasets. For example, the user community can be notified through conference presentations, newsletter brief, and links on WMD websites.

- Provide Documentation and Descriptions – The current document, which completely describes the methods and data, likely contains more information than most users require. A brief document should be available on the USGS web page.

- User Community Feedback - The ability for users to provide input and feedback on the datasets will help to identify user communities, prioritize community needs and identify any problems with the datasets.

- Develop Monthly and Annual Datasets – The current volume of data may be somewhat overwhelming and beyond the requirements of users. Intermediate products including annual and monthly values by point may provide much of the desired information.

- Create new Florida PET and RET Maps – Florida Water Atlas has long been the benchmark used to estimate reasonable PET and RET values. New maps in paper (.pdf) and GIS format of the intermediate products would be a welcome update.

- Comparison to Existing Datasets – Users with existing datasets will wish to determine differences between the GOES ET dataset and their existing dataset. For example, SJRWMD agricultural water permitting uses the AFSIRS dataset. Other users continue to rely on ET pans. Comparisons to broadly used datasets should be conducted and results documented for dissemination to eliminate duplicate efforts.

- Recommended Approaches to Applications – Similar to existing datasets, input formats required for broadly used models should be developed to eliminate duplicate efforts.

6.2 Dataset Applications

This new dataset can be used to address a number of water resource questions. It was designed specifically for permitting, planning, and analysis using existing WMD tools. It is anticipated that the data sets will add immediate value to numerous specific applications and modeling activities. In addition to these anticipated activities, several broad analysis applications are recommended to enhance water resources analysis and to develop new benchmarks.

- Apply GOES ET datasets with Distributed Rainfall Products – The GOES ET dataset has the same distribution in space as the ONERAIN rainfall product. Using these two products, it is possible to map Florida water resources characteristics by undertake a series of analyses. Potential analyses could include ratios of PET and precipitation, irrigation demand, recharge, and water allocation needs.

- Characterizing spatial distribution patterns – The 2 km spatial scale will facilitate the examination of PET patterns due to location (e.g., coastal, latitude, inland water body, and elevation impacts). These maybe quantified using spatial statistics.

- Using patterns to distribute long-term PET point data in space – The spatial patterns identified using the 10-year, daily data set can be used in conjunction with long-term climate data to provide a more meaningful distribution in space and time. The datasets would have significant value for examining historical impacts on water resources.

- Optimizing measurement locations – To date, the selection of ET and climate measurements have been primarily based on the land-use and region of interest. Evaluation of the new PET and RET datasets can provide a quantitative means to optimally site new sites.

6.3 Calibration and Validation

In the process of developing the new dataset, a range of methods were evaluated, the best performing method was identified and, as necessary, datasets were calibrated. While validation exercises were performed for many aspects of the project, some key activities still need to be addressed regarding the final product.

- Validation of PET Datasets –The final ET datasets have not been compared to measured data. A series of in-situ ET measurements sites were used to select the PET method. These datasets are readily available and highly recommended for this type of analysis. Other measured datasets would be valuable for independent validation, but would require more effort to collect and identify potential conditions.

- Error Quantification of PET Datasets – Increasingly, models have the ability to incorporate knowledge of measurement precision. In any validation exercise, it would be extremely valuable to determine errors statistics, biases on annual and seasonal time scales as well as spatial. Error quantification should also examine the error sources and provide feedback regarding priorities to improve the dataset.

- Validation of Model Output – Ultimately the new datasets should enhance model performance. Comparisons should be made between measured data and model output using existing datasets and revised datasets. This will be a challenge for those models that will require parameter modifications prior to use. Others models will be able to use the dataset directly. For example, the RET data can be used directly in crop models. This model output could be compared to Benchmark Farms data.

6.4 Future Data and Measurements Needs

In the process of developing the new dataset, gaps in existing measurements were identified. In the future, measurement campaigns would be served well by including additional instrumentation, by providing measurements to support site intercomparisons, and by focusing on the need to distinguish differences across land uses.

- Four component net radiation measurements – The Priestley-Taylor method requires net radiation to be calculated. Only SJRWMD had four component net radiation measurement sites. These sites were critical in method selection and error characterization. It was assumed that these sites are representative of the entire state, but additional validation data would be extremely valuable to support this assumption.

- Albedo measurements – The same SJRWMD sites used for net radiation were also used to determine the albedo. Again a broader range of sites would be appropriate. In addition, the selected method used two constant albedo values; one for land and a different one for water. There is clear and compelling evidence that

albedo varies seasonally and across land uses. However, attempts to account for those variations had the same or worse errors as constant values. This should be examined in the future when better datasets exist. Remote sensing methods also showed some promise, but were not adequately mature at the time of this project. In the future, remote sensing will likely become a reliable source.

- Continue PET and RET dataset updates – While the datasets provided here are excellent community resources, the most valuable contribution of this project is the methods that were developed to produce the products. The solar radiation and ET datasets will need to be routinely updated to accommodate future years. Continuity in this process is strongly recommended to maintain a consistent product without lapses in institutional memory. It is recognized that the methods are not static and will advance to reflect new scientific knowledge. Thus, the supporting climate dataset should be archived and documented so that they can be used with new methods to recalculate the ET datasets across all years.

- Continue solar radiation measurements and calibration – The solar radiation product required calibration coefficients that change over time. A host of quality ground measurement sites were used to develop these coefficients. Future efforts will continue to rely on these or comparable sites.

- Ability to distinguish PET conditions from stressed conditions – In the process of identifying the best method to estimate PET it was determined that there is no systematic means and measurements available to differentiate between potential and stressed conditions. Standard methods in the field use leaf level measurements and/or soil moisture and depth to groundwater as indicators. However, most sites did not have either of these measurements. Those which did were located at a range of depths making it difficult to develop a consistent approach across sites. It is recommended that Florida ET experiments measure soil moisture and depth to ground water. A consistent approach to making these measurements is also recommended.

- Ability to distinguish PET differences across land uses/FLUCCS – This project determined that WMDs want to be able to distinguish among a minimum of 18 different land uses as derived from FLUCCS codes. Unfortunately, there is not adequate measurement data across this range of land uses. This project showed a distinct difference among open water, wetland, and other land uses. However, it was difficult to differentiate the PET across those other land uses for a range of reasons including variations within a single land use. The current PET data set only uses different parameters for cells with significant open water and for those without open water. Additional comparisons across sites are strongly recommended to further differentiate among land uses. Initial work should focus on differentiating those land uses with significant acreage and importance for water resources management.

- Extend Dataset to Actual ET – The current datasets only provide ET estimates for well watered conditions. The project clearly identified differences between ET during well watered conditions and ET for the typical annual cycle of Florida climate conditions. Most water resources applications need actual ET rather than PET. While there are a number of possible means to estimate actual ET including modeling, to date there is no systematic dataset available to provide the actual ET need for managing Florida water resources across land uses and for understanding impacts of climate change/climate variability and landscape changes on ET. The robust set of experimental data provides an opportunity to evaluate the viability of modeling, first principle, and remote sensing approaches to produce a consistent, statewide actual ET dataset.

7. References

Abtew, W. 1996. Evapotranspiration measurements and modeling for three wetland systems in South Florida, Water Resources Bulletin, 32 (3): 465-473.

Abtew, W., S. Newman, K. Pietro, and T. Kosier. 1995. Canopy resistance studies of cattails, Trans. of ASAE, 38 (1): 113-119.

Allen, R. G. 1996. Assessing integrity of weather data for use in reference evapotranspiration estimation. J. Irrig. and Drain. Engrg., ASCE. 122, 97-106.

Allen, R. G., L. S. Periera, D. Raes, and M. Smith. 1998. Crop evapotranspiration: Guidelines for computing crop requirements. Irrigation and Drainage Paper No. 56. Rome, Italy: FAO.

Allen, R. G., I. A. Walter, R. L. Elliott, T. A. Howell, D. Itenfisu, M. E. Jensen, R.L. Snyder. 2005. The ASCE standardized reference evapotranspiration equation, American Society of Civil Engineers, Reston, Virginia.

Anderson, M. C., W. L. Bland, J. M. Norman, and G. R. Diak. 2001. Canopy wetness and humidity prediction using satellite and synoptic-scale meteorological observations, Plant Dis., 85, 1018–1026.

Anderson, M. C., W. P. Kustas, and J. M. Norman. 2003. Upscaling and downscaling - A regional view of the soil-plant-atmosphere continuum, Agron. J., 95, 1408–1432.

Anderson, M. C., J. M. Norman, J. R. Mecikalski, R. D. Torn, W. P. Kustas, and J. B. Basara. 2004. A multiscale remote sensing model for disaggregating regional fluxes to micrometeorological scales, J. Hydrometeor., 5, 343–363.

Breuer, L., K. Eckhardt, and H-G. Frede. 2003. Plant parameter values for models in temperate climates, Ecological Modeling, 169: 237-293.

Brutsaert, W. 1975. On a derivable formula for long-wave radiation from clear skies. Water Resources Research, 11(5): 742–744.

Brutsaert, W. 1982. Evaporation into the Atmosphere—Theory, History and Application. Kluwer Academic Publishers, Dordrecht.

Crawford, T.M. and C.E.Duchon. 1999. An improved parameterization for estimating effective atmospheric emissivity for use in calculating daytime downwelling longwave radiation. J. Appl. Meteorol. 38, 474–480.

Darnell, W. L., W. F. Staylor, S. K. Gupta, and F. M. Denn. 1988. Estimation of surface insolation using sun-synchronous satellite data, J. Climate, 1, 820–835.

Dedieu, G., P. Y. Deschamps, and Y. H. Kerr. 1987. Satellite estimates of solar irradiance at the surface of the earth and of surface albedo using a physical model applied to meteosat data, J. Climate Appl. Meteor., 26, 79–87.

Diak, G. R., and C. Gautier. 1983. Improvements to a simple physical model for estimating insolation from GOES data, J. Climate Appl. Meteor., 22, 505–508.

Diak, G. R., W. L. Bland, and J. R. Mecikalski. 1996. A note on first estimates of surface insolation from GOES-8 visible satellite data, Agric. For. Meteor., 82, 219–226.

Diak, G. R., M. C. Anderson, W. L. Bland, J. M. Norman, J. R. Mecikalski, and R. M. Aune. 1998. Agricultural management decisions aids driven by real-time satellite data, Bull. Amer. Meteor. Soc., 79, 1345–1355.

Duarte, H.F., N.L. Diaz, and S.R. Maggiotto. 2006. Assessing daytime downward longwave radiation estimates for clear and cloudy skies in Southern Brazil. Agric. and Forest Meteorol., 139: 171-181.

Duffie, J. A. and W. A. Beckman. 1980. Solar Engineering of Thermal Processes. John Wiley and Sons, New York, pp. 1-109.

Frouin, R., C. Gautier, K. B. Katsaros, and J. Lind. 1988. A comparison of satellite and empirical formula techniques for estimating insolation over the oceans, J. Appl. Meteor., 27, 1016–1023.

Frouin, R., and B. Chertock. 1992. A technique for global monitoring of net solar irradiance at the ocean surface. Part I: Model, J. Appl. Meteor., 31, 1056–1066.

Gautier, C., G. R. Diak, and S. Masse. 1980. A simple physical model to estimate incident solar radiation at the surface from GOES satellite data, J. Appl. Meteor., 19, 1007–1012.

Gautier, C., G. R. Diak, and S. Masse. 1984. An investigation of the effects of spatially averaging satellite brightness measurements on the calculation of insolation, J. Climate Appl. Meteor., 23, 1380–1386.

Gu, J., E. A. Smith, and J. D. Merritt. 1999. Testing energy balance closure with GOES-retrieved net radiation and in situ measured eddy correlation fluxes in BOREAS, J. Geophys. Res,. 104, 27881–27893.

Hoblit, B. C., C. Castello, L. Liu, and D. Curtis. 2003. Creating a seamless map of gage-adjusted radar rainfall estimates for the State of Florida, paper presented at EWRI World Water and Environmental Congress, Philadelphia, Pennsylvania, 23-26 June.

Idso, S.B., and R.D. Jackson. 1969. Thermal radiation from the atmosphere. J. Geophysical Res., 74(23): 5397–5403.

Jacobs, J.D. 1978. Radiation climate of Broughton Island. In: Barry, R.G., Jacobs, J.D. (Eds.), Energy Budget Studies in Relation to Fast-ice Breakup Processes in Davis Strait. Inst. of Arctic and Alp. Res. Occas. Paper No. 26. University of Colorado, Boulder, CO, pp. 105–120.

Jacobs, J.M., S.L. Mergelsberg, A.F. Lopera, and D.A. Myers. 2002. Evaporation from a wet prairie wetland under drought conditions: Paynes Prairie Preserve, Florida, USA, Wetlands, Vol. 22, (2): 374–385.

Jacobs, J. M., D. A. Myers, M. C. Anderson, and G. R. Diak. 2002. GOES surface insolation to estimate wetlands evapotranspiration, J. Hydrol., 56, 53–65.

Jacobs, J. M., M. C. Anderson, L. C. Friess, and G. R. Diak. 2004. Solar radiation, longwave radiation and emergent wetland evapotranspiration estimates from satellite data in Florida, USA, Hydrological Sciences Journal, 49, 461-476.

Konzelmann, T., R.S.W. Van de Wal, W. Greuell, R. Bintanja, E.A.C.Henneken, and A. Abe-Ouchi. 1994. Parameterization of global and longwave incoming radiation for the Greenland ice sheet. Global Planet. Change 9, 143–164.

Llasat, M.C., and R.L. Snyder. 1998. Data error effects on net radiation and evapotranspiration estimation. Agric. and Forest Meteorol., 91: 209-221.

MacQuarrie, P. and L.C. Nkemdirim. 1991. Potential, actual and equilibrium evapotranspiration in a wheat field, Water Resources Bulletin, 27 (1): 73-82.

Maykut, G.A. and P.E. Church. 1973. Radiation climate of Barrow, Alaska, 1962–1966. J. Appl. Meteorol. 12, 620–628.

Mecikalski, J. M., G. R. Diak, M. C. Anderson, and J. M. Norman. 1999. Estimating fluxes on continental scales using remotely sensed data in an atmosphere–land exchange model, J. Appl. Meteor., 38, 1352–1369.
Monteith, J.L. 1965. Evaporation and environment. pp. 205-234. In G.E. Fogg (ed.) Symposium of the Society for Experimental Biology, The State and Movement of Water in Living Organisms, Vol. 19, Academic Press, Inc., NY.
Möser, W., and E. Raschke. 1984. Incident solar radiation over Europe from METEOSAT data, J. Climate Appl. Meteor., 23, 166–170.
Offerle, B., C.S.B. Grimmond and T.R. Oke. 2003. Parameterization of net all-wave radiation for urban areas. J. of Applied Meteorology, 42: 1157-1173.
Otkin, J.A., M.C. Anderson, J.R. Mecikalski, and G.R. Diak. 2005. Validation of GOES-Based Insolation Estimates Using Data from the U.S. Climate Reference Network. Journal of Hydrometeorology, 6, 460–475.
Penman, H.L. 1948. Natural evaporation from open water, bare soil, and grass. Proc. Roy. Soc. London A193:120-146.
Pinker, R. T., and J. A. Ewing. 1985. Modeling surface solar radiation: Model formulation and validation, J. Climate Appl. Meteor., 24, 389–401.
Pinker, R. T., and I. Laszlo. 1992. Modeling surface solar irradiance for satellite applications on global scale, J. Appl. Meteor., 31, 194–211.
Pinker, R. T., R. Frouin, and Z. Li. 1995. A review of satellite methods to derive surface shortwave irradiance, Remote Sens. Environ., 51, 105–124.
Pinker, R. T., J. D. Tarpley, I. Laszlo, K. E. Mitchell, P. R. Houser, E. F. Wood, J. C. Schaake, A. Robock, D. Lohmann, B. A. Cosgrove, J. Sheffield, Q. Duan, L. Luo, and R. W. Higgins. 2003. Surface radiation budgets in support of the GEWEX Continental-Scale International Project (GCIP) and the GEWEX Americas Prediction Project (GAPP), including the North American Land Data Assimilation System (NLDAS) project, J. Geophys. Res., 108(22), 8798, doi: 10.1029/2002JDO03301.
Powell, T. L., G. Starr, K.L. Clark, T.A. Martin, and H.R. Gholz. 2005. Ecosystem and understory water and energy exchange for a mature, naturally regenerated flatwood
Prata, A.J. 1996. A new long-wave formula for estimating downward clear-sky radiation at the surface. Q. J. R. Meteorol. Soc. 122, 1127–1151.
Priestley, C.H.B. and R.J. Taylor. 1972. On the assessment of surface heat flux and evaporation using large-scale parameters, Monthly Weather Review 100:81-92.
Raphael, C., and J. E. Hay. 1984. An assessment of models which use satellite data to estimate solar irradiance at the Earth's surface, J. Climate Appl. Meteor., 23, 832–844.
Satterlund, D.R. 1979. An improved equation for estimating long-wave radiation from the atmosphere. Water Resour. Res. 15, 1649-1650.
Schmetz, J. 1989. Towards a surface radiation climatology. Retrieval of downward irradiance from satellites, Atmos. Res., 23, 287–321.
Sellers, W.D. 1965. Physical Climatology. University of Chicago Press, Chicago, Ill.
Shuttleworth, W. J. 1993. Evaporation, Chapter 4 in Handbook of Hydrology, D. R. Maidment, editor in chief, McGraw-Hill, Inc.
Stewart, J. B., C. J. Watts, J. C. Rodriguez, H. A. R. De Bruin, A. R. van den Berg, and J. Garatuza-Payan. 1999. Use of satellite data to estimate radiation and evaporation for northwest Mexico, Agric. Water Manage., 38, 181–193.

Sugita, M. and W. Brutsaert. 1993. Cloud effect in the estimation of instantaneous downward longwave radiation. Water Resour. Res. 29 (3), 599–605.
Sumner, D.M. and J.M. Jacobs. 2005. Utility of Penman–Monteith, Priestley–Taylor, reference evapotranspiration, and pan evaporation methods to estimate pasture evapotranspiration, Journal of Hydrology, 308: 81–104.
Tarpley, J. D. 1979. Estimating incident solar radiation at the surface from geostationary satellite data, J. Appl. Meteor., 18, 1172–1181.
The National Centers for Environmental Prediction (NCEP) Reanalysis data provided by the NOAA/OAR/ESRL PSD, Boulder, Colorado, USA, from their Web site at http://www.cdc.noaa.gov/cdc/reanalysis/reanalysis.shtml).
Weymouth, G., and J. LeMarshall. 1999. An operational system to estimate global solar exposure over the Australian region from satellite observations, Aust. Meteor. Mag., 48, 181–195.

Appendix 2.1:
Units Correction for Penman-Monteith Equation

Appendix I

Working out the units in Penman Monteith (eqn 4.2.27 in Maidment, 1993)

$$\text{Radiation term} = \frac{1}{\lambda \rho_w} \frac{\Delta A}{\Delta + \gamma (1 + r_s/r_a)}$$

where λ in $MJ\ Kg^{-1}$

ρ_w in $Kg\ m^{-3}$

Δ in $KPaC^{-1}$

γ in $KPaC^{-1}$

A in $MJ\ m^{-2}\ d^{-1}$

r_s, r_a in $S\ m^{-1}$

$$\frac{1}{(MJ\ Kg^{-1})(1000\ Kg\ m^{-3})} \quad \frac{(KPaC^{-1})(MJ\ m^{-2}\ d^{-1})}{KPaC^{-1} + KPaC^{-1}(1 + \frac{S\ m^{-1}}{S\ m^{-1}})}$$

$$= \frac{1}{1000\ MJ\ m^{-3}} \quad \frac{(KPaC^{-1})(MJ\ m^{-2}\ d^{-1})}{KPaC^{-1}}$$

$$= \frac{m\ d^{-1}}{1000} \times \frac{1000\ mm}{m} = \boxed{mm\ d^{-1}}$$

$$\text{Advection term} = \frac{1}{\lambda \rho_w} \frac{\rho_a C_p D / r_a}{\Delta + \gamma(1 + r_s/r_a)}$$

where ρ_a in $kg\ m^{-3}$
C_p in $kJ\ kg^{-1}\ C^{-1}$
D in kPa
others as before

$$\frac{1}{(MJ\ kg^{-1})(1000\ kg\ m^{-3})} \quad \frac{(kg\ m^{-3})(kJ\ kg^{-1}\ C^{-1})(kPa)}{(kPa\ C^{-1})(s\ m^{-1})}$$

$1000\ kJ$

$$= \frac{m\ s^{-1}}{1000 \cdot 1000} \times \frac{1000\ mm}{m} \times \frac{86400\ s}{d} = \boxed{86.4\ \frac{mm}{d}}$$

→ must introduce a constant = 86.4 into advection term in order to get the units to work out to $mm\ d^{-1}$

Appendix 2.2:

Additional site information

			Instrument heights (m)					
Site name	Longitude (decimal degrees)	Latitude (decimal degrees)	Air temperature/humidity	Eddy flux	Anemometer	Pyanometer	Radiometer	Canopy height (m)
Alachua County (Donaldson)	-82.1633	29.7548		15	15			9.1 - 11
Alachua County (Austin Cary)	-82.2188	29.7381		32	32			22.00
Belleview	-82.0000	29.0000	6.65	7.28	7.28	6.75	6.50	5.50
Blue Cypress Marsh	-80.7114	27.6953	2.00	4.00	3.00	2.00	3.00	2.10
Blue Springs Tact	-83.1969	30.5067		8.50	8.50			6.00
Carlton Ranch	-81.7731	27.1783		10.00	6.40			5.00
Disney Wilderness	-81.4002	28.0488	1.20	3.40	3.60	3.00	3.40	0.40
Duda Farm	-80.7760	28.2740	1.10	3.20	2.70	2.70	2.70	0.10
Everglades-L1	-80.7022	25.6164	2.35	4.27	4.27			1.52
Everglades-P33	-80.5294	25.3597	1.62	3.66	3.66			1.07
Everglades-X1.5	-80.7381	26.2583	2.50	5.49	5.49			1.83
Ferris Farms	-82.2762	28.7613	1.90	2.70	3.30	2.80	2.70	0.10
Indian River Lagoon	-80.5761	28.0561		4.60	4.60			--
Kennedy Space Center	-80.6715	28.6086		3.50	3.50			1.50
Kennedy Space Center	-80.6709	28.4583		18.00	18.00			13.00
Starkey	-82.5592	28.2253	1.40	1.50	2.20	1.20	1.00	0.35
Reedy Lake	-81.6132	28.4161		1.50	1.90			--
WCA	-80.6695	25.9736		3.20	3.70			--

Appendix 2.3:

Residual versus julian day for all “good” days

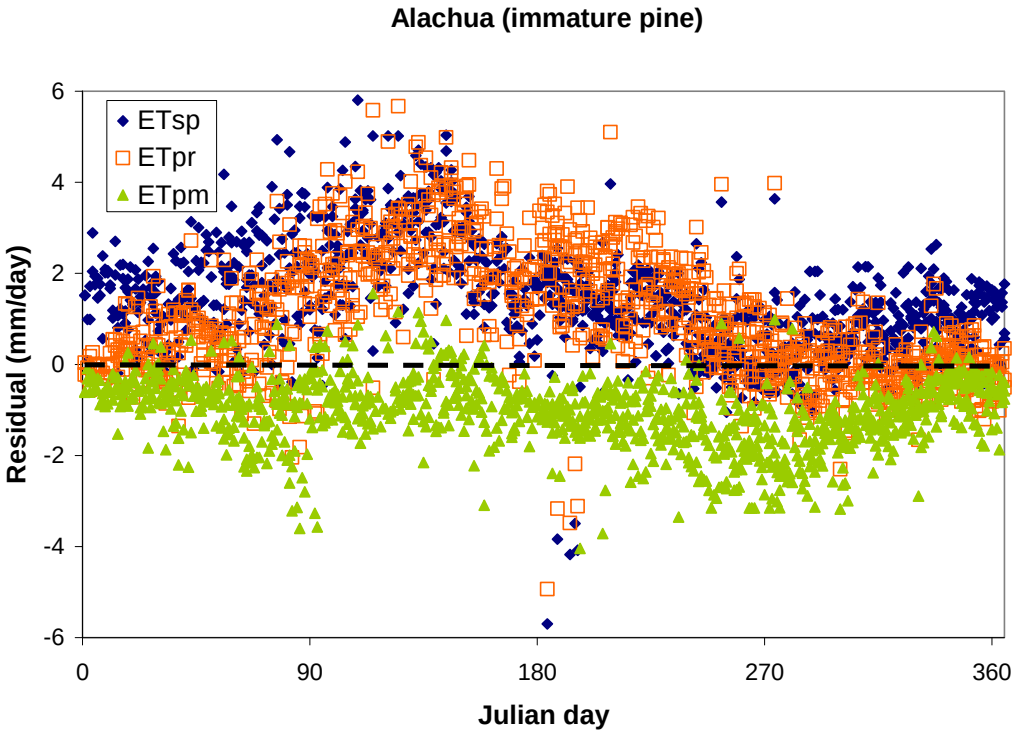
Alachua (immature pine)
ETsp
ETpr
ETpm
Residual (mm/day)
6
4
2
0
-2
-4
-6
0
90
180
270
360
Julian day

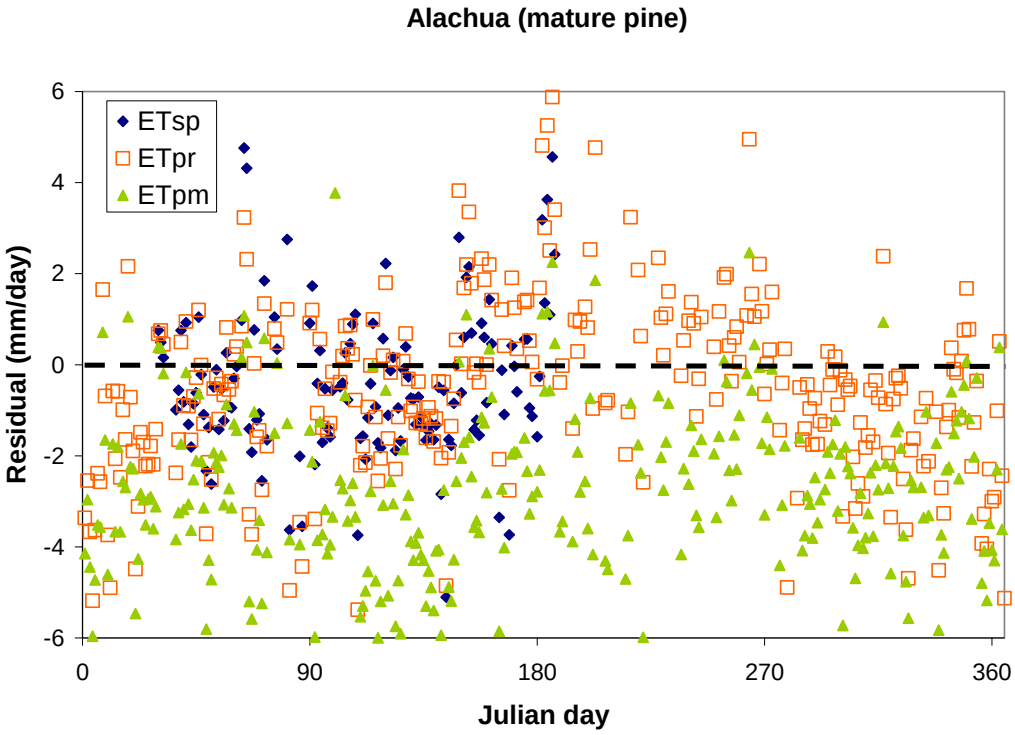
Alachua (mature pine)
ETsp
ETpr
ETpm
Residual (mm/day)
6
4
2
0
-2
-4
-6
0
90
180
270
360
Julian day

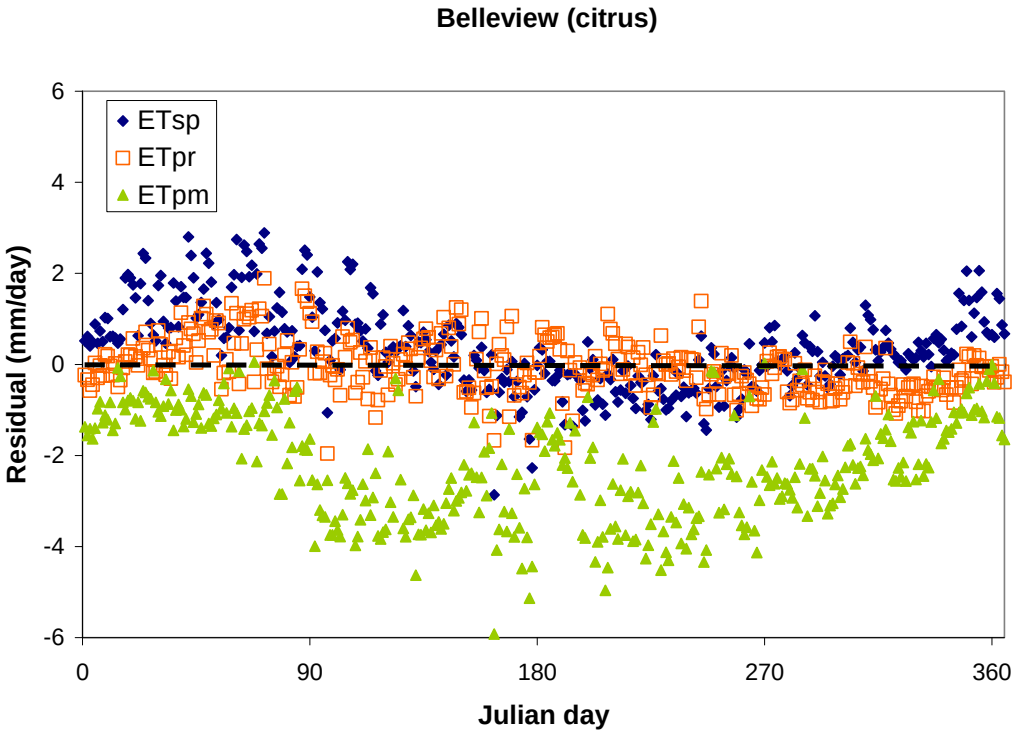
Belleview (citrus)
ETsp
ETpr
ETpm
Residual (mm/day)
6
4
2
0
-2
-4
-6
0
90
180
270
360
Julian day

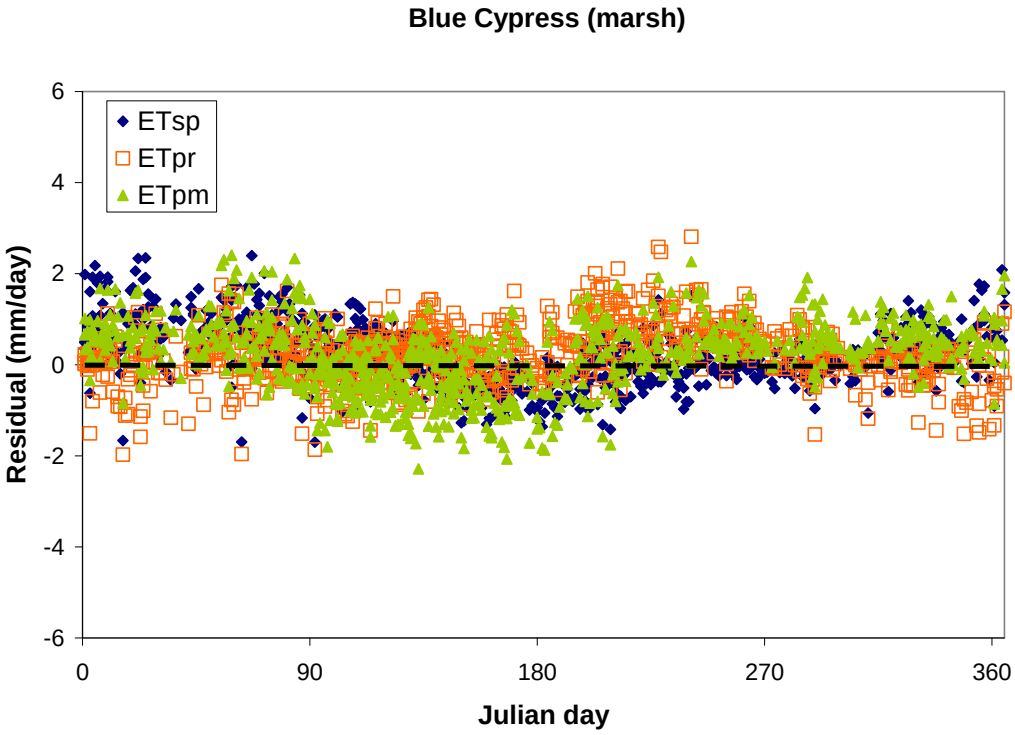
Blue Cypress (marsh)
ETsp
ETpr
ETpm
Residual (mm/day)
6
4
2
0
-2
-4
-6
0
90
180
270
360
Julian day

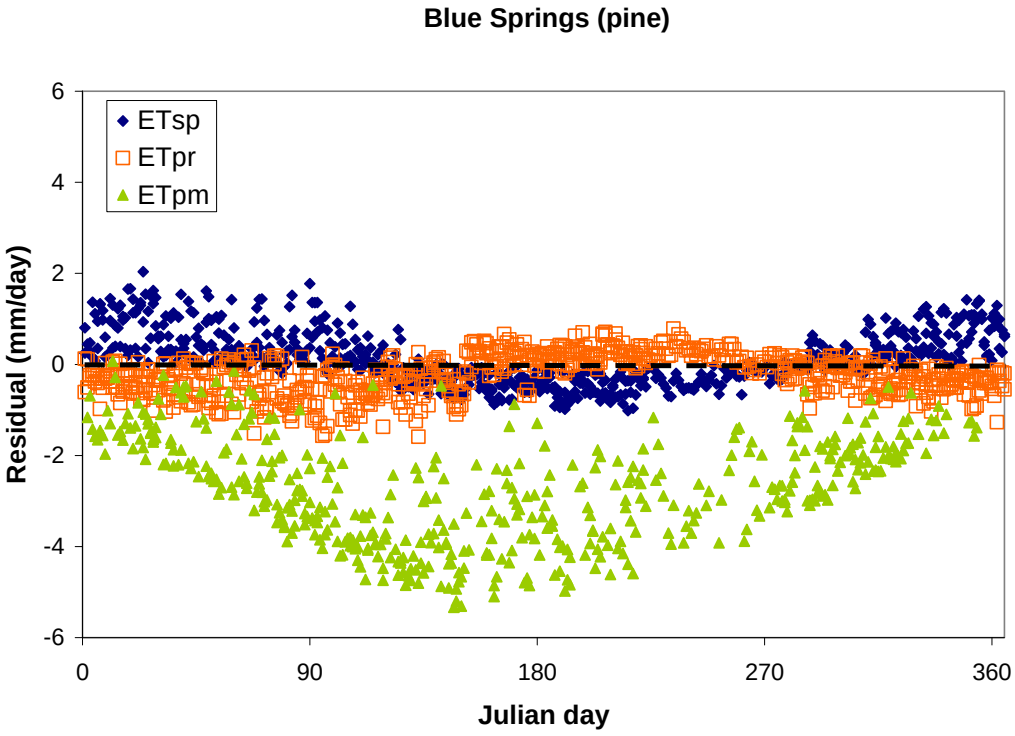
Blue Springs (pine)
ETsp
ETpr
ETpm
Residual (mm/day)
6
4
2
0
-2
-4
-6
0
90
180
270
360
Julian day

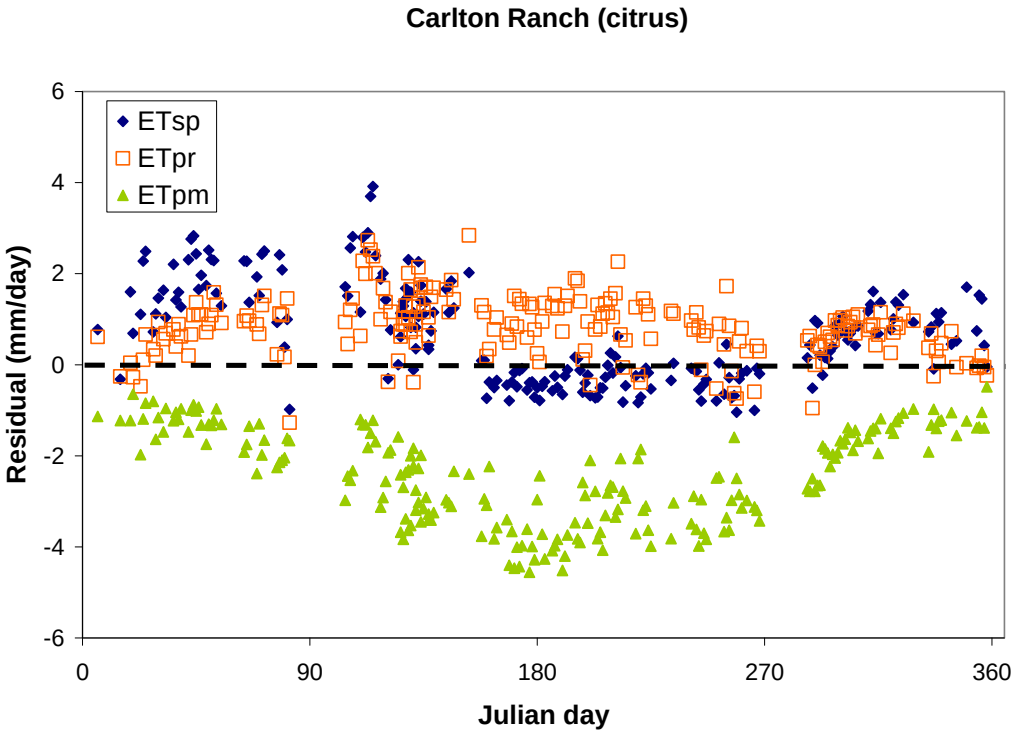
Carlton Ranch (citrus)
ETsp
ETpr
ETpm
Residual (mm/day)
6
4
2
0
-2
-4
-6
0
90
180
270
360
Julian day

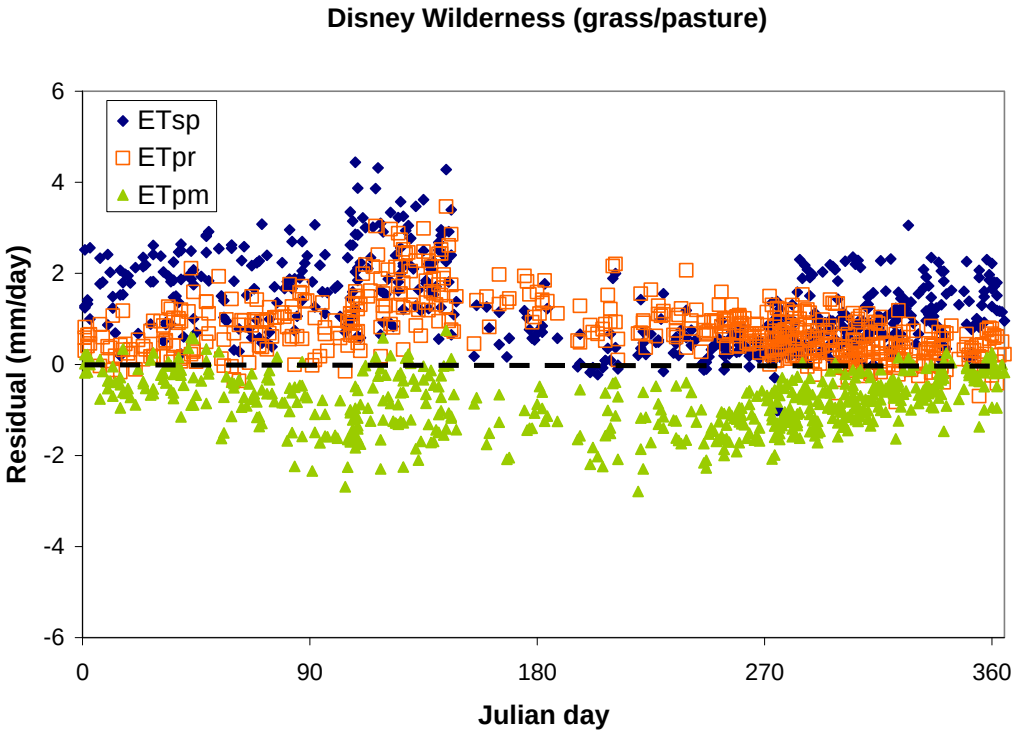
Disney Wilderness (grass/pasture)
ETsp
ETpr
ETpm
Residual (mm/day)
6
4
2
0
-2
-4
-6
0
90
180
270
360
Julian day

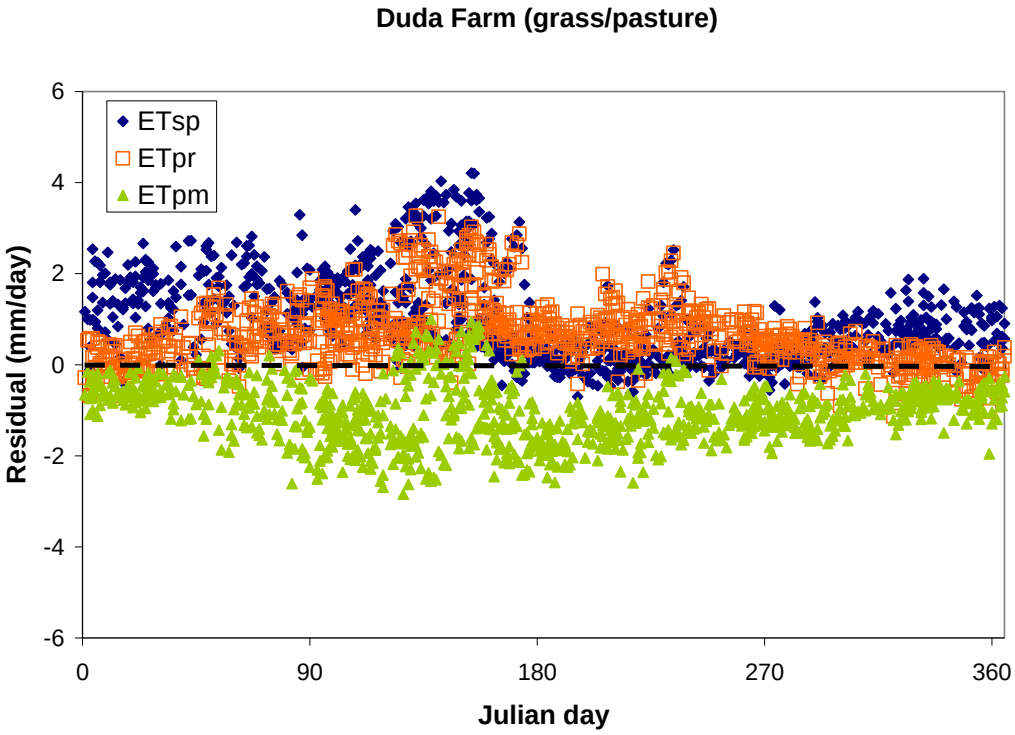
Duda Farm (grass/pasture)
ETsp
ETpr
ETpm
Residual (mm/day)
6
4
2
0
-2
-4
-6
0
90
180
270
360
Julian day

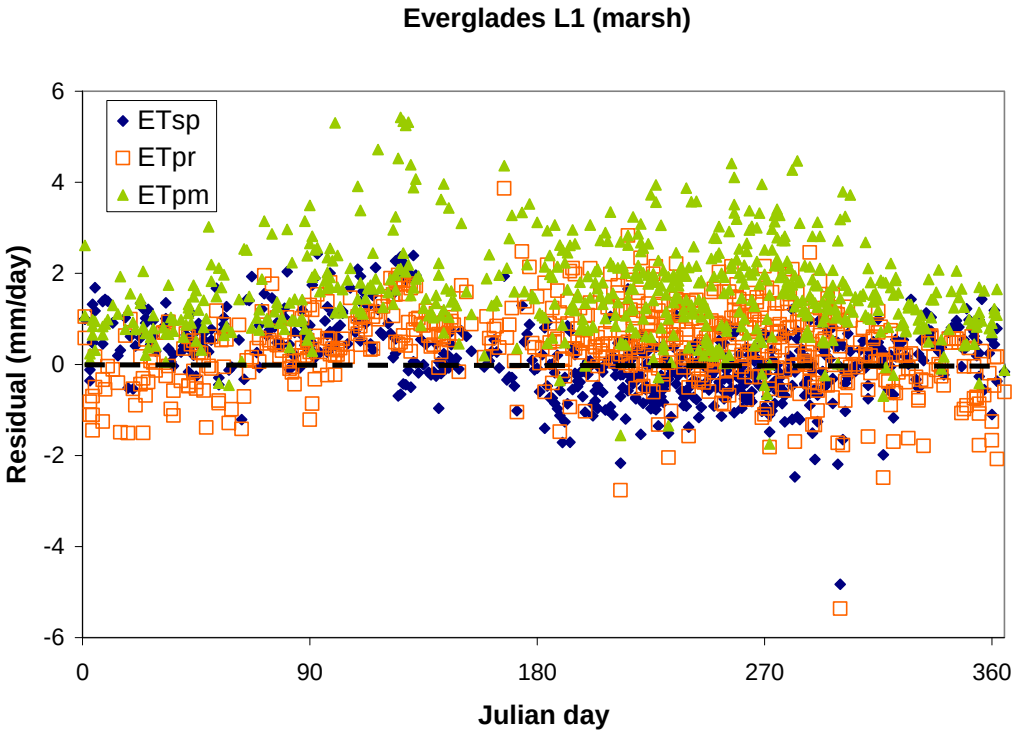
Everglades L1 (marsh)
ETsp
ETpr
ETpm
Residual (mm/day)
6
4
2
0
-2
-4
-6
0
90
180
270
360
Julian day

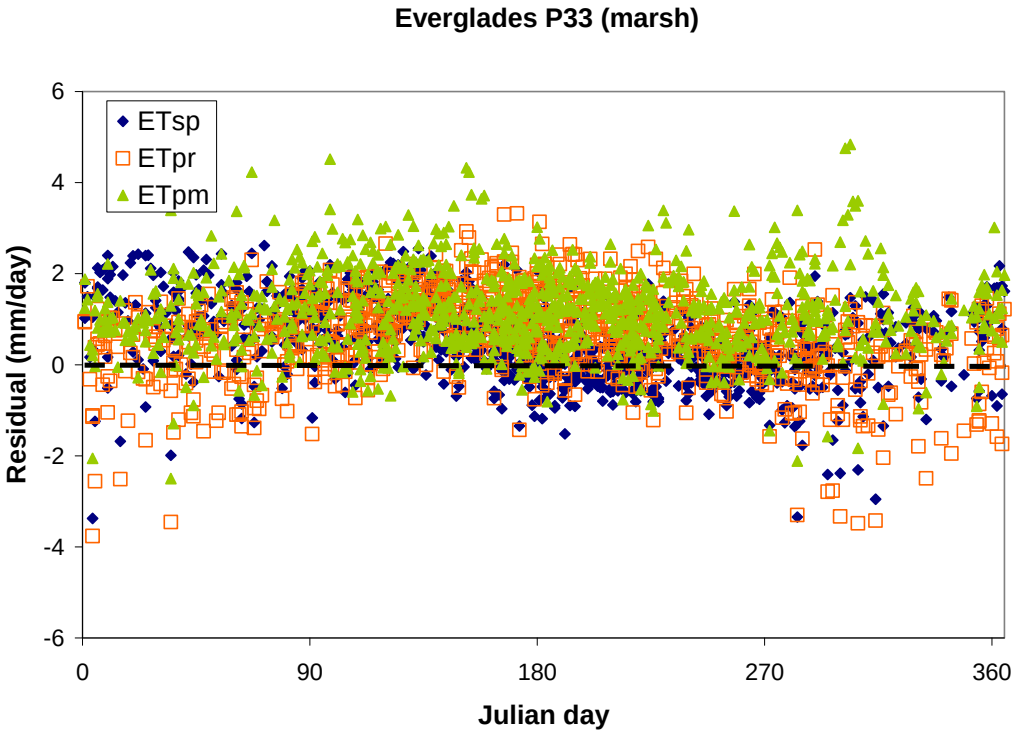
Everglades P33 (marsh)
ETsp
ETpr
ETpm
Residual (mm/day)
6
4
2
0
-2
-4
-6
0
90
180
270
360
Julian day

Everglades X1.5 (marsh)

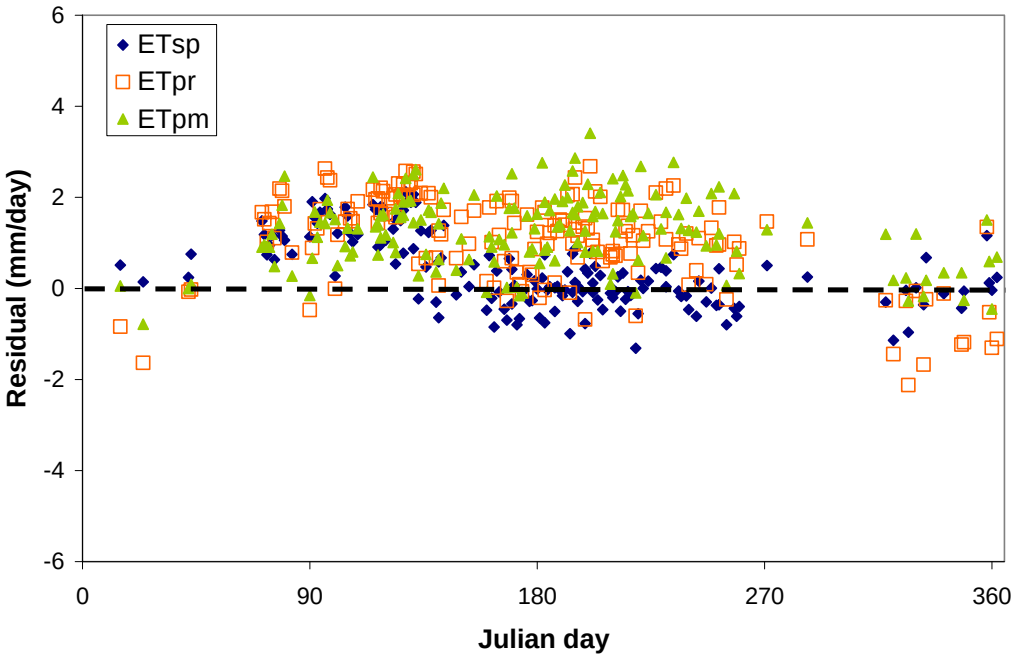

Ferris Farm (grass/pasture)

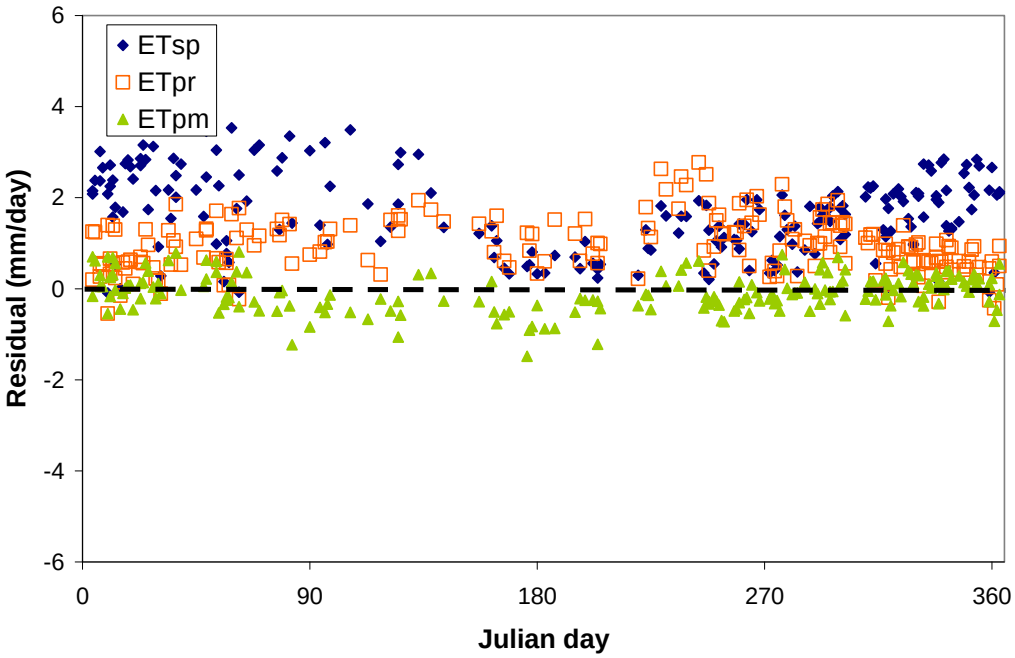

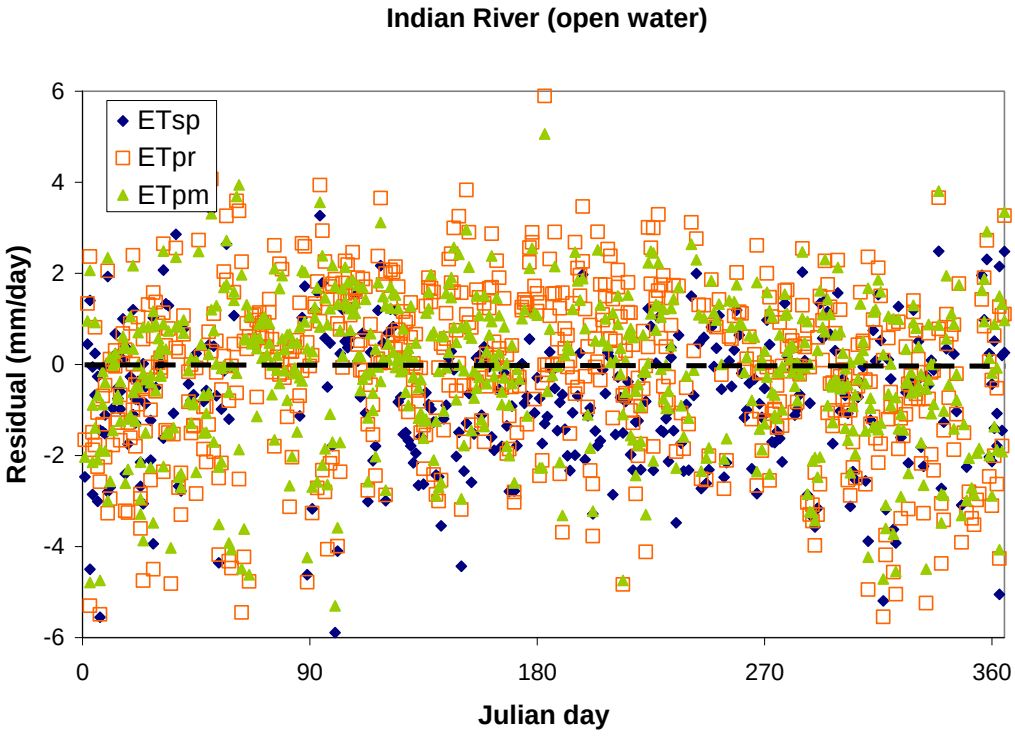
Indian River (open water)
ETsp
ETpr
ETpm
Residual (mm/day)
6
4
2
0
-2
-4
-6
0
90
180
270
360
Julian day

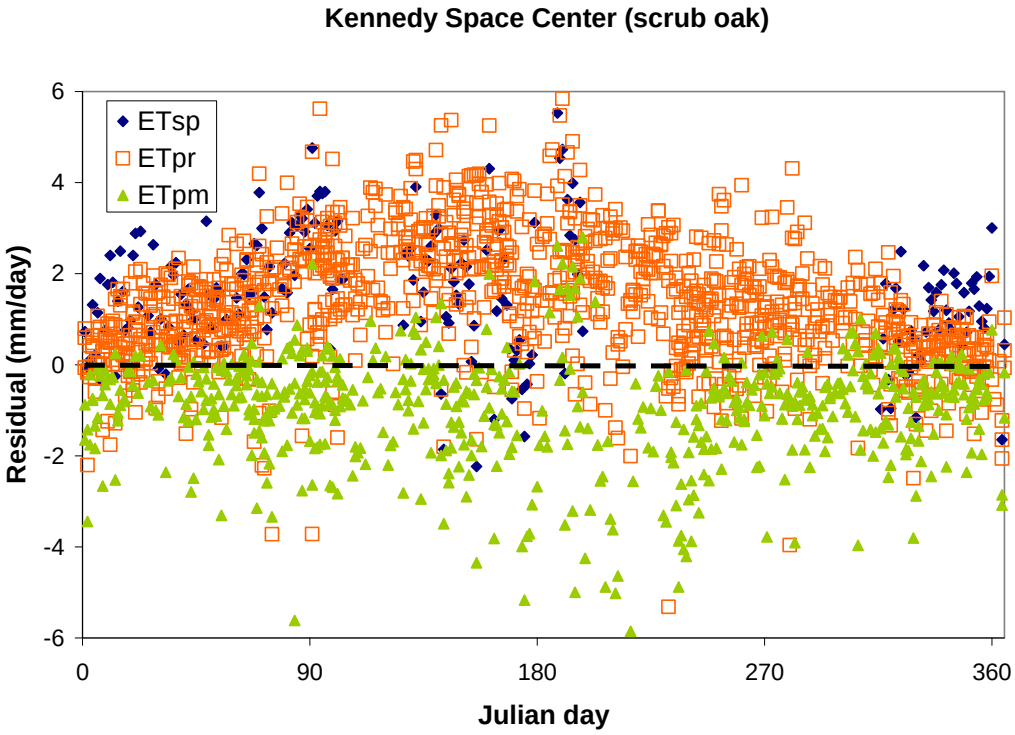
Kennedy Space Center (scrub oak)
ETsp
ETpr
ETpm
Residual (mm/day)
6
4
2
0
-2
-4
-6
0
90
180
270
360
Julian day

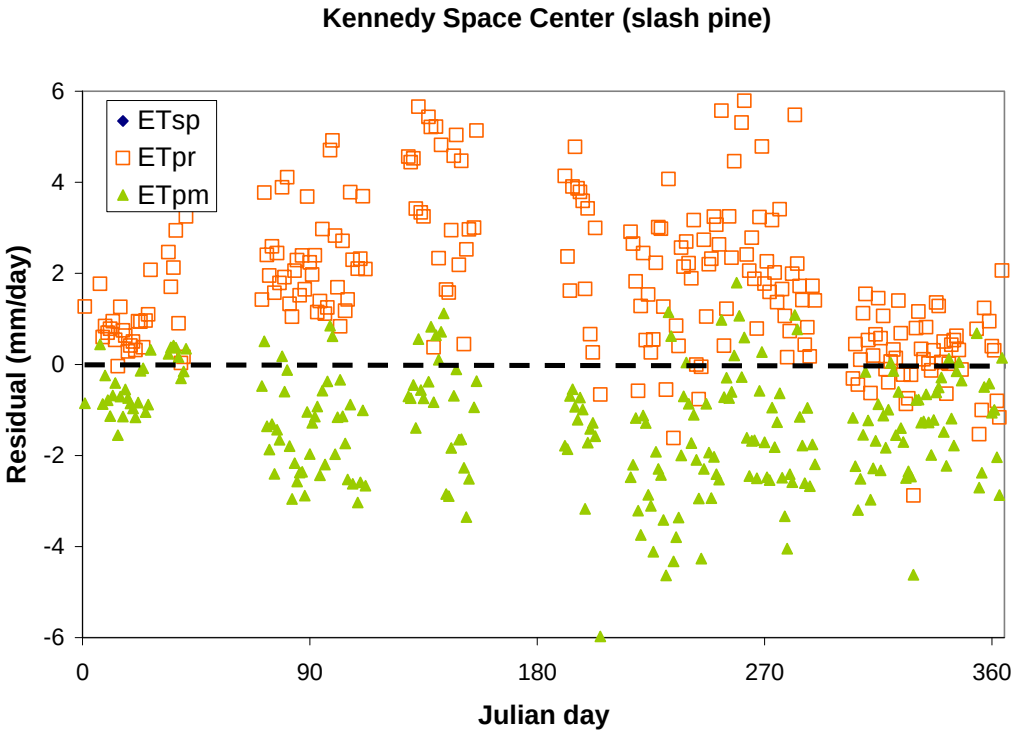
Kennedy Space Center (slash pine)
ETsp
ETpr
ETpm
Residual (mm/day)
6
4
2
0
-2
-4
-6
0
90
180
270
360
Julian day

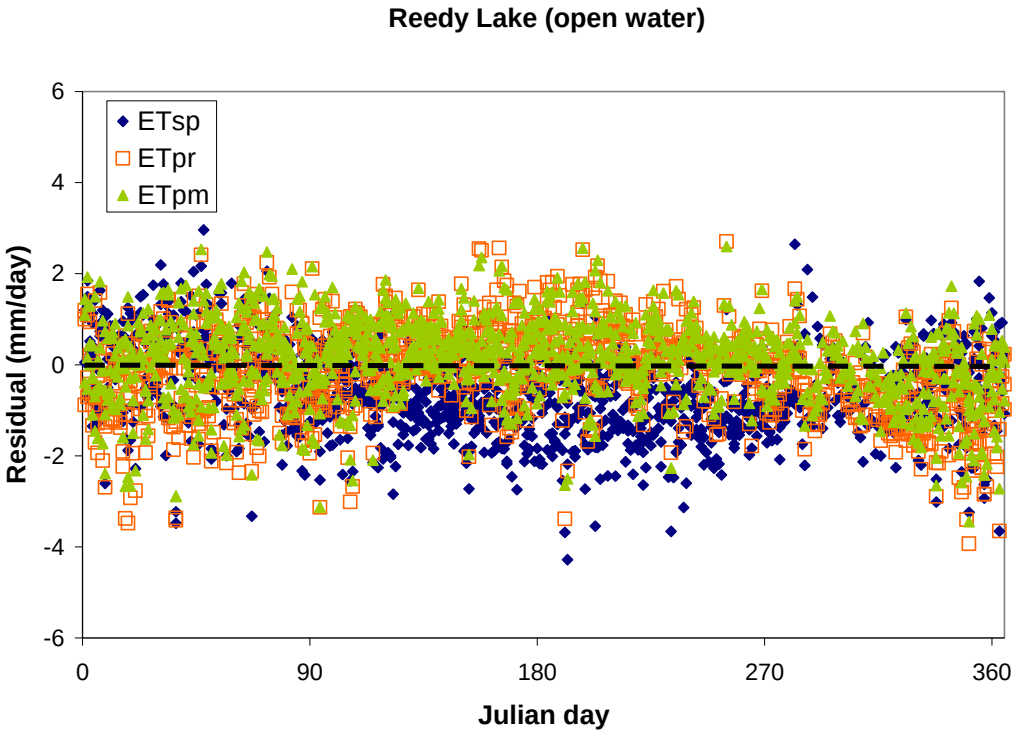
Reedy Lake (open water)
ETsp
ETpr
ETpm
Residual (mm/day)
6
4
2
0
-2
-4
-6
0
90
180
270
360
Julian day

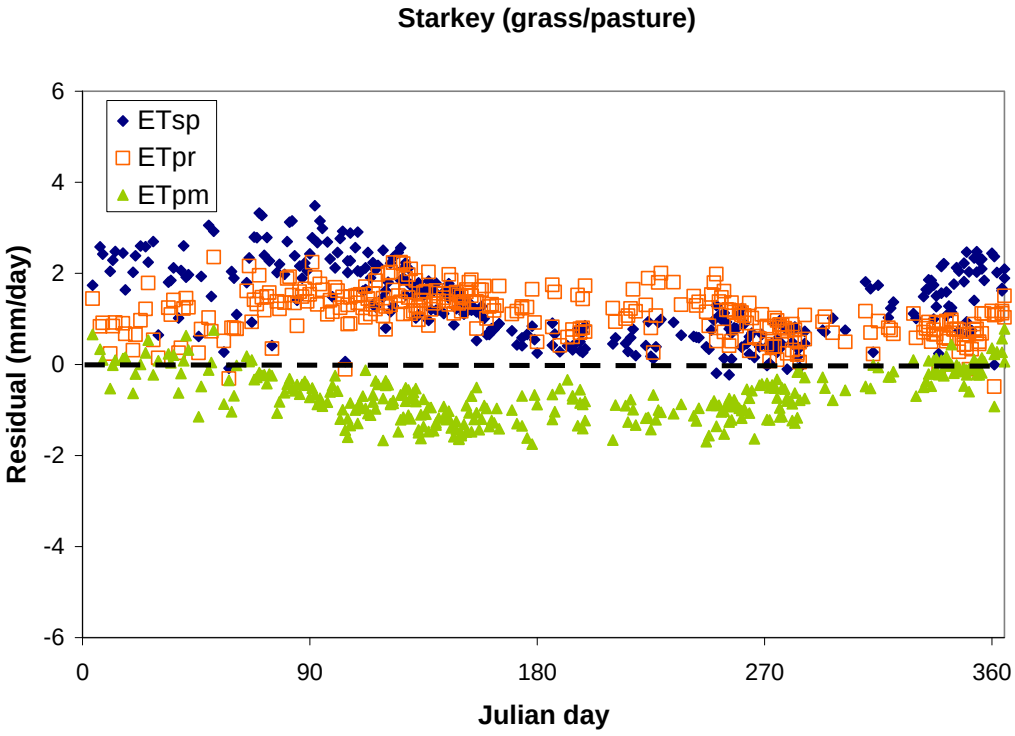
Starkey (grass/pasture)
ETsp
ETpr
ETpm
Residual (mm/day)
6
4
2
0
-2
-4
-6
0
90
180
270
360
Julian day

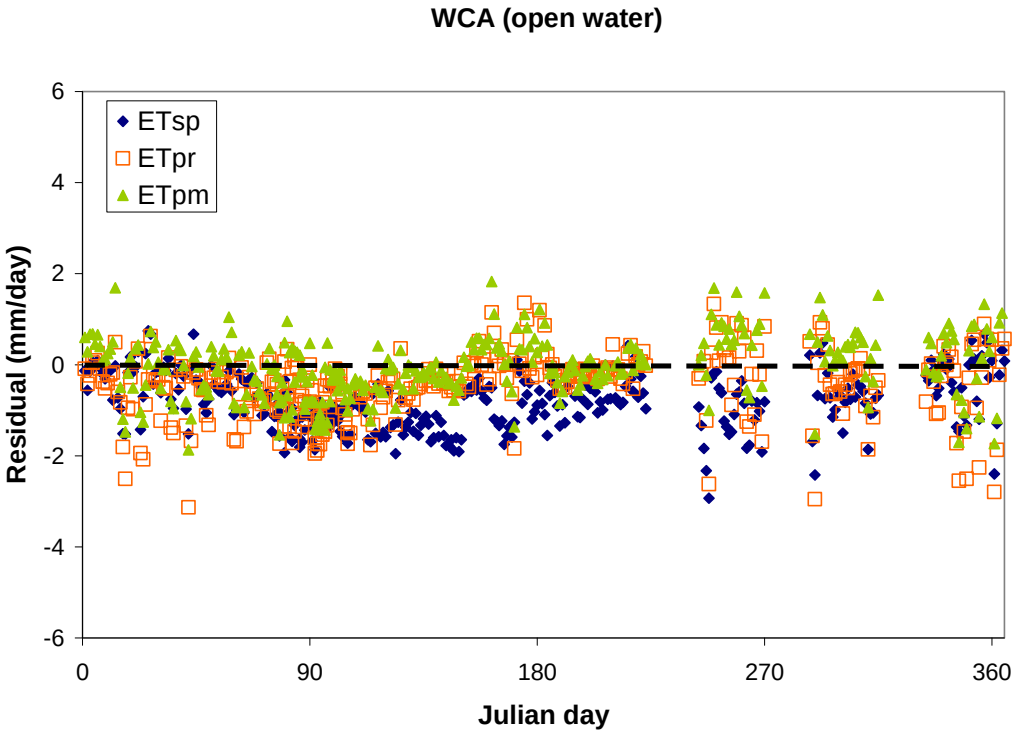
WCA (open water)
ETsp
ETpr
ETpm
Residual (mm/day)
6
4
2
0
-2
-4
-6
0
90
180
270
360
Julian day

Appendix 2.4:

Residual versus observed DAET for all “good” days

Table A2.4. The slopes of the residuals versus the daily observed evapotranspiration plots that follow for the Simple (ETsp), Priestley-Taylor (ETpr) and Penman-Monteith (ETpm) models, respectively. * Indicates that the slope is significant at the p = 0.05 level.

	Slope		
Site	Sp	PT	PM
Alachua (mature pine)	-0.58*	-0.58*	-0.84*
Alachua (immature pine)	-0.29*	0.05	-0.67*
Belleview	-0.23*	0.08*	-0.74*
Blue Cypress	-0.27*	0.02	-0.37*
Blue Springs Tract	--	--	--
Carlton Ranch	-0.26*	0.24*	-0.73*
Disney Wilderness	0.03	0.27*	-0.38*
Duda Farm	-0.12*	0.23*	-0.35*
Everglades L1	-0.28*	0.14*	0.41*
Everglades P33	-0.25*	0.07*	0.01
Everglades X1.5	-0.23*	0.28*	0.31*
Ferris Farm	0.23*	0.45*	-0.16*
Indian River	-0.68*	-0.54*	-0.54*
KSC (scrub oak)	-0.41*	-0.19*	-0.75*
KSC (slash pine)	--	-0.29*	-0.84*
Reedy Lake	-0.04*	-0.04*	-0.12*
Starkey	0.17*	0.38*	-0.34*
WCA	-0.28*	-0.12*	-0.19*

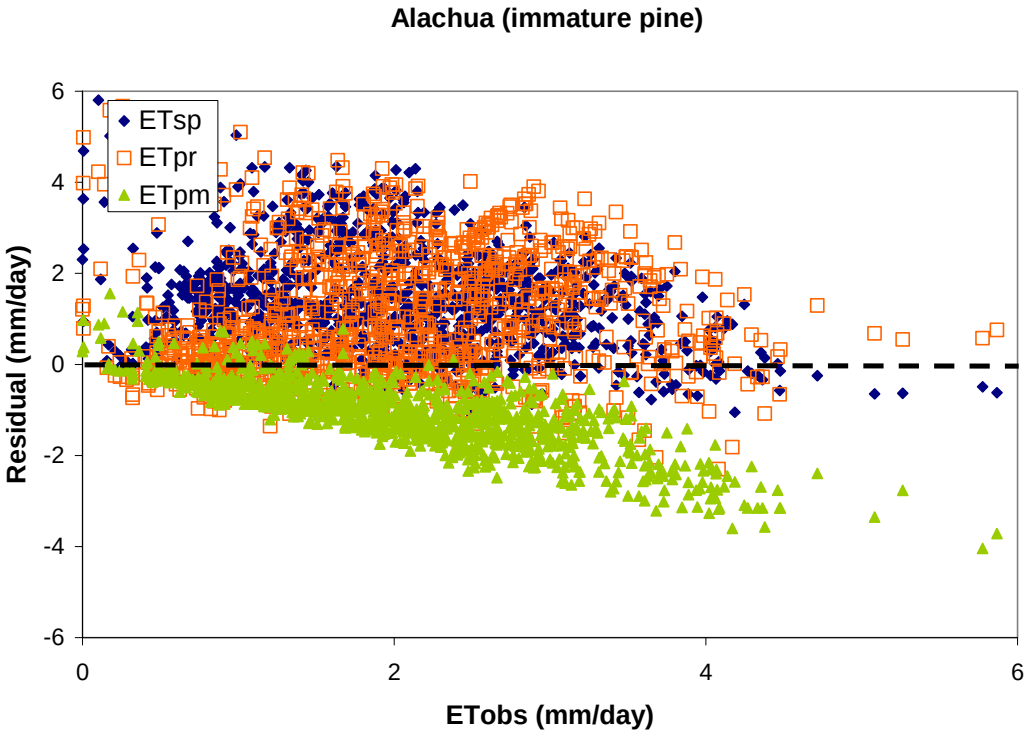
Alachua (immature pine)
ETsp
ETpr
ETpm
Residual (mm/day)
ETobs (mm/day)
6
4
2
0
-2
-4
-6
0
2
4
6

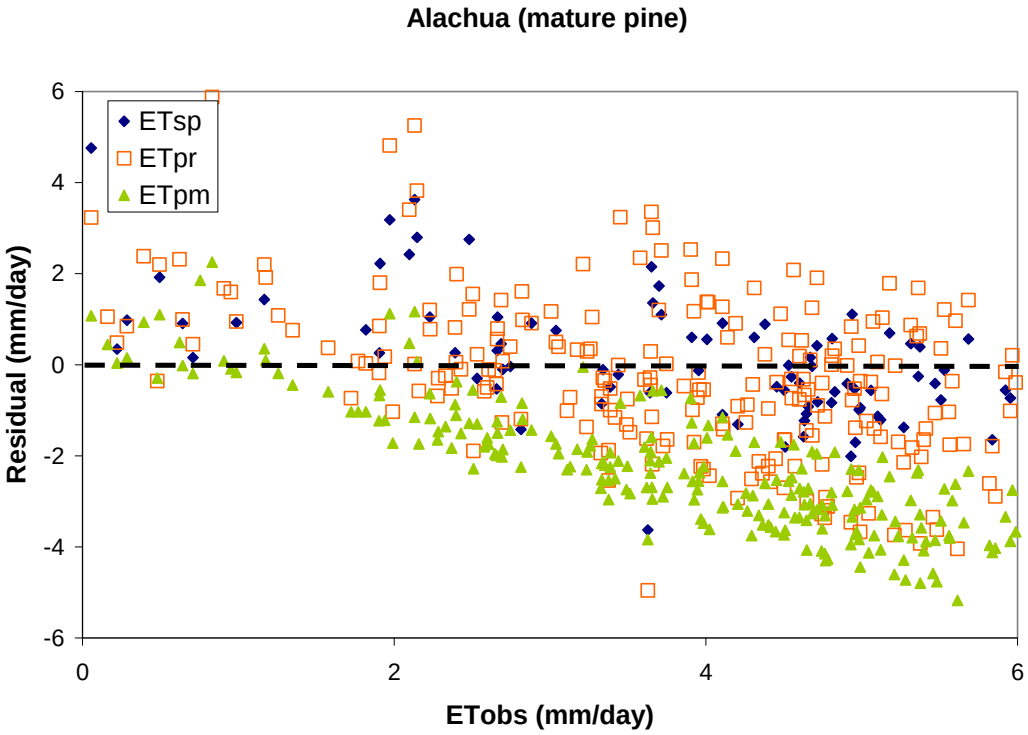
Alachua (mature pine)
ETsp
ETpr
ETpm
Residual (mm/day)
ETobs (mm/day)
6
4
2
0
-2
-4
-6
0
2
4
6

Belleview (citrus)

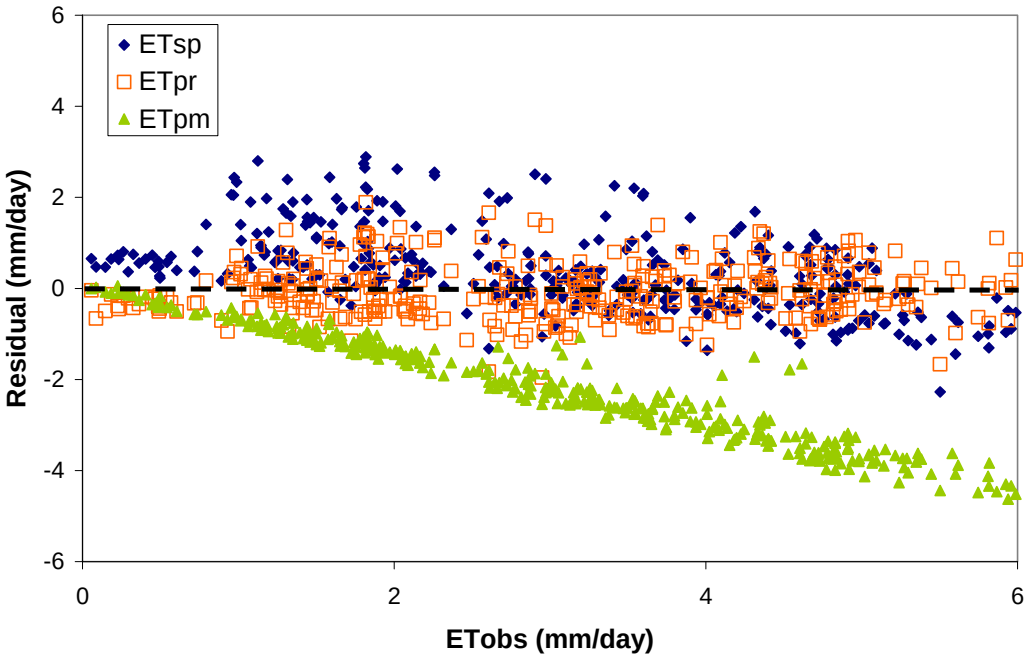

Blue Cypress (marsh)

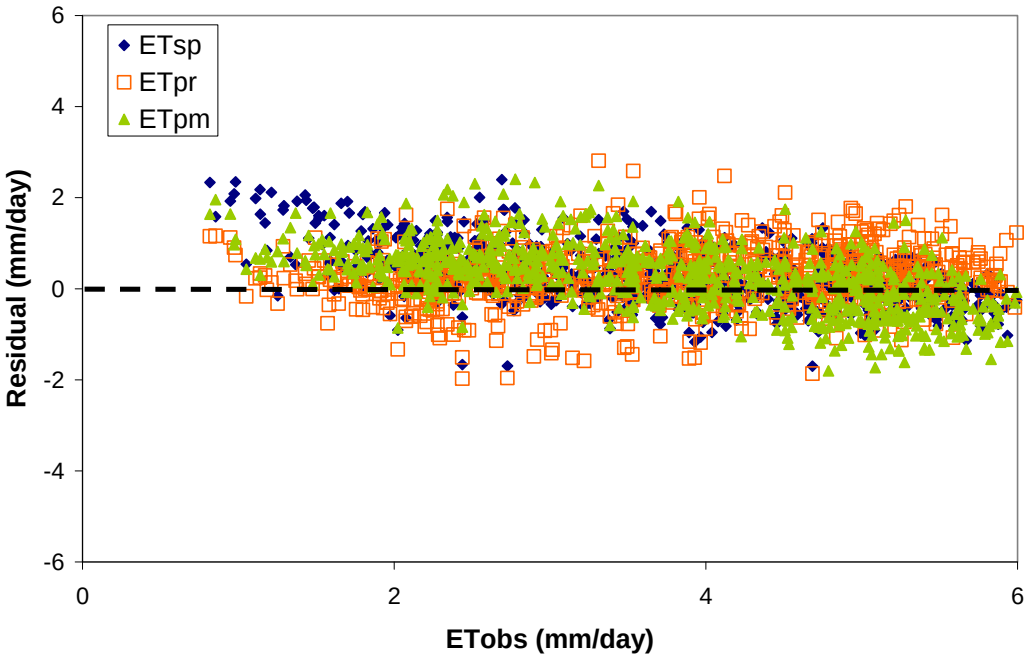

Blue Springs (pine)

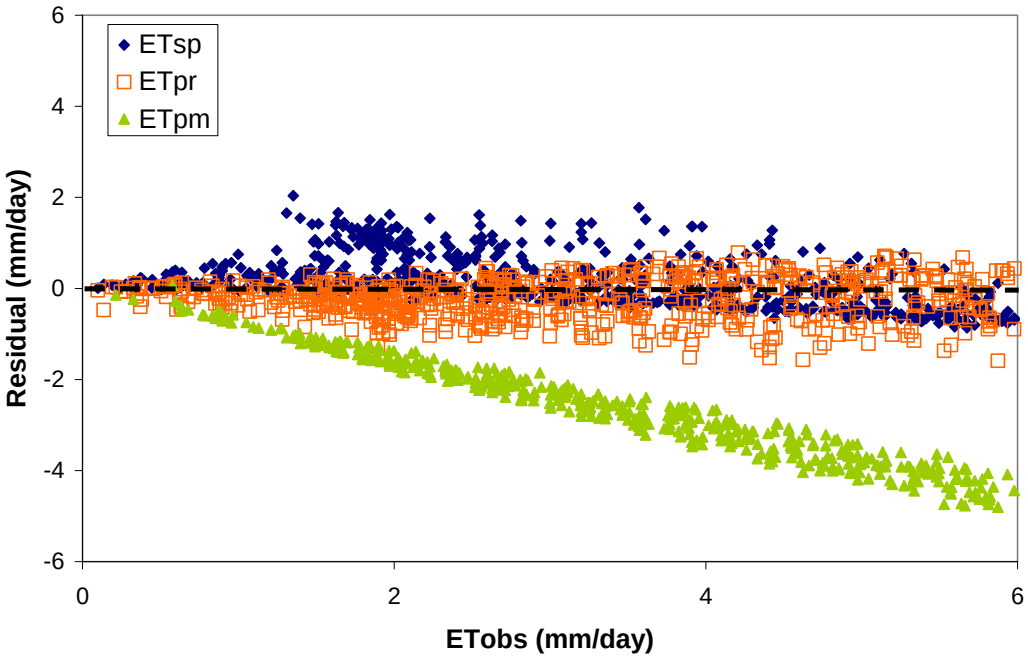

Carlton Ranch (citrus)

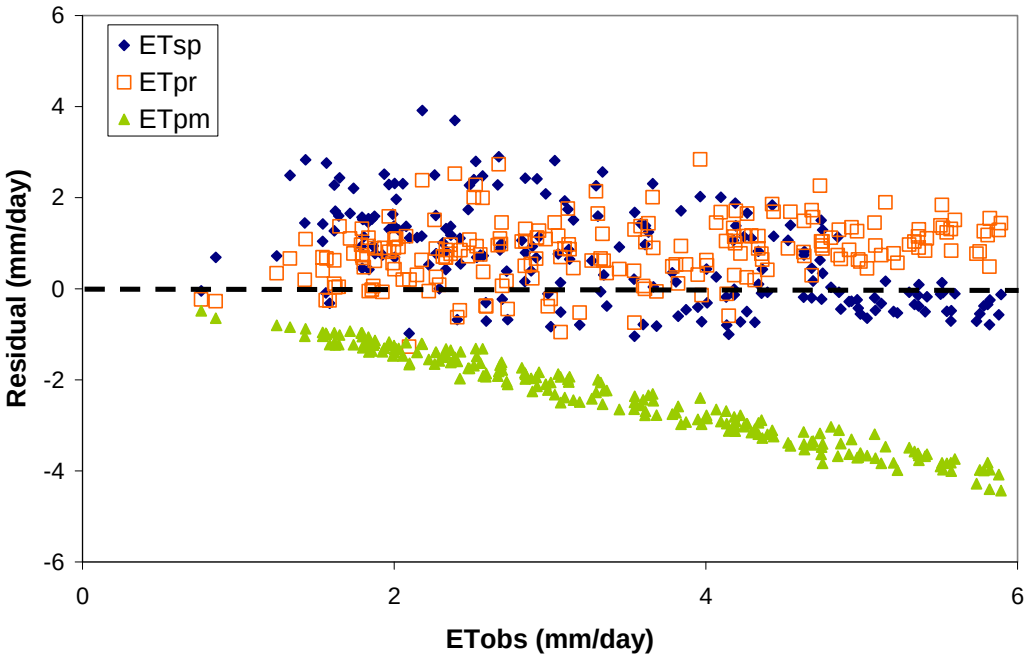

Disney Wilderness (grass/pasture)

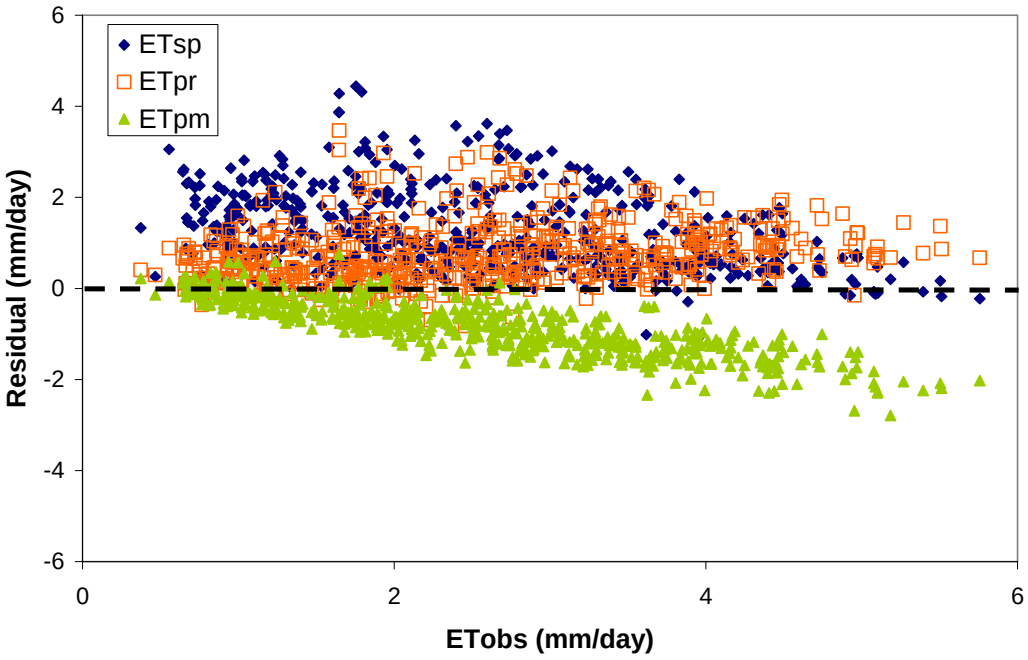

Duda Farm (grass/pasture)

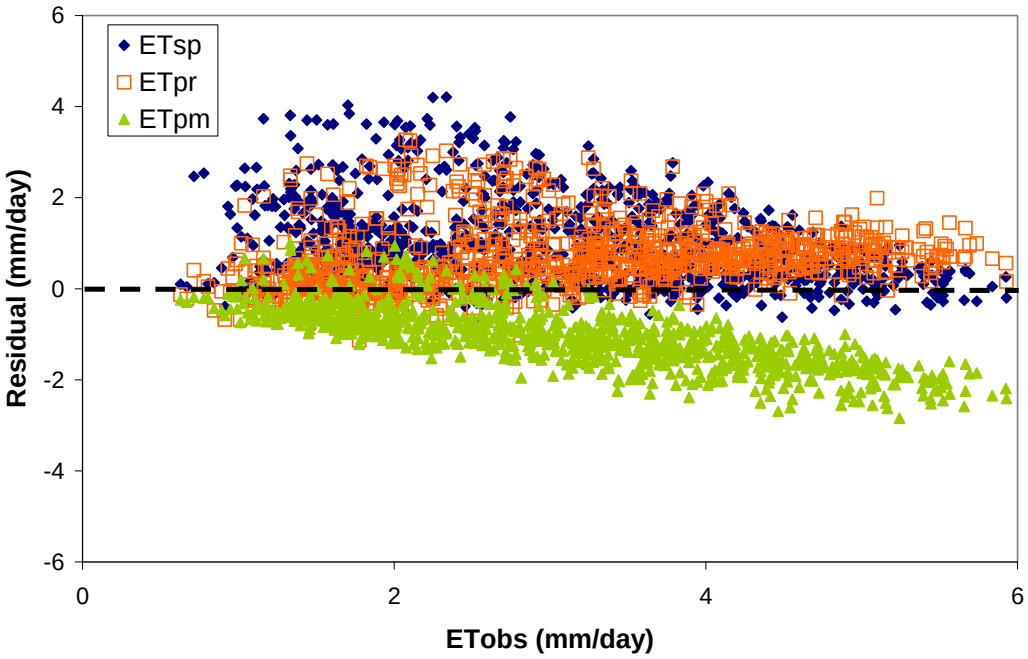

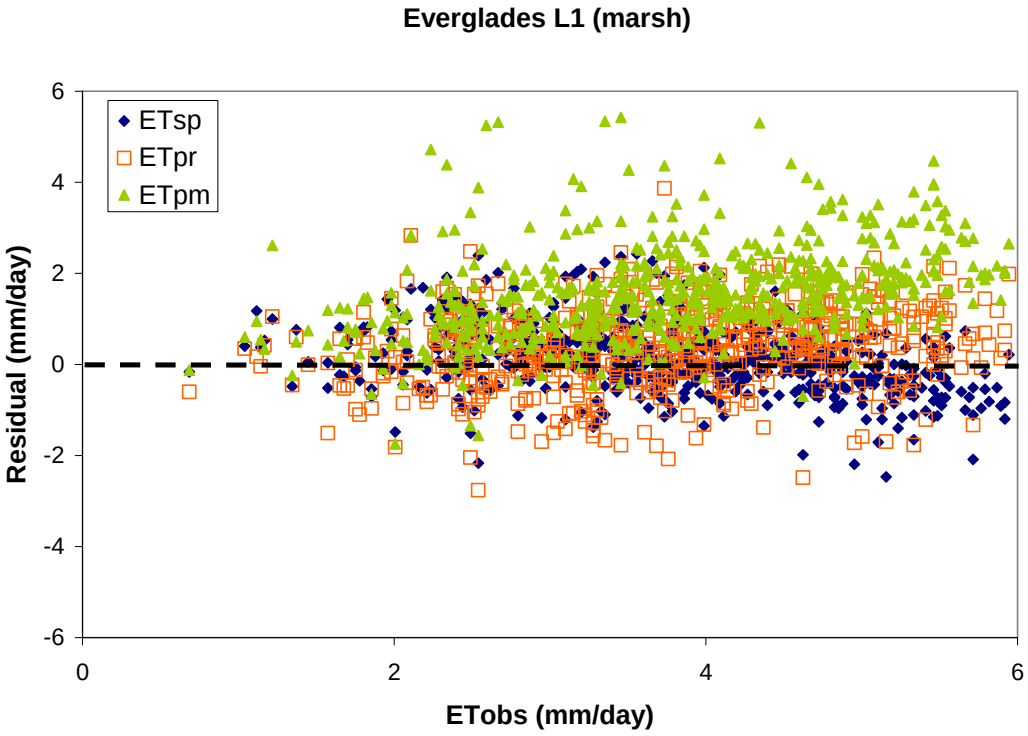
Everglades L1 (marsh)
ETsp
ETpr
ETpm
Residual (mm/day)
ETobs (mm/day)
6
4
2
0
-2
-4
-6
0
2
4
6

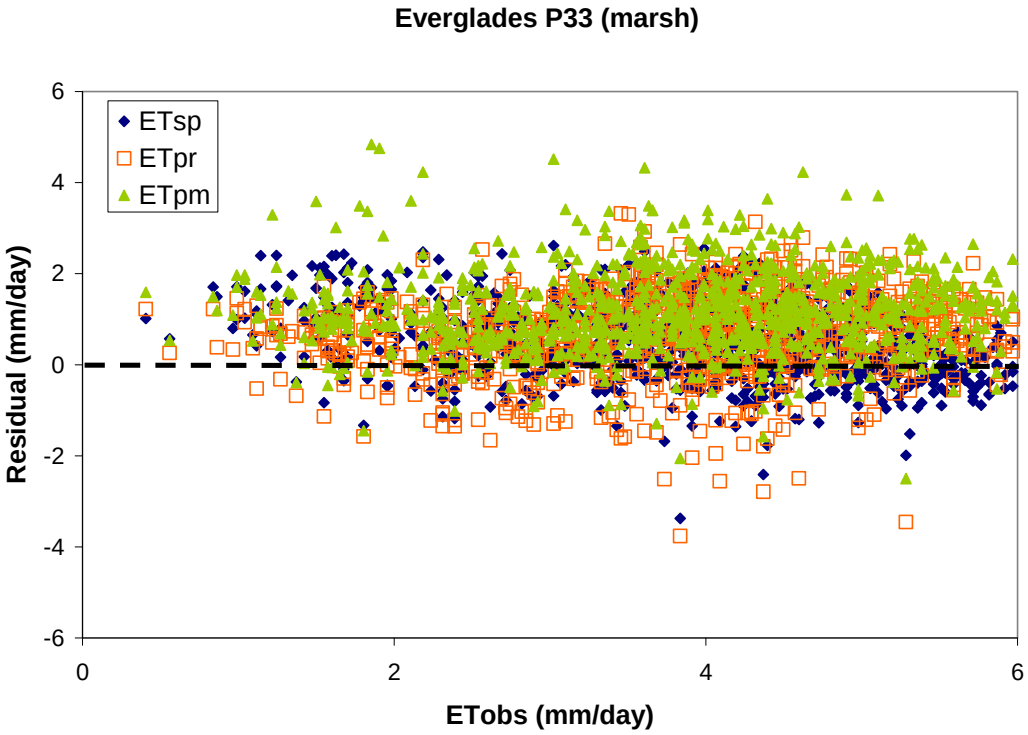
Everglades P33 (marsh)
ETsp
ETpr
ETpm
Residual (mm/day)
ETobs (mm/day)
6
4
2
0
-2
-4
-6
0
2
4
6

Everglades X1.5 (marsh)

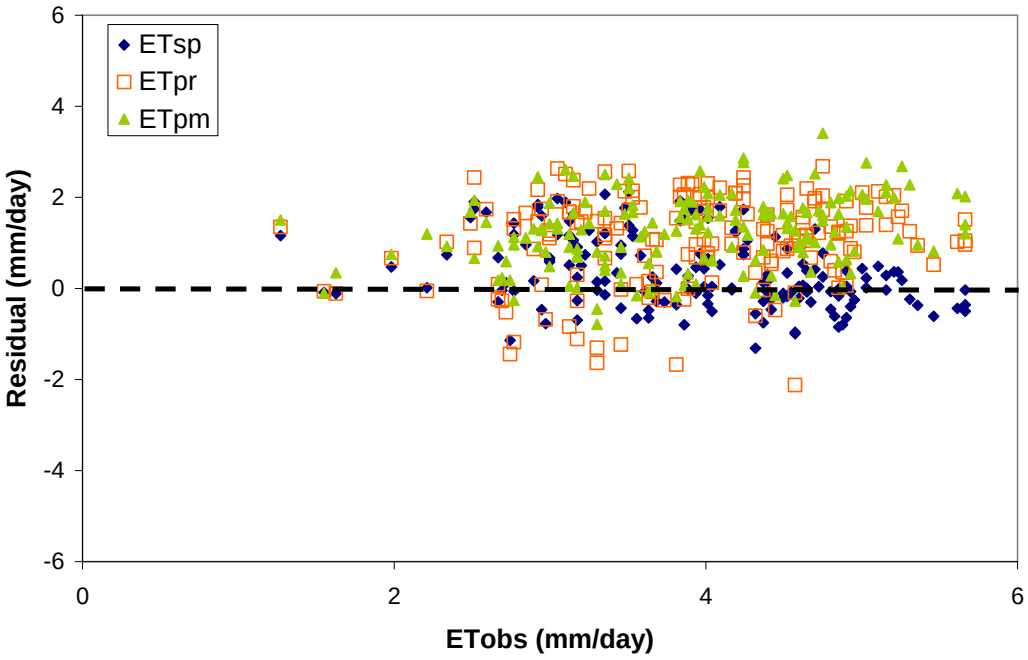

Ferris Farm (grass/pasture)

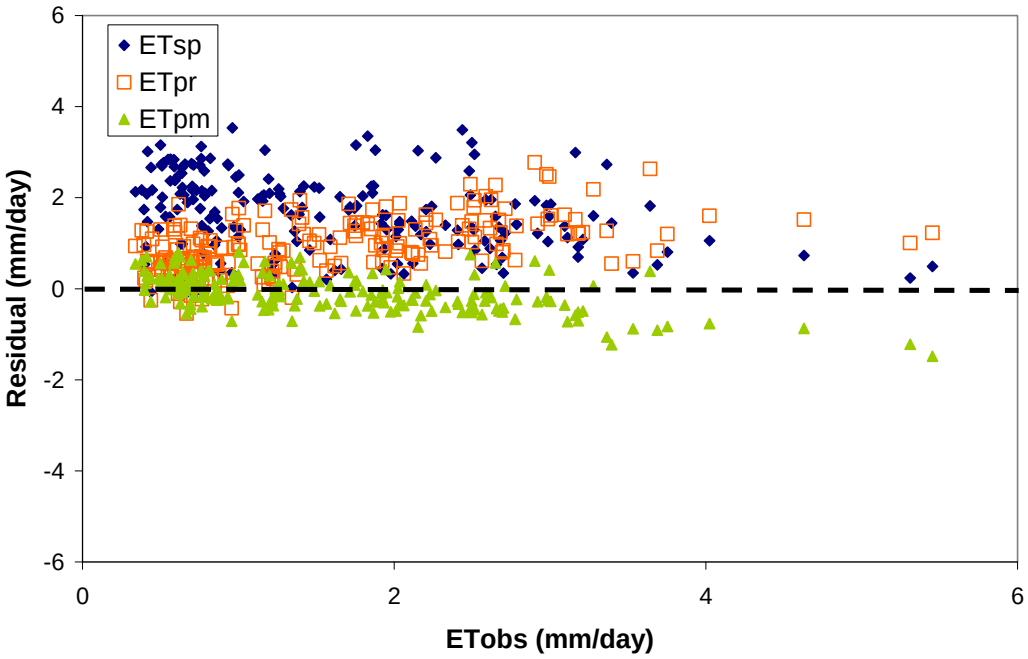

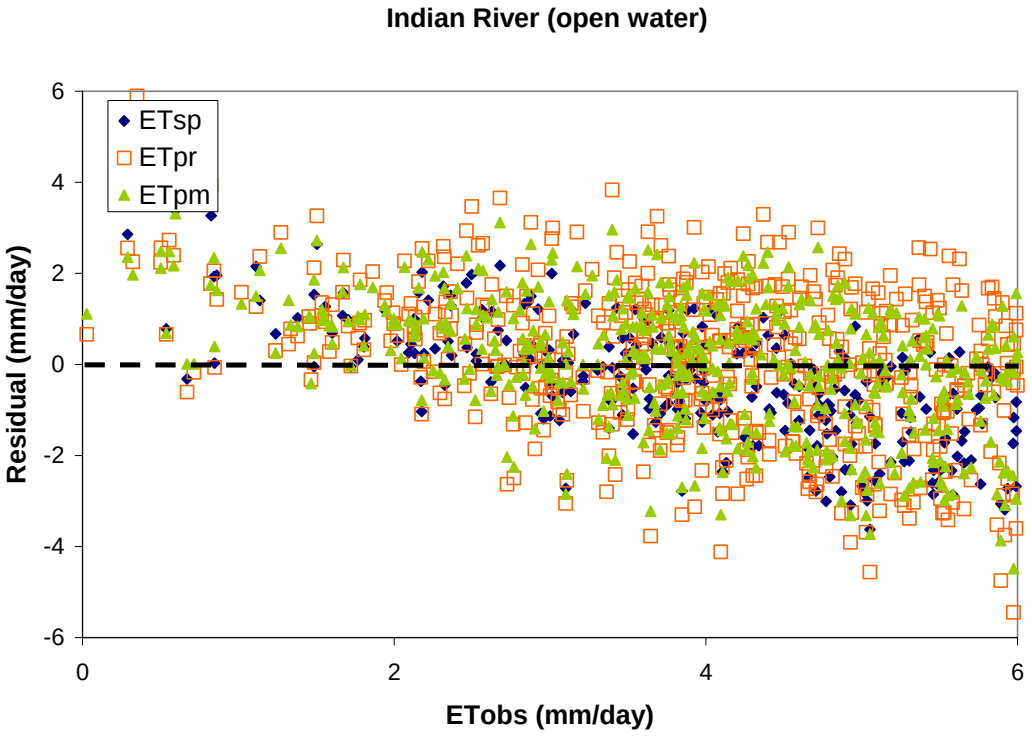
Indian River (open water)
ETsp
ETpr
ETpm
Residual (mm/day)
ETobs (mm/day)
6
4
2
0
-2
-4
-6
0
2
4
6

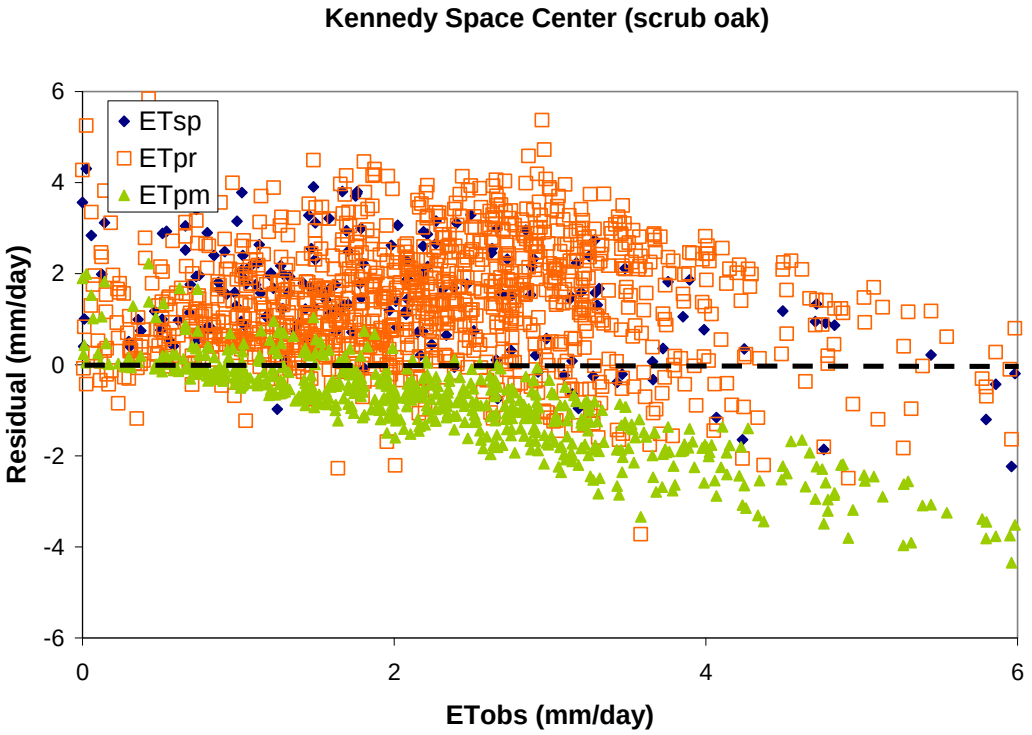
Kennedy Space Center (scrub oak)
ETsp
ETpr
ETpm
Residual (mm/day)
ETobs (mm/day)
6
4
2
0
-2
-4
-6
0
2
4
6

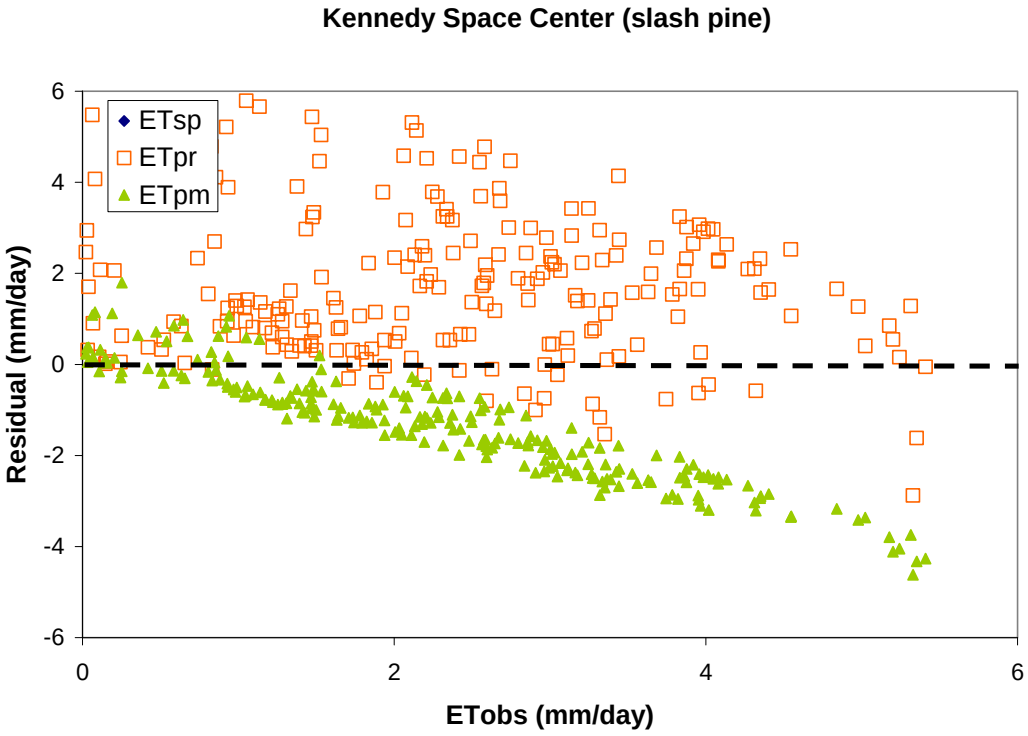
Kennedy Space Center (slash pine)
ETsp
ETpr
ETpm
Residual (mm/day)
ETobs (mm/day)
6
4
2
0
-2
-4
-6
0
2
4
6

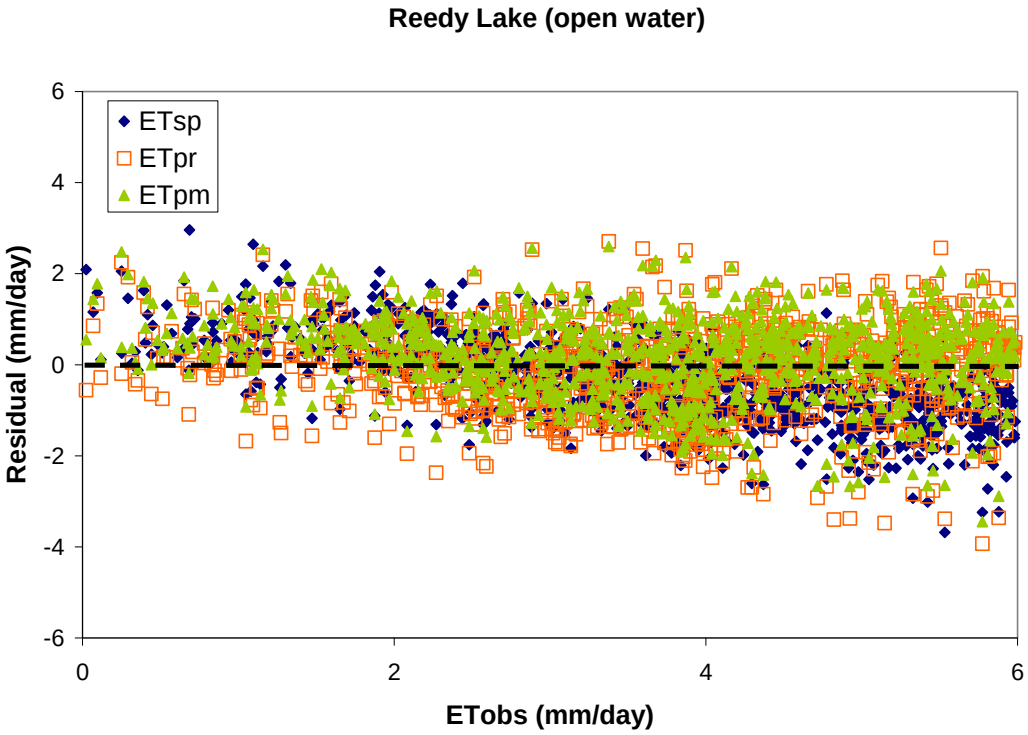
Reedy Lake (open water)
ETsp
ETpr
ETpm
Residual (mm/day)
ETobs (mm/day)
6
4
2
0
-2
-4
-6
0
2
4
6

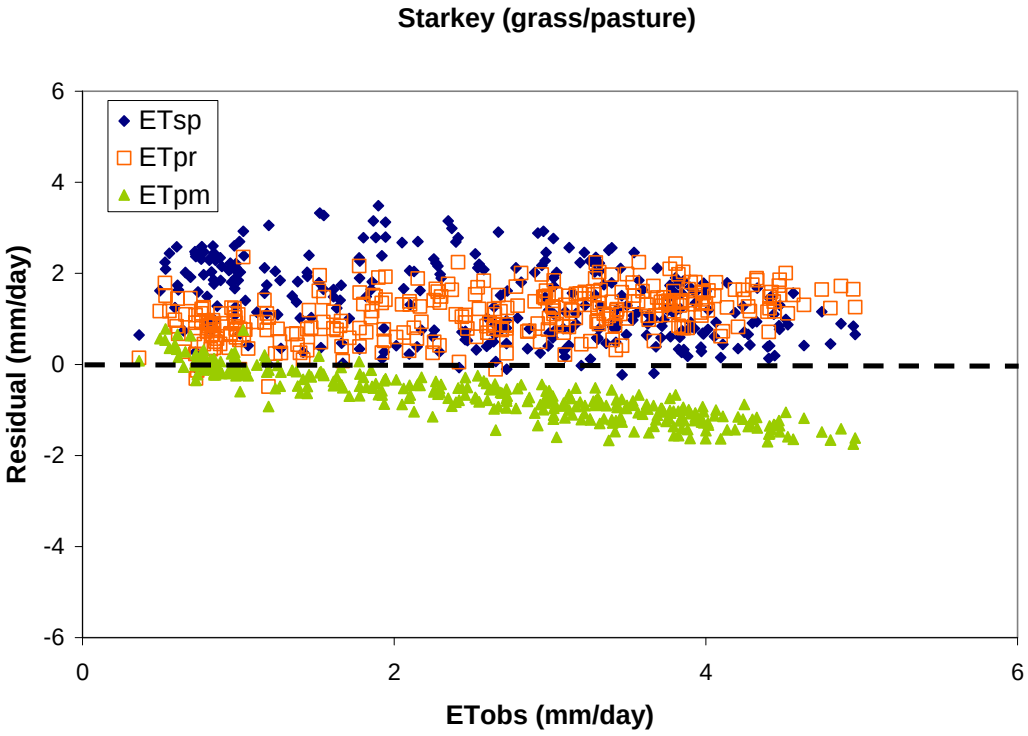
Starkey (grass/pasture)
ETsp
ETpr
ETpm
Residual (mm/day)
ETobs (mm/day)
6
4
2
0
-2
-4
-6
0
2
4
6

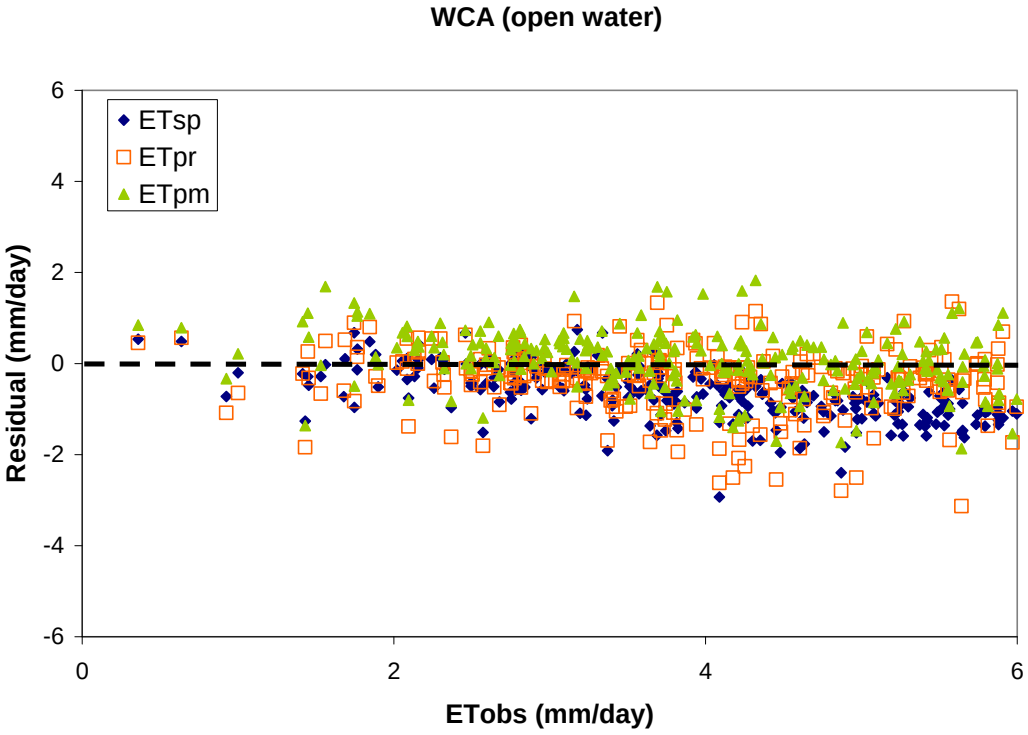
WCA (open water)
ETsp
ETpr
ETpm
Residual (mm/day)
ETobs (mm/day)
6
4
2
0
-2
-4
-6
0
2
4
6

Appendix 2.5:

Penman-Monteith forest ET compared to observed DAET with estimated stomatal resistance and 50% of with estimated stomatal resistance

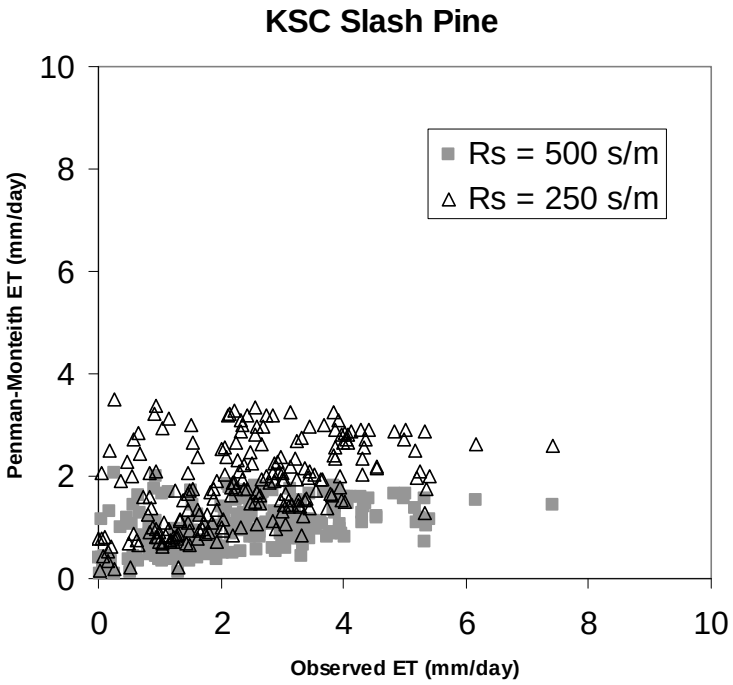
KSC Slash Pine
Rs = 500 s/m
Rs = 250 s/m
Penman-Monteith ET (mm/day)
Observed ET (mm/day)
0
2
4
6
8
10

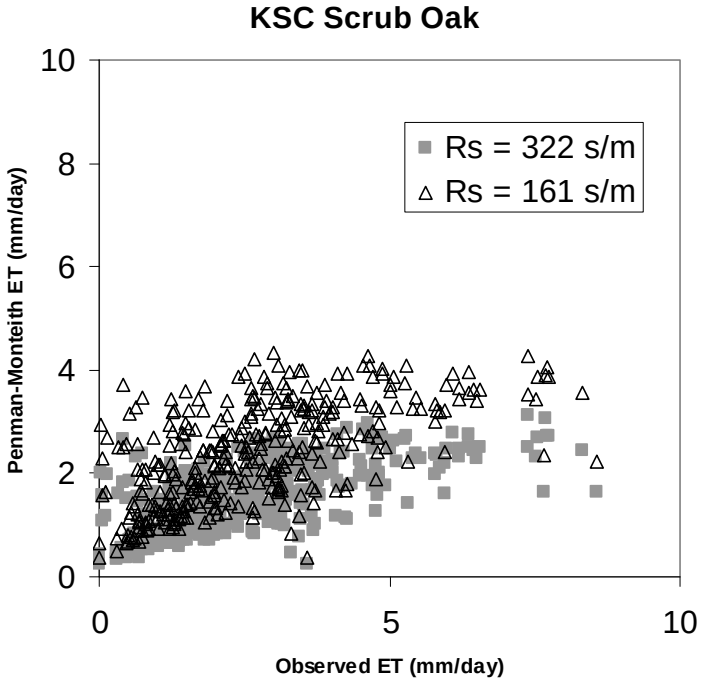
KSC Scrub Oak
Rs = 322 s/m
Rs = 161 s/m
Penman-Monteith ET (mm/day)
Observed ET (mm/day)
0
5
10

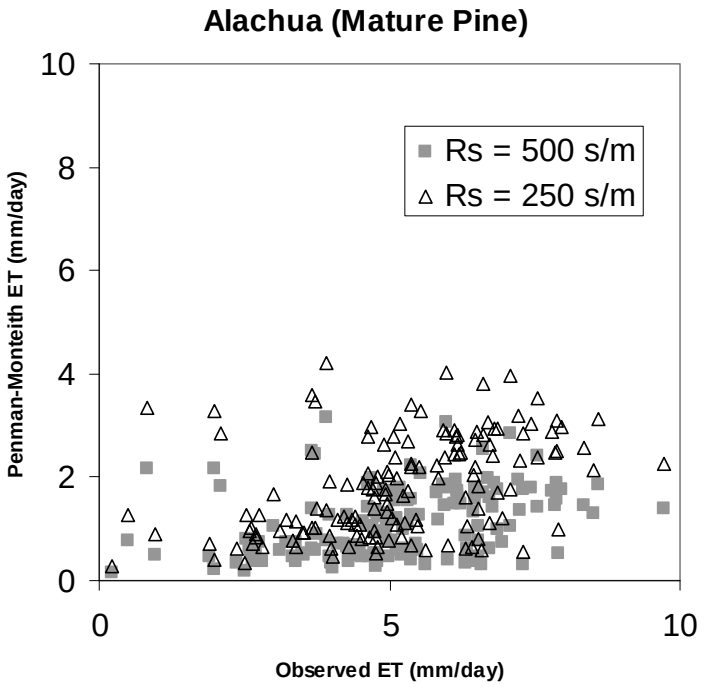
Alachua (Mature Pine)
Rs = 500 s/m
Rs = 250 s/m
Penman-Monteith ET (mm/day)
Observed ET (mm/day)
0
2
4
6
8
10
0
5
10

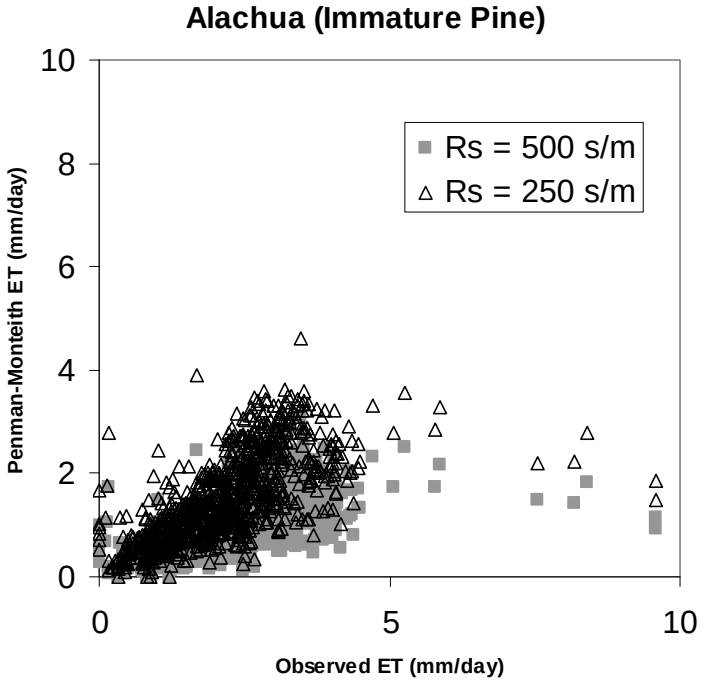
Alachua (Immature Pine)
Rs = 500 s/m
Rs = 250 s/m
Penman-Monteith ET (mm/day)
Observed ET (mm/day)
0
2
4
6
8
10
0
5
10

Appendix 5.1:

Directory Structure of PET and RET Backup Drive

Reference ET and Priestley-Taylor ET data

1) Climate data (Climate data in 2 km grid)
- Folder name: Climate
- Subfolders: \output, Temp, RH, Wind
  Each subfolder contains subfolder for each year dataset
  Each year contains Fortran source code, i.e., Interpolation_IDW_3_Temp.f90
  Fortan code requires input files:
  2km_grid.txt (Latitude and Longitude for all pixels)
  list_climatemax.dat (list of output files)
  list_climatemin.dat (list of output files)
  year_StationsRH.txt (list of local climate stations)
  #_#_yearRH.txt (max, min for each pixel by stations)
  Output climate files for each day of year contains latitude and longitude and climate
  - In Fortran source code, change date (Ln 15), available sites (Ln 16), and file name for sites (Ln 46).

2) ET analysis
- Folder name: ET_com (contains each subfolder for reference ETo and PET analysis)
- Subfolders: ETo_2004, ETo_2003, etc.
- Input data required: 6 list files
  list_GOES_RS.dat (list for GOES insolation files)
  list_Tmax.dat (list for max. temperature files)
  list_Tmin.dat (list for min. temperature files)
  list_RHmax.dat (list for max. humidity files)
  list_RHmin.data (list for min. humidity files)
  list_wind.dat (list for wind files)
  4 fixed input files
  Julian.dat (DOY for year)
  Longitude.dat (longitude for each pixel)
  Latitude.dat (latitude for each pixel)
  LAT_LON_Albedo_FL.txt (Albedo value for land and water for each pixel)

Climate data
GOES-Dsolar_UAH-TIRGCL_**cal**.date.Q#
Tmax.yeardate
Tmin.yeardate
RHmax.yeardate
RHmin.yeardate
Wind.yeardate

For reference ET
Note) 6 list files and corresponding climate input files are copied from interpolation folder.

- Process file
ETo_only.f90 (calculate reference ET)
Only change between year date in the code (Ln 10).
- Make input file: list_ETo_out.dat (list for output files for ETo)

Output files: ETo.yeardate (-9999.900 is missing by GOES solar radiation)

For PET

Note) Albedo data were obtained from WMD (LAT_LON_Albedo_FL.txt)
- Albedo needed for only PET calculation, not Reference ET.
- Process file
PET_only.f90 (calculate PET)
Only change between year date in the code (Ln 10).
- Make input file: list_PET_out.dat (list for output files for PET)
Need to create from list_ETo 1995 to 2003

Output files: PET.yeardate (-9999.900 is missing by GOES solar radiation)

For 1995, GOES solar radiation was available from DOY 152 to DOY 365. As a matter of convenience and in order to not modify source code to account for the limited days, a dummy set of solar radiation data was used from DOY 1 to DOY 151 (1996 GOES solar radiation was used). PET output files for DOY 1 to 151 are labeled as ETo.YearDOY_dummy. Valid result files for reference ET and PET are available from DOY 152.

3) Final Data from UAH
- Folder name: GOESRS (Final dataset from Simon Paech, 07/2007)
- contains final Daily solar radiation for 1995 to 2004
Daily solar radiation (GOES-Dsolar_UAH-TIRGCL_**cal**.date.Q#)
list_GOES_RS.dat (list of solar radiation files)
list.dat (intermediate file used to create list_GOES_RS.dat)

4) Data from UAH for 2004 only (Received from Simon Paech, 02/2007 to analyze albedo)
- Folder name: GOESAlbedo_UAH
- Subfolders: GOES_Insolation_2004

Albedo_2004 Un-projected data (Data used for daily GOES albedo data extractions corresponding with 11 local sites)

Input: GOES-Albedo_UAH-TIRGCL.date
List_goes_albedo.dat (Iist of GOES Albedo files)
extract_raw_goes_albedo_specs.dat (list of extracted sites)
Input data modified at line 6 data directory
at line 9 for year, start, and end day

Source code: extract_goes_albedo.pro (run using IDL)

Output: SJR_#_year_date_GOES_min_alb.dat

Albedo_2005 Un-projected data (Data used for daily GOES albedo data extractions corresponding with 11 local sites)

Input: FLORALB.date
List_goes_albedo.dat (Iist of GOES Albedo files)
extract_raw_goes_albedo_specs.dat (list of extracted sites)
Input data modified at line 6 data directory
at line 9 for year, start, and end day

Source code: extract_raw_goes_albedo.pro (run using IDL)

Output: SJR_#_year_date_raw_GOES_min_alb.dat

Calibration (contains Albedo extraction program coding by IDL, calibrations, and readmes)

- Other subfolders: Not used by UNH

5) ArcGIS dataset
- Folder name: FLGIS (contains Net Radiation sites in FL)

6) Net Radiation analysis
- Folder name: NetRadiation_Computation (contains all R_{ld} and RN analysis for 11 experiment sites)
- Subfolders: Data\Analysis

All files that has "Minha" suffix modified and created by Minha

Albedo_calcs_minha.xls (contains all albedo values and plots)

Ex) LakeApopka.RN_minha.xls contains

Experiment data
clear sky R_{ld} (subsheet: Rld_clear)
cloudy sky R_{ld} (subsheet: Rld_clear)
RN (subsheet: Rld_clear)

GOES data (Same as above, but GOES albedo values inserted in Col. J)
clear sky R_{ld} (subsheet: Rld_clear(GOES_Albedo))
cloudy sky R_{ld} (subsheet: Rld_clear(GOES_Albedo))
RN (subsheet: Rld_clear(GOES_Albedo))

Annual average albedo (Same as above, but net solar radiation and constant albedo values inserted in Cols. I and J)
clear sky R_{ld} (subsheet: Rld_clear(Avg_Albedo))
cloudy sky R_{ld} (subsheet: Rld_clear(Avg_Albedo))
RN (subsheet: Rld_clear(Avg_Albedo))

- Summary tables for all sites' results

Rldc_Summary_Minha.xls (contains longwave radiation results)
Rld_Clear (Table 5)
Rld_Cloudy (Table 6)

Rn_Summary_Minha.xls (contains RN results)
11 Sites (Tables 7 and 8)

11 Sites Ave Albedo (Tables 9 and 10)

Rn_Summary_avg_albedo.xls (contains RN results using local, GOES, and annual average albedo) Same as previous – sent for conference call July 2007

ASCE_RN_Graph.xls (contains all results for ASCE spring meeting, 2007)

- Subfolders: Data\FW_Analysis (contains BlueCypress and DudaFarm analysis)
  Sites_fw.xls (intermediate albedo values)
  LakeApopka.RN_minha.xls (comparable to 11 sites given above)

- Subfolders: Data\Net Radiation (Contains raw data for daily and hourly)

Appendix 5.2:

Meteorological Station Tables

The following tables summarize the available data by measurement, station, year, and quality. X indicates the data were valid for the corresponding year, blank indicates the data were not available, and, where present, 99Y indicates the data were available, but were not used due to data quality issues. The flag value indicated the extent of the data's problems. A 991 flag indicated minor problems while a 999 flag indicated major problems.

Temperature Meteorological Station Tables

File Names	Latitude	Longitude	Station Name (NOAA)	95	96	97	98	99	00	01	02	03	04
80211_12832_1995T.txt	29.73	-85.017	APALACHICOLA	X	X	X	X	X	991	X	991	X	X
80228_99999_1995T.txt	27.22	-81.867	ARCADIA	991	991	X	999	999	991	992	999	X	X
80236_99999_1995T.txt	27.18	-81.350	ARCHBOLD BIO STATION	X	X	991	X	X	X	X	X	X	X
80369_99999_1995T.txt	27.60	-81.533	AVON PARK	X	X	X	X	991	991	991	991	991	991
80478_99999_1995T.txt	27.90	-81.850	BARTOW	X	991	X	X	991	992	992	991	X	992
80598_99999_1995T.txt	29.77	-82.917	BELL 4 WNW						999	X	X	X	999
80611_99999_1995T.txt	26.683	-80.667	BELLE GLADE EXP STN	X	X	X	X	X	X	991	999	999	999
80737_99999_1995T.txt	26.33	-81.000	BIG CYPRESS								999	999	X
80945_99999_1995T.txt	27.450	-82.500	BRADENTON 5 ESE	X	X	X	X	X	991	999		999	X
81022_99999_1995T.txt	30.38	-84.983	BRISTOL 2 S							999	991	991	X
81046_99999_1995T.txt	28.62	-82.367	BROOKSVILLE CHIN HILL	X	X	X	999	991	991	X	X	X	X
81276_99999_1995T.txt	26.87	-80.633	CANAL POINT USDA	991	X	X	X	992	992	991	991	X	999
81544_99999_1995T.txt	30.78	-85.483	CHIPLEY 3 E	X	X	999	999	999	991	992	X	X	999
81641_99999_1995T.txt	28.45	-81.750	CLERMONT 6 SSW	X	991	X	X	991	999	991	X	992	992
81651_99999_1995T.txt	26.73	-81.050	CLEWISTON NO. 2	999	999	999	999	999		999	999	999	999
81858_99999_1995T.txt	26.27	-80.283	CORAL SPRINGS	X	X	991	X	991	992	999	999	999	999
81986_13884_1995T.txt	30.78	-86.517	CRESTVIEW BOB SIKES AP	999	X	999		999	999	X	X	X	X
82008_99999_1995T.txt	29.65	-83.167	CROSS CITY 2	X	X	992	999	999	999	999	999	999	999
82150_99999_1995T.txt	29.18	-81.067	DAYTONA BEACH				999		999	999	X	999	999
82158_12834_1995T.txt	29.18	-81.050	DAYTONA BEACH MUNICIPAL ARPT	999	999	991		X	X	X	X	X	X
82220_99999_1995T.txt	30.75	-86.083	DE FUNIAK SPRINGS	991	999	X	X	X	X	991	X	X	999
82229_99999_1995T.txt	29.02	-81.317	DELAND	X	X	X	X	X	X	X	X	X	X

File Names	Latitude	Longitude	Station Name	95	96	97	98	99	00	01	02	03	04
82298_99999_1995T.txt	26.6	-81.133	DEVILS GARDEN TOWER	991	999	999	999	999	999	999	999	X	9991
82441_99999_1995T.txt	24.77	-80.900	DUCK KEY	X	X	999	999	999	991	X	X	999	X
82915_99999_1995T.txt	29.75	-81.533	FEDERAL POINT	991	991	999	999	999	999	991	X	X	991
82944_99999_1995T.txt	30.67	-81.467	FERNANDINA BEACH	991	X	X	X	X	991	X	X	X	X
83020_99999_1995T.txt	25.15	-80.917	FLAMINGO RANGER STN	991	X	999	999	999	999	999	999	999	999
83163_99999_1995T.txt	26.1	-80.200	FORT LAUDERDALE	X	X	X	X	X	991	991	X	X	991
83165_12849_1995T.txt	26.07	-80.150	FORT LAUDERDALE HOLLYWOOD INT						999	999	X	X	X
83168_99999_1995T.txt	26.13	-80.100	FORT LAUDERDALE BAHIA MA						999	999	X	X	991
83186_12835_1995T.txt	26.58	-81.867	FORT MYERS PAGE FIELD	999			999	X	X	X	X	X	X
83207_99999_1995T.txt	27.47	-80.350	FORT PIERCE	X	X	X	X	X	991	991	991	X	991
83322_99999_1995T.txt	29.68	-82.500	GAINESVILLE 11 WNW	X	X	X	X	X	X				
83326_12816_1995T.txt	29.7	-82.283	GAINESVILLE MUNI ARPT	X	X	991	999	X	X	X	X	X	X
83470_99999_1995T.txt	30.27	-82.183	GLEN ST MARY NURSERIES	X	991	X	999	991	991	992	X	991	991
83874_99999_1995T.txt	29.75	-81.467	HASTINGS ARC	X	X	X	X	X	991	X	X	X	X
83909_99999_1995T.txt	25.83	-80.283	HIALEAH	X	X	991	999	991	992	992	992	992	991
83956_99999_1995T.txt	29.83	-82.600	HIGH SPRINGS	991	991	991	999	991	X	991	991	992	999
84050_99999_1995T.txt	26.03	-80.133	HOLLYWOOD								999	X	991
84095_99999_1995T.txt	25.5	-80.550	HOMESTEAD GEN AVIATION AP	999	X	999	X	991	991	991	999	X	X
84210_99999_1995T.txt	26.42	-81.417	IMMOKALEE 3 NNW	999	999	X	X	999				999	999
84289_99999_1995T.txt	28.8	-82.317	INVERNESS	X	X	X	999	991	991	991	991	X	991
84358_13889_1995T.txt	30.5	-81.700	JACKSONVILLE MUNICIPAL ARPT	X	991	X	999	X	991	X	X	X	X
84366_99999_1995T.txt	30.28	-81.400	JACKSONVILLE BEACH	X	X	X	X	991	991	X	X	X	999
84394_99999_1995T.txt	30.52	-82.950	JASPER 9 ESE	991	999	X	X	991	X	X	X	999	X
84570_12836_1995T.txt	24.55	-81.750	KEY WEST BOCA CHICA AP	X	991	991	999	X	X	X	X	X	991
84625_99999_1995T.txt	28.28	-81.417	KISSIMMEE 2	999	X	X	X	991	991	992	991	X	X

File Names	Latitude	Longitude	Station Name	95	96	97	98	99	00	01	02	03	04
84707_99999_1995T.txt	28.10	-81.717	LAKE ALFRED EXP STN	X	X	X	999	992	999				
84723_99999_1995T.txt	29.95	-82.333	LAKE BUTLER					999	999	999	999	999	X
84731_99999_1995T.txt	30.18	-82.600	LAKE CITY 2 E		X	X	X	991	999	X	X	X	X
84802_99999_1995T.txt	27.98	-82.017	LAKELAND 2	999	X	X	X	X	X	X	X	X	999
85076_99999_1995T.txt	28.87	-81.783	LISBON	X	X	991	999	X	X	991	X	X	991
85099_99999_1995T.txt	30.28	-82.967	LIVE OAK		X	X	X	991	991	992	991	991	991
85275_99999_1995T.txt	30.45	-83.417	MADISON		X	999	X	991	991	X	991	X	999
85359_99999_1995T.txt	25.95	-81.717	MARCO ISLAND								999	X	X
85539_99999_1995T.txt	30.05	-83.183	MAYO 5 NW		X	X	X	999	991	X	X	X	X
85549_3853_1995T.txt	30.4	-81.417	MAYPORT NS		X	X	999	992	999	999	991	999	999
85612_12838_1995T.txt	28.1	-80.650	MELBOURNE EAU GALLIE AP	X	X	X	X	X	X	X	X	X	X
85658_92811_1995T.txt	25.78	-80.133	MIAMI BEACH		X	X	X	X	X	X	X	991	X
85663_12839_1995T.txt	25.78	-80.317	MIAMI INTL AP		X	991	999	X	X	X	X	X	X
85667_99999_1995T.txt	25.75	-80.383	MIAMI NWSFO					999	X	X	999	X	X
85793_99999_1995T.txt	30.78	-87.133	MILTON EXPERIMENT STN	999	X	999	X	X	999	X	X	999	999
85879_99999_1995T.txt	30.57	-83.867	MONTICELLO 2 S	X	X	999	999	999	999	999	999	999	999
85895_99999_1995T.txt	26.83	-81.083	MOORE HAVEN LOCK 1	999	X	X	X	X	X	999	X	X	X
85973_99999_1995T.txt	27.93	-81.600	MOUNTAIN LAKE	X	X	X	X	991	991	X	X	X	999
86065_99999_1995T.txt	27.25	-82.317	MYAKKA RIVER STATE PARK	X	X	X	X	X	X	991	X	991	999
86076_12897_1995T.txt	26.15	-81.783	NAPLES MUNICIPAL AP								999	991	X
86078_99999_1995T.txt	26.02	-81.717	NAPLES 1 S	999	991	X	999	991	992	999	X	X	991
86129_99999_1995T.txt	30.95	-85.883	NEW HOPE							999	992	X	991
86240_99999_1995T.txt	30.53	-86.500	NICEVILLE	991	X	X	999	991		991	X	992	X
86315_99999_1995T.txt	25.95	-80.217	NORTH MIAMI BEACH #2							999	X	999	X
86406_99999_1995T.txt	25.85	-81.033	OASIS RANGER STN	999	X	X	X	X	X	991	X	992	X
86414_99999_1995T.txt	29.08	-82.083	OCALA	X	X	X	X	991	991	999	X	X	X
86485_99999_1995T.txt	27.2	-80.833	OKEECHOBEE HRCN GATE 6		999	999	999		992	999	X	999	999
86618_99999_1995T.txt	29.48	-81.967	ORANGE SPRINGS 2 SSW						999	X	X	X	991

File Names	Latitude	Longitude	Station Name	95	96	97	98	99	00	01	02	03	04
86628_12815_1995T.txt	28.43	-81.333	ORLANDO INTL ARPT	X	X	991	999	X	X	X	X	X	X
86753_99999_1995T.txt	29.65	-81.667	PALATKA				999	X	991	999	X	X	991
86767_99999_1995T.txt	29.63	-81.200	PALM COAST 6 NE					999	999	992	X	X	991
86828_99999_1995T.txt	30	-84.483	PANACEA							999	991	999	X
86842_99999_1995T.txt	30.25	-85.667	PANAMA CITY 5 NE	X	X	991	X	999	991	X		999	X
86880_99999_1995T.txt	27.62	-82.350	PARRISH	991	991	991	X	991	991	999	999	992	992
86997_13899_1995T.txt	30.48	-87.183	PENSACOLA MUNICIPAL ARPT	X	X	X	999	X	X	X	X	X	X
87020_99999_1995T.txt	25.58	-80.433	PERRINE		999	X	X	X	X	X	X	991	991
87025_99999_1995T.txt	30.1	-83.567	PERRY 3 S		X	X	X	X	991	991	X	992	X
87189_99999_1995T.txt	26.12	-80.267	PLANTATION							999	999	X	X
87205_99999_1995T.txt	28.02	-82.150	PLANT CITY	X	X	X	X	992	992	992	X	X	999
87397_99999_1995T.txt	26.92	-82.000	PUNTA GORDA 4 ESE	X	X	X	X	991	991	991	X	X	992
87429_99999_1995T.txt	30.6	-84.550	QUINCY 3 SSW	X	999	999	999	999	999	999	999	999	999
87760_99999_1995T.txt	25.38	-80.600	ROYAL PALM RANGER ST		999	999	X	X	991	991	991	X	X
87826_99999_1995T.txt	29.88	-81.300	ST AUGUSTINE WFOY		X	X	X	991	991	992	X	X	991
87851_99999_1995T.txt	28.33	-82.267	ST LEO	X	X	X	X	X	X	X	X	X	X
87886_92806_1995T.txt	27.77	-82.633	ST PETERSBURG ALBERT WHITTED	X	X	X	X	991	991	X	X	X	X
87982_99999_1995T.txt	28.8	-81.267	SANFORD EXPERIMENT STN	X	X	X	999	991	991	999	X	991	991
88368_99999_1995T.txt	26.47	-80.633	SOUTH BAY 15 S								999	X	991
88529_99999_1995T.txt	29.93	-82.117	STARKE 3 E					999	999	999	X	999	X
88565_99999_1995T.txt	29.72	-83.300	STEINHATCHEE 2	999	X	999	999	992	999	999			
88620_99999_1995T.txt	27.2	-80.167	STUART 1 N	X	X	999	999	999	999	999	999	999	999
88756_99999_1995T.txt	30.4	-84.350	TALLAHASSEE AIRPORT	X	991	991	999	999				999	999
88758_93805_1995T.txt	30.4	-84.350	TALLAHASSEE DALE MABRY FIELD						X	X	991	X	X

File Names	Latitude	Longitude	Station Name	95	96	97	98	99	00	01	02	03	04
88780_99999_1995T.txt	25.77	-80.817	TAMIAMI TRAIL 40 MI BEND	999	X	X	999	992	991	999	992	992	999
88788_12842_1995T.txt	27.97	-82.533	TAMPA INTERNATIONAL AP	991	991	991	999	X	X	X	X	X	X
88824_99999_1995T.txt	28.15	-82.750	TARPON SPRINGS	X	X	X	999	X	991	991	X	X	999
88841_99999_1995T.txt	25	-80.517	TAVERNIER	999	991	999	999	999	991	992	X	X	X
88942_99999_1995T.txt	28.63	-80.833	TITUSVILLE	991	991	999	X	991	991	991	X	X	X
89120_99999_1995T.txt	29.42	-82.817	USHER TOWER	X	X	X	X	X	X	X	X	X	X
89176_99999_1995T.txt	27.1	-82.433	VENICE	991	X	991	X	X	992	991	X	X	X
89214_12843_1995T.txt	27.65	-80.417	VERO BEACH MUNICIPAL ARPT	X	X	999	999	991	991	991	X	991	991
89219_99999_1995T.txt	27.65	-80.400	VERO BEACH 4 W	X	X	X	X	992	X	999	999	992	992
89401_99999_1995T.txt	27.55	-81.800	WAUCHULA 2 N	991	X	X	X	X	991	X	999	X	991
89430_99999_1995T.txt	28.52	-82.583	WEEKI WACHEE	X	X	991	999	999	999	999	999	999	999
89525_12844_1995T.txt	26.68	-80.100	WEST PALM BEACH MORRISON FIEL	999	991	X	X	X	X	X	X	X	X
89566_99999_1995T.txt	30.12	-85.200	WEWAHITCHKA	X	X	999	X	992	999	991	999	992	999
89640_99999_1995T.txt		-82.783	WHITE SPRINGS 7 N					999	999	999	999	999	999
89707_99999_1995T.txt	28.02	-81.733	WINTER HAVEN	X	X	999	999	999	991	991	X	992	992
999999_3855_1995T.txt	30.35	-87.317	PENSACOLA FOREST SHERMAN NAS	X	X	X	999	991	991	999	991	999	999
999999_12849_1995T.txt	26.07	-80.150	FORT LAUDERDALE NAS					999	999	X	991	999	
999999_12850_1995T.txt	24.58	-81.683	KEY WEST NAS	X	X	991	999	991	991	991	991	999	999
999999_93832_1995T.txt	30.22	-81.883	JACKSONVILLE CECIL FLD NAS	X	X	X	999	992		991			
999999_93837_1995T.txt	30.23	-81.667	JACKSONVILLE NAS	X	X	X	999	992	X		992	999	
999999_93841_1995T.txt	30.72	-87.017	WHITING FIELD NAS	X	X	X	999	999	999	999	999	999	

FAWN File Names '98	FAWN File Names	Latitude	Longitude	Station Name	98	99	00	01	02	03	04
	Fawndata_AL_2004T.txt	29.803	-82.41	ALACHUA			X	X	X	X	X
F_AP_1998T.txt	Fawndata_AP_2004T.txt	28.642	-81.55	APOPKA	X	X		X	X	X	X
F_AV_1998T.txt	Fawndata_AV_2004T.txt	28.473	-81.648	AVALON	X	X	X	X	X	X	X
	Fawndata_BA_2004T.txt	27.76	-82.223	BALM							X
	Fawndata_BR_2004T.txt	29.402	-82.587	BRONSON						X	X
	Fawndata_BV_2004T.txt	28.635	-82.285	BROOKSVILLE				X	X	X	X
	Fawndata_CA_2004T.txt	29.843	-84.695	CARRABELLE							X
	Fawndata_CI_2004T.txt	29.41	-82.17	CITRA				X	X	X	X
	Fawndata_DO_2004T.txt	28.017	-82.233	DOVER		X	X	X	X	X	X
	Fawndata_FL_2004T.txt	26.087	-80.242	FORT LAUDERDALE					X	X	X
	Fawndata_FP_2004T.txt	27.427	-80.402	FT.PIERCE		X	X	X		X	X
	Fawndata_HA_2004T.txt	29.693	-81.445	HASTINGS			X	X	X	X	X
F_HO_1998T.txt	Fawndata_HO_2004T.txt	25.51	-80.498	HOMESTEAD	X	X	X	X	X	X	X
F_IM_1998T.txt	Fawndata_IM_2004T.txt	26.462	-81.44	IMMOKALEE	X	X	X	X	X	X	X
	Fawndata_JY_2004T.txt	30.775	-87.14	JAY						X	X
	Fawndata_KN_2004T.txt	27.963	-81.05	KENANSVILLE							X
F_LA_1998T.txt	Fawndata_LA_2004T.txt	28.102	-81.712	LAKE ALFRED	X	X	X	X	X	X	X
	Fawndata_LO_2004T.txt	30.303	-82.9	LIVE OAK						X	X
	Fawndata_MC_2004T.txt	30.28	-82.138	MACCLENNY						X	X
	Fawndata_MA_2004T.txt	30.85	-85.165	MARIANNA						X	X
	Fawndata_MO_2004T.txt	30.538	-83.917	MONTICELLO							X
	Fawndata_OC_2004T.txt	29.02	-81.968	OCKLAWAHA		X	X	X	X	X	X
F_OK_1998T.txt	Fawndata_OK_2004T.txt	28.682	-81.887	OKAHUMPKA	X	X	X	X	X	X	X
	Fawndata_ON_2004T.txt	27.398	-81.94	ONA		X	X	X	X	X	X
	Fawndata_PA_2004T.txt	26.925	-81.402	PALMDALE							X
	Fawndata_PI_2004T.txt	29.223	-81.448	PIERSON		X	X	X	X	X	X
	Fawndata_PH_2004T.txt	29.697	-81.98	PUTNAM HALL						X	X
	Fawndata_QU_2004T.txt	30.545	-84.597	QUINCY						X	X
	Fawndata_SE_2004T.txt	27.422	-81.402	SEBRING							X
F_UM_1998T.txt	Fawndata_UM_2004T.txt	28.92	-81.632	UMATILLA	X	X	X	X	X		X

Relative Humidity Meteorological Station Tables

File Name	Latitude	Longitude	Site Name	FAWN SITES	95	96	97	#	99	00	O1	O2	O3	O4
Fawndata_AL_1995RH	29.803	-82.410	ALACHUA							X	X	X	X	X
Fawndata_AP_1995RH	28.642	-81.550	APOPKA					X	X	X		X	X	X
Fawndata_AV_1995RH	28.473	-81.648	AVALON									X	X	X
Fawndata_BA_1995RH	27.760	-82.223	BALM											X
Fawndata_BR_1995RH	29.402	-82.587	BRONSON											
Fawndata_BV_1995RH	28.635	-82.285	BROOKSVILLE									X	X	
Fawndata_CA_1995RH	29.843	-84.695	CARRABELLE											X
Fawndata_CI_1995RH	29.410	-82.170	CITRA									X	X	X
Fawndata_DO_1995RH	28.017	-82.233	DOVER						X	X	X	X	X	X
Fawndata_FL_1995RH	26.087	-80.242	FORTLAUDERDALE									X	X	X
Fawndata_FP_1995RH	27.427	-80.402	FT. PIERCE						X	X	X	X	X	X
Fawndata_HA_1995RH	29.693	-81.445	HASTINGS							X	X	X	X	X
Fawndata_HO_1995RH	25.510	-80.498	HOMESTEAD					X	X	X	X	X	X	X
Fawndata_IM_1995RH	26.462	-81.440	IMMOKALEE					X	X	X	X	X	X	X
Fawndata_JY_1995RH	30.775	-87.140	JAY											
Fawndata_KN_1995RH	27.963	-81.050	KENANSVILLE											X
Fawndata_LA_1995RH	28.102	-81.712	LAKE ALFRED					X	X	X	X	X	X	X
Fawndata_LO_1995RH	30.303	-82.900	LIVE OAK											
Fawndata_MC_1995RH	30.280	-82.138	MACCLENNY										X	
Fawndata_MA_1995RH	30.850	-85.165	MARIANNA											
Fawndata_MO_1995RH	30.538	-83.917	MONTICELLO											
Fawndata_OC_1995RH	29.020	-81.968	OCKLAWAHA						X	X	X	X	X	X
Fawndata_OK_1995RH	28.682	-81.887	OKAHUMPKA										X	X
Fawndata_ON_1995RH	27.398	-81.940	ONA						X	X	X	X	X	X
Fawndata_PA_1995RH	26.925	-81.402	PALMDALE											X
Fawndata_PI_1995RH	29.223	-81.448	PIERSON						X	X	X	X		X
Fawndata_PH_1995RH	29.697	-81.980	PUTNAM HALL											
Fawndata_QU_1995RH	30.545	-84.597	QUINCY											
Fawndata_SE_1995RH	27.422	-81.402	SEBRING											X
Fawndata_UM_1995RH	28.920	-81.632	UMATILLA								X	X		X

File Name	Latitude	Longitude	Site Name	SJRWMD SITES	95	96	97	#	99	00	O1	O2	O3	O4
SJ_01350583_1995RH	27.59	-80.69	Ft Drum Ws				X		X					
SJ_01540709_1995RH	27.83	-80.81	Tucker WS					X						
SJ_02103140_1995RH	29.66	-81.69	DHQ											
SJ_02333020_1995RH	29.25	-81.46	Pierson AP								X			
SJ_02363021_1995RH	29.41	-81.62	Marvin Jones Rd											
SJ_02373022_1995RH	29.22	-81.32	SR40 & 11											
SJ_02441371_1995RH	29.78	-81.44	Elkton				X							
SJ_02731502_1995RH	28.75	-81.21	Lk Jessup WS											
SJ_02741537_1995RH	29.48	-82.13	Orange Lk WS											
SJ_19004202_1995RH	27.85	-80.46	Coconut Point IRL141											
SJ_30233134_1995RH	29.01	-81.83	Sunny Hill WS				X							
SJ_50000404_1995RH	28.63	-81.62	Lk Apopka Cntr									X		
File Name	Latitude	Longitude	Site Name	SFWMD SITES	95	96	97	#	99	00	O1	O2	O3	O4
SFWMD_12513_1995RH	26.96	-80.97	L005		X						X	X		
SFWMD_12523_1995RH	26.82	-80.78	L006		X	X	X		X	X		X		
SFWMD_13079_1995RH	26.90	-80.79	LZ40		X		X	X	X	X	X		X	
SFWMD_15085_1995RH	25.22	-80.54	JBTS		X		X		X					X
SFWMD_15482_1995RH	28.14	-81.35	S61W		X	X		X	X	X		X	X	
SFWMD_15493_1995RH	26.79	-81.30	S78W		X	X	X	X	X	X		X	X	X
SFWMD_15504_1995RH	26.17	-80.83	S140W			X		X	X		X	X	X	X
SFWMD_15515_1995RH	26.74	-80.90	CFSW		X	X	X	X	X		X	X	X	
SFWMD_15686_1995RH	26.32	-81.07	BIG CY SI				X	X		X	X	X	X	
SFWMD_15856_1995RH	26.66	-80.41	ENR105		X	X	X	X	X			X		
SFWMD_15883_1995RH	26.62	-80.44	ENR308		X		X	X	X	X	X		X	
SFWMD_16026_1995RH	27.14	-80.79	L001			X			X	X	X	X	X	X
SFWMD_16259_1995RH	25.61	-80.51	S331W			X	X	X	X	X	X	X	X	X
SFWMD_DJ240_1995RH	27.40	-81.11	S65CW		X	X	X	X	X	X	X	X	X	
SFWMD_DO529_1995RH	26.66	-80.63	BELLE GL				X	X	X	X	X	X		
SFWMD_DU552_1995RH	26.50	-80.22	LOXWS		X	X	X			X				

File Name	Latitude	Longitude	Site Name	NOAA SITES	95	96	97	#	99	00	O1	O2	O3	O4
81986_13884_1997RH	30.78	-86.52	CRESTVIEW BOB S. AP								X	X	X	X
82158_12834_1997RH	29.18	-81.05	DAYTONA BEACH MUNIARPT		X	X	X	X	X	X	X	X	X	X
83165_12849_1997RH	26.07	-80.15	FORT LAUDERDALE HW. INT											X
83186_12835_1997RH	26.58	-81.87	FORT MYERS PAGE FIELD						X	X	X	X	X	X
83326_12816_1997RH	29.70	-82.28	GAINESVILLE MUNI ARPT		X	X	X	X	X	X	X	X	X	X
84358_13889_1997RH	30.50	-81.70	JACKSONVILLE MUNIARPT		X	X	X	X	X	X	X	X	X	X
84570_12836_1997RH	24.55	-81.75	KEY WEST BOCA CHICA AP		X	X	X	X	X	X	X	X	X	X
85549_03853_1997RH	30.40	-81.42	MAYPORT NS		X	X	X		X	X	X	X		
85663_12839_1997RH	25.78	-80.32	MIAMI INTL AP		X	X	X	X	X	X	X	X	X	X
86076_12897_1997RH	26.15	-81.78	NAPLES MUNICIPAL AP											X
86628_12815_1997RH	28.43	-81.33	ORLANDO INTL ARPT		X	X	X	X	X	X	X	X	X	X
86997_13899_1997RH	30.48	-87.18	PENSACOLA MUNI ARPT					X	X	X	X	X	X	X
88758_93805_1997RH	30.40	-84.35	TALLAHASSEE D.M. FIELD		X	X	X	X	X	X	X	X	X	X
88788_12842_1997RH	27.97	-82.53	TAMPA INTERNATIONAL AP		X	X	X	X	X	X	X	X	X	X
89214_12843_1997RH	27.65	-80.42	VERO BEACH MUNI ARPT		X							X	X	X
89525_12844_1997RH	26.68	-80.10	WEST PALM BEACH MOR. FIEL		X	X	X	X	X	X	X	X	X	X
999999_3855_1997RH	30.35	-87.32	PENSACOLA FOREST SHERMAN NAS		X	X	X	X		X	X	X		
99999_12833_1997RH	29.33	-83.10	CROSS CITY AIRPORT							X				
99999_12849_1997RH	26.07	-80.150	FORT LAUDERDALE NAS								X	X		
99999_12850_1997RH	24.58	-81.68	KEY WEST NAS		X	X	X	X	X	X	X	X		
99999_12859_1997RH	25.77	-80.20	MIAMI											
99999_12897_1997RH	26.15	-81.77	NAPLES AIRPORT											
99999_53860_1997RH	30.33	-81.52	JACKSONVILLE CRAIG MUNI AP											
99999_93832_1997RH	30.22	-81.88	JACKSONVILLE CECIL FLD NAS		X	X	X							
99999_93837_1997RH	30.23	-81.67	JACKSONVILLE NAS		X	X	X	X	X	X	X			
99999_93841_1997RH	30.72	-87.02	WHITING FIELD NAS		X	X	X	X						
15478_72223_1997RH	30.68	-88.25	MOBILE REG ARPT		X	X	X	X	X	X				

Wind Meteorological Station Tables

File Name	Latitude	Longitude	Site Name	FAWN SITES	95	96	97	98	99	OO	O1	O2	O3	O4
Fawndata_AL_1998W.txt	29.803	-82.410	ALACHUA					X		X	X	X	X	X
Fawndata_AP_1998W.txt	28.642	-81.550	APOPKA					X	X	X	X	X	X	X
Fawndata_AV_1998W.txt	28.473	-81.648	AVALON							X	X	X	X	X
Fawndata_BA_1998W.txt	27.760	-82.223	BALM											X
Fawndata_BR_1998W.txt	29.402	-82.587	BRONSON										X	X
Fawndata_BV_1998W.txt	28.635	-82.285	BROOKSVILLE								X	X	X	X
Fawndata_CA_1998W.txt	29.843	-84.695	CARRABELLE											X
Fawndata_CI_1998W.txt	29.410	-82.170	CITRA								X	X	X	X
Fawndata_DO_1998W.txt	28.017	-82.233	DOVER						X	X	X	X	X	X
Fawndata_FL_1998W.txt	26.087	-80.242	FORTLAUDERDALE									X	X	X
Fawndata_FP_1998W.txt	27.427	-80.402	FT. PIERCE						X	X	X	X	X	X
Fawndata_HA_1998W.txt	29.693	-81.445	HASTINGS							X	X	X	X	X
Fawndata_HO_1998W.txt	25.510	-80.498	HOMESTEAD					X	X	X	X	X	X	X
Fawndata_IM_1998W.txt	26.462	-81.440	IMMOKALEE						X	X	X	X	X	X
Fawndata_JY_1998W.txt	30.775	-87.140	JAY										X	X
Fawndata_KN_1998W.txt	27.963	-81.050	KENANSVILLE											X
Fawndata_LA_1998W.txt	28.102	-81.712	LAKE ALFRED					X	X	X	X	X	X	X
Fawndata_LO_1998W.txt	30.303	-82.900	LIVE OAK										X	X
Fawndata_MC_1998W.txt	30.280	-82.138	MACCLENNY										X	X
Fawndata_MA_1998W.txt	30.850	-85.165	MARIANNA										X	X
Fawndata_MO_1998W.txt	30.538	-83.917	MONTICELLO											X
Fawndata_OC_1998W.txt	29.020	-81.968	OCKLAWAHA						X	X	X	X	X	X
Fawndata_OK_1998W.txt	28.682	-81.887	OKAHUMPKA							X	X		X	X
Fawndata_ON_1998W.txt	27.398	-81.940	ONA						X	X	X	X	X	X
Fawndata_PA_1998W.txt	26.925	-81.402	PALMDALE											X
Fawndata_PH_1998W.txt	29.697	-81.980	PUTNAM HALL											X
Fawndata_QU_1998W.txt	30.545	-84.597	QUINCY										X	X
Fawndata_SE_1998W.txt	27.422	-81.402	SEBRING											X
Fawndata_UM_1998W.txt	28.920	-81.632	UMATILLA							X	X	X	X	X

File Name	Latitude	Longitude	Site Name	SJRWMD SITES	95	96	97	98	99	OO	O1	O2	O3	O4
SJ_01350586_1997W.txt	27.59	-80.69	Ft Drum Ws				X	X						
SJ_02741546_1997W.txt	29.48	-82.13	Orange Lk WS					X						
SJ_30233135_1997W.txt	29.01	-81.83	Sunny Hill WS				X							
SJ_00640273_1996W.txt	28.714	-81.037	SJR at SR46 nr Geneva											
SJ_02571452_1996W.txt	30.007	-81.360	Stokes Landing nr St. Augustine											
SJ_00530223_1996W.txt	28.341	-80.933	S-164 Lower nr Cocoa			X	X	X						
SJ_00700321_1996W.txt	28.253	-80.850	Lake Winder nr Viera		X									
SJ_00960396_1996W.txt	27.826	-80.741	S-96B West nr Fellsmere		X		X							
SJ_01060424_1996W.txt	27.560	-80.689	C-52 Canal West nr Fells		X	X								
SJ_00540104_1996W.txt	27.727	-80.776	Blue Cypress Lake nr Fells		X	X								
SJ_02161117_1996W.txt	29.691	-81.487	Dick Reid					X						
SJ_02401326_1996W.txt	29.280	-81.717	Hopkins Prairie					X						
SJ_02431345_1996W.txt	29.597	-81.527	Hell Cat Bay				X	X						
SJ_02441366_1996W.txt	29.775	-81.443	Elkton		X	X								
SJ_02481390_1996W.txt	29.457	-81.530	Newbold Fernery											
SJ_21902191_1996W.txt	28.656	-81.706	Clay Island Weir nr Astatula		X	X								
SJ_22002206_1996W.txt	28.668	-81.706	Clay Island WS nr Astatula											
SJ_50004996_1996W.txt	28.629	-81.625	Lake Apopka Center											

File Name	Latitude	Longitude	Site Name	SFWMD SITES	95	96	97	98	99	OO	O1	O2	O3	O4
SFWMD_12510_1995W.txt	26.96	-80.97	L005		X	X	X	X	X		X	X	X	X
SFWMD_12520_1995W.txt	26.82	-80.78	L006											
SFWMD_15069_1995W.txt	25.26	-80.42	MBTS		X				X	X		X	X	
SFWMD_15104_1995W.txt	26.68	-80.37	S5A_WIND		X	X	X							
SFWMD_15466_1995W.txt	27.40	-81.11	S65CW		X		X	X		X	X	X	X	X
SFWMD_15476_1995W.txt	28.14	-81.35	S61W			X	X	X				X	X	
SFWMD_15498_1995W.txt	26.17	-80.83	S140W			X	X							
SFWMD_15509_1995W.txt	26.74	-80.90	CFSW		X	X	X	X			X	X	X	X
SFWMD_15879_1995W.txt	26.62	-80.44	ENR308		X	X	X	X	X	X	X	X	X	
SFWMD_16253_1995W.txt	25.61	-80.51	S331W			X	X	X	X	X	X	X	X	X
SFWMD_DU558_1995W.txt	26.50	-80.22	LOXWS		X	X	X						X	X
SFWMD_F9559_1995W.txt	26.33	-80.88	L3BRS				X							
SFWMD_FF837_1995W.txt	28.05	-81.40	WRWX					X	X	X				

File Name	Latitude	Longitude	Site Name	NOAA SITES	95	96	97	98	99	OO	O1	O2	O3	O4
81986_13884_1995W.txt	30.78	-86.52	CRESTVIEW BOB S.AP								X	X	X	X
82158_12834_1995W.txt	29.18	-81.05	DAYTONA BEACH MUNIARPT		X	X	X	X	X	X	X	X	X	X
83165_12849_1995W.txt	26.07	-80.15	FORT LAUDERDALE HW.INT											X
83186_12835_1995W.txt	26.58	-81.87	FORT MYERS PAGE FIELD						X	X	X	X	X	X
83326_12816_1995W.txt	29.70	-82.28	GAINESVILLE MUNI ARPT		X	X	X	X	X	X	X	X	X	X
84358_13889_1995W.txt	30.50	-81.70	JACKSONVILLE MUNIARPT		X	X	X	X	X	X	X	X	X	X
84570_12836_1995W.txt	24.55	-81.75	KEY WEST BOCA CHICA AP		X			X	X	X	X	X	X	X
85549_03853_1995W.txt	30.40	-81.42	MAYPORT NS		X	X	X		X	X		X		
85663_12839_1995W.txt	25.78	-80.32	MIAMI INTL AP		X	X	X	X	X	X	X	X	X	X
86076_12897_1995W.txt	26.15	-81.78	NAPLES MUNICIPAL AP											X
86628_12815_1995W.txt	28.43	-81.33	ORLANDO INTL ARPT		X	X	X	X	X	X	X	X	X	X
86997_13899_1995W.txt	30.48	-87.18	PENSACOLA MUNI ARPT					X	X	X	X	X	X	X
88758_93805_1995W.txt	30.40	-84.35	TALLAHASSEE D.M.FIELD		X	X	X	X	X	X	X	X	X	X
88788_12842_1995W.txt	27.97	-82.53	TAMPA INTERNATIONAL AP		X	X	X	X	X	X	X	X	X	X
89214_12843_1995W.txt	27.65	-80.42	VERO BEACH MUNI ARPT		X			X	X	X	X	X	X	X
89525_12844_1995W.txt	26.68	-80.10	WEST PALM BEACH MOR. FIEL		X	X	X	X	X	X	X	X	X	X
999999_3855_1995W.txt	30.35	-87.32	PENSACOLA FOREST SHER.NAS		X	X	X	X	X	X	X	X		
99999_12833_1995W.txt	29.33	-83.10	CROSS CITY AIRPORT							X				
99999_12849_1995W.txt	26.07	-80.150	FORT LAUDERDALE NAS								X	X		
99999_12850_1995W.txt	24.58	-81.68	KEY WEST NAS		X	X	X	X	X	X	X	X		
99999_93837_1995W.txt	30.23	-81.67	JACKSONVILLE NAS		X	X	X	X	X	X	X	X		
99999_93841_1995W.txt	30.72	-87.02	WHITING FIELD NAS		X	X	X	X	X	X		X		